ABSTRACT

INTERFERENCE SUPPRESSION AND DIVERSITY FOR CDMA SYSTEMS

by
Xiaodong Cai

In code-division multiple-access (CDMA) systems, due to non-orthogonality of the spreading codes and multipath channels, the desired signal suffers interference from other users. Signal fading due to multipath propagation is another source of impairment in wireless CDMA systems, often severely impacting performance. In this dissertation, reduced-rank minimum mean square error (MMSE) receiver and reduced-rank minimum variance receiver are investigated to suppress interference; transmit diversity is applied to multicarrier CDMA (MC-CDMA) systems to combat fading; packet combing is studied to provide both interference suppression and diversity for CDMA random access systems.

The reduced-rank MMSE receiver that uses a reduced-rank estimated covariance matrix is studied to improve the performance of MMSE receiver in CDMA systems. It is shown that the reduced-rank MMSE receiver has much better performance than the full-rank MMSE receiver when the covariance matrix is estimated by using a finite number of data samples and the desired signal is in a low dimensional subspace. It is also demonstrated that the reduced-rank minimum variance receiver outperforms the full-rank minimum variance receiver. The probability density function of the output SNR of the full-rank and reduced-rank linear MMSE estimators is derived for a general linear signal model under the assumption that the signals and noise are Gaussian distributed.

Space-time coding that is originally proposed for narrow band systems is applied to an MC-CDMA system in order to get transmit diversity for such a wideband system. Some techniques to jointly decode the space-time code and

suppress interference are developed. The channel estimation using either pilot channels or pilot symbols is studied for MC-CDMA systems with space-time coding.

Performance of CDMA random access systems with packet combining in fading channels is analyzed. By combining the current retransmitted packet with all its previous transmitted copies, the receiver obtains a diversity gain plus an increased interference and noise suppression gain. Therefore, the bit error rate dramatically decreases with the number of transmissions increasing, which in turn improves the system throughput and reduces the average delay.

INTERFERENCE SUPPRESSION AND DIVERSITY FOR CDMA SYSTEMS

by
Xiaodong Cai

A Dissertation
Submitted to the Faculty of
New Jersey Institute of Technology
in Partial Fulfillment of the Requirements for the Degree of
Doctor of Philosophy of Electrical Engineering

Department of Electrical and Computer Engineering

January 2001

APPROVAL PAGE

INTERFERENCE SUPPRESSION AND DIVERSITY FOR CDMA SYSTEMS

Xiaodong Cai

Dr. Ali N. Akansu, Dissertation Advisor Professor of Electrical and Computer Engineering, NJIT	Date
Dr. Hongya Ge, Committee Member Assistant Professor of Electrical and Computer Engineering, NJIT	Date
Dr. Richard Haddad, Committee Member Professor of Electrical and Computer Engineering, NJIT	Date
Dr. Alexander M. Haimovich, Committee Member Associate Professor of Electrical and Computer Engineering, NJIT	Date
Dr. Jack H. Winters, Committee Member Member of Technical Staff, AT&T Labs-Research, Redbank, NJ	Date

BIOGRAPHICAL SKETCH

Author: Xiaodong Cai

Degree: Doctor of Philosophy

Date: January 2001

Undergraduate and Graduate Education:

- Doctor of Philosophy in Electrical Engineering,
  New Jersey Institute of Technology, Newark, NJ 2001
- Master of Engineering in Electrical Engineering,
  National University of Singapore, Singapore, 1997
- Bachelor of Science in Information and Electronic Engineering,
  Zhejiang University, Hangzhou, China, 1989

Major: Electrical Engineering

Publications and Presentations:

Xiaodong Cai, Yi Sun, and Ali N. Akansu,
"Performance of DS-CDMA random access systems with packet combining in fading channels," to be submitted to IEEE Journal in Selected Area on Communications.

Xiaodong Cai and Ali N. Akansu,
"Multicarrier CDMA systems with transmit diversity," IEEE VTC 2000, Boston, MA, Oct. 2000.

Xiaodong Cai, Hongya Ge, and Ali N. Akansu,
"Reduced rank minimum variance receiver for asynchronous CDMA Systems," IEEE ICC 2000, New Orleans, LA, pp. 1030-1033, June 2000.

Xiaodong Cai and Ali N. Akansu,
"A subspace method for blind channel identification in OFDM systems," IEEE ICC 2000, New Orleans, LA, pp 929-933, June 2000.

Xiaodong Cai, Hongya Ge, and Ali N. Akansu,
"Low-rank minimum variance CDMA receiver in multipath channels," IEEE ICASSP 2000, Istanbul, Turkey, pp. 2877-2880, June 2000.

Xiaodong Cai, Hongya Ge, and Ali N. Akansu,
"On the conditioned signal-to-noise ratio of linear MMSE estimators," 34th Annual Conference on Information Sciences and Systems, Princeton, NJ, pp. FA2:1-5, Mar. 2000.

Kun Wang, Xiaodong Cai, and Hongya Ge,
"A novel space-time rake receiver for DS-CDMA systems," 34th Annual Conference on Information Sciences and Systems, Princeton, NJ, pp. FA3:12-17, Mar. 2000.

Xiaodong Cai, Hongya Ge, and Ali N. Akansu,
" Low-rank MMSE detector for synchronous DS-CDMA," 33th Asilomar Conference on Signals, Systems and Computer, Pacific Grove, CA, pp. 940-944, Oct. 1999.

Mahalingam Ramkumar, Ali N. Akansu, and Xiaodong Cai,
"Floating signal constellations for multimedia steganography," IEEE ICC 2000, New Orleans, LA, pp. 249-253, June 2000.

Xiaodong Cai and Ali N. Akansu,
"OFDM systems embedded training sequence in the guard intervals," submitted to ICASSP 2001.

H.H. Chen and Xiaodong Cai ,
"Waveform optimization for OQAM-OFDM systems by using nonlinear programming algorithms," 1997 47th IEEE Vehicular Technology Conference, Phoenix, AZ, pp. 1385-1389, May 1997.

Hsiao-Hwa Chen and Xiaodong Cai,
"Optimization of transmitter and receiver filters for OQAM-OFDM systems using nonlinear programming," IEICE Transactions on Communications, v E80-B n 11 Nov 1997, pp. 1680-1687.

To my beloved parents

ACKNOWLEDGMENT

I wish to express my sincere gratitude to my advisor, Dr. Ali N. Akansu, for providing a stimulating and inspiring research environment. It was his constant encouragement, guidance and support that made this pursuit stimulating and rewarding.

I would like to express my appreciation to Dr. Hongya Ge, who spend much time to discuss with me on some ideas and details. I have benefited so much from her suggestions and comments. Thanks are due also to Dr. Yi Sun for his insightful discussions that lead to the research work on CDMA random access system with packet combing.

I must extend my gratitude to Dr. Richard Haddad, Dr. Alexander M. Haimovich and Dr. Jack H. Winters for serving as members of the dissertation committee and for their valuable comments.

No doctoral experience would be complete without the friends that have helped shape it. I would like to thank my good friends Anil, Bin, Burak, Feihong, Minyi, Sebnem and Surong for making my stay at the laboratory enjoyable.

Finally, words can never express the gratitude I feel toward my mother and father who teach me the importance of hard work and perseverance and instill in me the confidence that I could succeed at whatever I chose to do.

TABLE OF CONTENTS

TABLE OF CONTENTS
(Continued)

Chapter Page

TABLE OF CONTENTS
(Continued)

Chapter **Page**

LIST OF TABLES

Table **Page**

LIST OF FIGURES

Figure **Page**

LIST OF FIGURES
(Continued)

Figure **Page**

LIST OF FIGURES
(Continued)

CHAPTER 1

INTRODUCTION

1.1 CDMA Systems

In wireless communications, multiple access schemes are used to allow many users to share simultaneously a finite amount of radio spectrum. Frequency division multiple access (FDMA), time division multiple access (TDMA), and code division multiple access (CDMA) are the three major access techniques used to share the available bandwidth in a wireless communication systems. FDMA assigns a unique frequency band or channel to each user. Once the channel is assigned, no other user can share the same channel. TDMA systems divide the radio spectrum into time slots, and in each slot only one user is allowed to either transmit or receive. In CDMA systems, all the users share the same spectrum bandwidth and time slots. Each user is assigned a specific code that can be used to separate it from other users. In our work, we are particularly interested in some techniques to improve the performance and capacity of CDMA systems.

1.1.1 DS-CDMA

In direct sequence CDMA (DS-CDMA) systems, a narrowband signal that contains a message is multiplied by a signal with a very large bandwidth signal called the spreading signal. The spreading signal is compromised of chips that are defined by a pseudo random sequence which is known to both the transmitter and receiver. The chip rate is much greater than the data rate of the message. All users use the same carrier frequency and may transmit simultaneously. The receiver performs a correlation operation to detect the signal of the desired user. All other user's signal appear as noise at the output of the correlator. The noise coming from other users are called multiple access interference (MAI).

CDMA systems can tolerate some MAI. Introduction of each additional active user increase the overall level of interference to the other users. Each user introduces a unique level of interference that depends on power level, its timing synchronization relative to other signals in the system, and its specific cross-correlation with other CDMA signals. The tolerance to MAI is not unlimited and as the number of interfering users increases, the equivalent noise results in degradation of performance. Even if the number of users is not too large, some users may be received at such high signal levels that a lower power user may be swamped out. This is the near-far effect: users near the receiver are received at higher powers than those far away, and those further away suffer a degradation in performance.

To combat the near-far problem, power control is used in most CDMA systems. Power control is provided by each base station and assures that each mobile user with the base station coverage area provides the same signal level to the base station receiver. This solves the problem of a nearby user overpowering the base station receiver and drowning out the signals of far away users. Despite the use of power control, the performance and channel capacity DS-CDMA systems are limited by the MAI.

1.1.2 Multicarrier CDMA

The multicarrier CDMA transmitter spreads the original data stream over different subcarriers using a spreading code in the frequency domain. A fraction of the symbol corresponding to a chip of the spreading code is transmitted through a different carrier. In order to ensure that each carrier undergoes flat fading, the number of carrier may be greater than the processing gain. In this case, the original data steam is first converted into several parallel steams. Each parallel data steam is modulated over N (processing gain) carriers. Multicarrier modulation can be performed using inverse discrete Fourier transform (IDFT) which can be implemented very efficiently

with fast algorithms. A proper guard interval is inserted in between different data blocks to eliminate inter block interference. It has been shown [29] that the MC-CDMA has better performance than the DS-CDMA in fading channels.

1.2 Multiuser Detection

Multiuser detection techniques can substantially increase capacity relative to the matched filter receiver. The matched filter treats MAI the same as background Gaussian noise, whereas a multiuser detector exploits the specific structure of MAI. The optimal multiuser receiver proposed by Verdu [97] demonstrates that DS-CDMA is not fundamentally MAI limited and can be near-far resistant. The optimal detector comprises a bank of matched filters followed by a maximum-likelihood (ML) sequence detector whose decision algorithm is the Viterbi algorithm [70]. The computational complexity of the optimal detector grows exponentially with the number of users.

To reduce the complexity, many suboptimal detectors have been proposed. These suboptimal detectors can be put in three categories: nonlinear detector, linear detector and a hybrid of the nonlinear and linear detectors. The nonlinear multiuser detectors include successive interference cancellation (SIC) [40, 43, 67, 100], parallel inference cancellation (PIC) [17, 50, 51, 95, 111], decision-feedback detector [20] and iterative detector [2, 64, 102]. In successive interference cancellation, the users are ordered from strongest to weakest, and are successively demodulated. The interference are removed from users in that order. In parallel interference cancellation, estimated symbols from all users simultaneously regenerate and remove interference for each user. Whereas successive interference cancellation requires a nonuniform distribution of transmitted powers across users to achieve uniform performance across users, parallel interference cancellation is less sensitive to this power distribution. A decision-feedback multiuser detector is analogous to th decision-feedback equalizer for single-user channels. It consists of a linear feedforward filter followed by a feedback

loop which implements successive interference cancellation. That is, the feedback matrix is constrained to be lower-diagonal, so that users are demodulated successively. The iterative multiuser detector is inspired by iterative Turbo decoders [7]. Estimated symbols at the output of the decoder along with reliability information is used to cancel, or partially cancel, interference to other users. The performance of the iterative multiuser detector can reach the single-user bound.

The linear multiuser detector is an important class of suboptimal detector because it is near-far resistant and is easily implemented. The linear multiuser detector includes decorrelator [58, 59, 89] and linear MMSE detector [61, 110]. A decorrelator removes all cross correlations between users, therefore, eliminating multiple access interference. Decorrelators are also shown to be optimally near-far resistant [58]. However, in a manner analogous to zero-forcing equalization, noise enhancement may be a problem. The MMSE detector [61, 110] minimizes the mean squared-error between the transmitted symbol and the output of the detector. MMSE detector has also been shown to be near-far resistant [61]. As the level of background noise tends to be zero, or as energies of interferences increase to infinity, the MMSE linear detector converges to the decorrelating detector.

A combination of the decorrelating detector and PIC was consider in [96], combination of MMSE detector and PIC in [14, 39], and combination of the decorrelating detector and SIC in [19]. In these detectors, a linear multiuser detector is usually first used to generate initial symbol estimates. These estimates are then used in a parallel or successive interference canceler to remove residual interference from the received signal, giving a"cleaned-up" signal. This signal is again input to a linear multiuser detector, giving a refined set of estimates. This procedure can be iterated to improve the estimates further.

1.3 Diversity Techniques

In wireless environment, signal fading arises primarily from multipath propagation of a transmitted signal due to reflections off physical objects. The strength of the fading signal may be very weak due to destructive addition of multipaths in the propagation media. Severe attenuation in signal strength makes it impossible for the receiver to determine the transmitted signal. However, the effects of fading can be substantially mitigated through the use of diversity techniques. Three main forms of diversity are traditionally exploited to varying degrees in wireless communications systems: temporal diversity, spectral diversity, and spatial diversity.

Temporal diversity is effective when the fading is time-selective. Channel coding in conjunction with time interleaving effects temporal spreading of symbols, thereby providing for diversity. *Spectral diversity* is effective when the fading is frequency-selective. This form of diversity can be practically exploited when the available bandwidth for transmission is large enough that individual multipath components can begin to be resolved, or equivalently when it is large enough that different subbands of the transmission bandwidth experience effectively independent fading. In CDMA systems, the signal bandwidth is much larger than the coherent bandwidth of the channel. Thus, CDMA system can take advantage of frequency diversity. *Spatial diversity* involves the use of multiple antennas at either the receiver, the transmitter, or both. The signals received from sufficiently spaced antennas would have essentially uncorrelated envelopes. The receiver perform combining or selection and switching to improve the quality of the received signal.

The use of multiple antennas at the mobile makes the remote units larger and more expensive. It is more economical and feasible to add more antennas to the base stations rather than the remote units. For this reason, transmit diversity schemes are very attractive in a practical system. The early approaches on transmit diversity use signal processing at the transmitter to spread the information across the antennas.

In [108, 109, 104, 77, 107], orthogonal signaling is used at the transmitter. Phase sweeping is employed in [35, 53] so that the received signal is a fast fading signal even the channel is slow fading. The significant gain of the transmit diversity can be realized by view this problem from a coding perspective rather than purely from the signal processing point of view. Recently, Space-time trellis coding [87, 86] and space-time block coding [1, 85] are proposed for transmit diversity. General theory to construct effective space-time codes are given in [32, 36]

1.4 Thesis Overview

In this introductory chapter, we have attempted to review the CDMA systems, multiuser detection and diversity techniques, and thus lay the background for the subject material of this proposal.

Chapter 2 is about the reduced-rank MMSE receiver, the reduced-rank minimum variance receiver and the probability density of conditioned SNR of linear MMSE estimators. In Section 2.1, the reduced-rank MMSE receiver is first developed. Then, performance of the reduced-rank MMSE receiver in terms of the MSE at the output of the receiver is analyzed. Finally, an adaptive reduced-rank MMSE receiver is developed based on a subspace tracking algorithm. In Section 2.2, we start by developing a low-complexity minimum variance (MV) CDMA receiver, and then develop a reduced-rank MV receiver. In section 2.3, the probability density function of conditioned SNR of linear MMSE estimators is studied. These estimators are the full-rank estimator obtained by sample matrix inverse (SMI) method and the reduced-rank estimator obtained by the principal component inverse matrix (PCI) method.

In chapter 3, MC-CDMA systems with transmit diversity is studied. The space-time block code is used to introduce transmit diversity. Our emphasis is put on the design of linear receiver that decodes the space-time code and suppresses

interference. Channel estimation using pilot channels or pilot symbols is studied for the multicarrier CDMA system with space-time coding.

In chapter 4, the system performance of CDMA random access systems with linear receivers and packet combing in multipath fading channels is analyzed. By using packet combing, the receiver obtains a diversity gain and a interference suppression gain. Both the slotted CDMA system and unslotted CDMA system with random spreading signature are considered. The bit error rate of the MMSE receiver, decorrelator and matched filter receiver in fading channels is first calculated, and the system throughput and average delay is then analyzed. Chapter 5 contains concluding remarks and a summary of the thesis.

CHAPTER 2

REDUCED-RANK MINIMUM MEAN SQUARED ERROR RECEIVER AND REDUCED-RANK MINIMUM VARIANCE RECEIVER FOR DS-CDMA SYSTEMS

Minimum mean square error (MMSE) interference suppression methods have been proposed for DS-CDMA systems [61]. It has been shown that such schemes provide potentially large performance gains relative to the conventional matched filter receiver. The blind MMSE receiver in [37] minimizes the receiver's mean output energy (MOE) while constraining the response of the user of interest to a constant. It is shown that MOE and MMSE are directly related and minimizing one is equivalent to minimizing the other.

In [76], linear multiuser detectors for synchronous CDMA are derived within the framework of constrained optimization [44]. In the case of a single constraint that corresponds to knowledge of the desired user's code, the general constrained optimization detector reduces to the MOE detector in [37]. These linear detectors are similar in spirit to the minimum variance beamforming and generalized sidelobe canceler (GSC) in the context of array signal processing [44]. The spreading code of the desired user plays the same role as the steering vector. An extension of the constrained optimization approach to multipath CDMA channels was provided in [88, 90]. It is shown that the performance of the minimum variance receiver with optimal constraints approaches the performance of MMSE receiver at high SNR. The optimal constraint vector can be found by maximizing the output signal power after the interference is suppressed using a min/max approach.

In DS-CDMA systems, the number of active users, K, is usually less than the processing gain, N. Hence, the effective rank r of the noise-free signal covariance matrix is usually less or much less than the signal dimension, N. In this chapter, we explore the low rank nature of the CDMA signal to develop the reduced-rank

MMSE receiver and the reduced-rank minimum variance receiver. The objectives of reduced-rank MMSE receiver include reducing both the computational complexity and the amount of training data that is required for covariance estimation. Reduced-rank processing methods include the multistage Wiener filter (MWF) [27], the cross-spectral metric (CSM) [25, 24], principal components inverse (PCI) [93, 92, 49], eigencanceler [31, 30] and fixed transforms [68]. The effect of the number of data samples in covarinace matrix estimation on the reduced-rank MMSE filter is studied in [49, 68, 10]. Reduced rank multistage Wiener filter and PCI reduced rank MMSE filter have been applied to CDMA system [38, 101]. In this chapter, we will use CSM method to reduce the rank of MMSE receiver and minimum variance receiver. It will be shown that the reduced-rank receiver can outperform full-rank receiver when the covariance matrix is estimated from an finite number of data samples. To further understand the performance of the full-rank and reduced-rank receiver, we study the density function of the conditioned output SNR of the linear MMSE estimators based on a general signal model.

2.1 Reduced-Rank MMSE Receiver

We consider a DS-CDMA system with K users simultaneously transmitting over an additive white Gaussian noise (AWGN) channel. The received baseband signal can be modeled as

$$r(t) = \sum_{k=1}^{K} A_k \sum_{i=-\infty}^{\infty} b_k(i) s_k(t - iT - \tau_k) + n(t) \tag{2.1}$$

where $n(t)$ is AWGN with power spectral density σ^2, A_k is the received signal amplitude from user k, T is the symbol duration, τ_k is relative delay with respect to the receiver, and $s_k(t)$ is the normalized spreading waveform. It is assumed that $\{b_k(i)\}$ is a set of independent equiprobable ± 1 random variables, and that $s_k(t)$ is

supported only on the interval $[0, T]$. Spreading waveform, $s_k(t)$, is expressed as

$$s_k(t) = \frac{1}{\sqrt{N}} \sum_{j=0}^{N-1} s_k[j]\psi(t - jT_c), \qquad t \in [0, T]. \tag{2.2}$$

Here, $\{s_k[0], s_k[1], \ldots s_k[N-1]\}$ is a signature sequence of $\pm 1s$ assigned to the kth user, $\psi(t)$ is a normalized chip waveform of duration T_c, and $N = T/T_c$ is the processing gain.

In this section, we restrict our attention to the synchronous case of model (2.1), in which $\tau_1 = \tau_2 = \ldots = \tau_K = 0$. It is then sufficient to consider the received signal during one symbol duration, and the received signal model becomes

$$r(t) = \sum_{k=1}^{K} A_k b_k s_k(t) + n(t), \qquad t \in [0, T]. \tag{2.3}$$

An asynchronous system of K users can be viewed as equivalent to a synchronous system with $2K - 1$ users [61]. Thus the results of this section apply in this context as well.

Consider the synchronous model (2.3). Sampling the chip-matched filter output at chip rate, we get an $N \times 1$ vector within a symbol interval T

$$\mathbf{r} = \sum_{k=1}^{K} A_k \mathbf{s}_k \mathbf{b} + \mathbf{n}, \tag{2.4}$$

where $\mathbf{s}_k = (1/\sqrt{N})[s_k[0], s_k[1], \ldots s_k[N-1]]^T$ is the normalized signature waveform vector of the kth user, and $\mathbf{n}$ is a white Gaussian noise vector with mean $\mathbf{0}$ and covariance matrix $\sigma^2 \mathbf{I}_N$ ($\mathbf{I}_N$ denotes the $N \times N$ identity matrix). We can also express (2.4) as

$$\mathbf{r} = \mathbf{SAb} + \mathbf{n} \tag{2.5}$$

where $\mathbf{S} = [\mathbf{s}_1, \mathbf{s}_2, \ldots, \mathbf{s}_K]$, $\mathbf{A} = diag(A_k)$ and $\mathbf{b} = [b_1, b_2, \ldots, b_K]$.

2.1.1 Reduced-Rank MMSE Receiver

Suppose the desired user is user 1, a linear multiuser detector for demodulating this user's data bit in (2.5) is in the form of a linear filter followed by a hard limiter

$$\hat{b}_1 = sgn(\mathbf{c}^T\mathbf{r}) \tag{2.6}$$

where $\mathbf{c} \in \mathcal{R}^N$. The linear MMSE detector minimizes the mean-squared error that is given by

$$MSE = E\{(b_1 - \mathbf{c}^T\mathbf{r})^2\} \tag{2.7}$$

It is easily shown that the MMSE solution for $\mathbf{c}$ is

$$\mathbf{c} = \mathbf{C}^{-1}\mathbf{p} \tag{2.8}$$

where $\mathbf{p} = E\{b_1\mathbf{r}\} = A_1\mathbf{s}_1$ is the cross-correlation between b_1 and $\mathbf{r}$, and matrix $\mathbf{C}$ is the covariance matrix of $\mathbf{r}$. We call this detector full-rank MMSE detector. The covariance matrix is given by

$$\mathbf{C} = E\{\mathbf{r}\mathbf{r}^T\} = \mathbf{S}\mathbf{A}\mathbf{A}\mathbf{S}^T + \sigma^2\mathbf{I}_N. \tag{2.9}$$

It can also be expressed in terms of its singular value decomposition

$$\mathbf{C} = \mathbf{U}\mathbf{\Lambda}\mathbf{U}^T = [\mathbf{U}_s \ \mathbf{U}_n] \begin{bmatrix} \Lambda_s & \\ & \Lambda_n \end{bmatrix} \begin{bmatrix} \mathbf{U}_s^T \\ \mathbf{U}_n^T \end{bmatrix} \tag{2.10}$$

where $\mathbf{U} = [\mathbf{U}_s \ \mathbf{U}_n]$, $\Lambda = diag(\Lambda_s, \Lambda_n)$; $\Lambda_s = diag(\lambda_1, \ldots, \lambda_K)$ contains the K largest eigenvalues of $\mathbf{C}$ in descending order and $\mathbf{U}_s = [\mathbf{u}_1 \ \ldots \mathbf{u}_K]$ contains the corresponding orthonormal eigenvectors; $\Lambda_n = \sigma^2\mathbf{I}_{N-K}$ and $\mathbf{U}_n$ contains the $N - K$ orthonormal eigenvectors with the eigenvalue σ^2. The range space of $\mathbf{U}_s$ is called the signal space since it has the same range as $\mathbf{S}$. The range of $\mathbf{U}_n$ is called the noise space.

Since $\mathbf{s}_1$ is orthogonal to the noise space, it is easily shown that the full-rank MMSE detector in (2.8) can also be expressed in terms of the signal space parameters

$$\mathbf{c} = \mathbf{U}_s\Lambda_s^{-1}\mathbf{U}_s^T\mathbf{p} \tag{2.11}$$

and mean-squared error is written as

$$MSE = 1 - \mathbf{p}^T \mathbf{U}_s \Lambda_s^{-1} \mathbf{U}_s^T \mathbf{p}. \tag{2.12}$$

It can be seen from (2.11) that the MMSE detector $\mathbf{c}$ is a vector lying in the signal space. The dimension of the signal space is K, hence, we call this detector rank-K detector. It has the same performance as the full-rank detector because the desired user's signature is orthogonal to the noise space. We will see later that the rank-K detector performs better than the full-rank detector when the covariance matrix is estimated. In the following theorem, we derive the proposed reduced-rank MMSE detector that lies in a subspace of the signal space.

Theorem 1 *Suppose that matrix* $\mathbf{U}_r$ *contains* $r(r \leq K)$ *columns of* $\mathbf{U}_s$ *and* Λ_r *consists of corresponding eigenvalues, and the reduced-rank MMSE detector lies in the range space of* $\mathbf{U}_r$*, then the rank-r MMSE detector* $\mathbf{c}_r$ *is given by*

$$\mathbf{c}_r = \mathbf{U}_r \Lambda_r^{-1} \mathbf{U}_r^T \mathbf{p}, \tag{2.13}$$

and the mean-squared error is found as

$$MSE_r = 1 - \mathbf{p}^T \mathbf{U}_r \Lambda_r^{-1} \mathbf{U}_r^T \mathbf{p}. \tag{2.14}$$

Proof: Let $\mathbf{w} = [w_1, w_2, \ldots, w_r]^T$ and $\mathbf{c}_r = \mathbf{U}_r \mathbf{w}$, then the mean-squared error is calculated by

$$\begin{aligned} MSE_r &= E\{(b_1 - \mathbf{c}_r^T \mathbf{r})^2\} \\ &= \mathbf{c}_r^T \mathbf{C} \mathbf{c}_r - 2\mathbf{c}_r^T \mathbf{p} + 1 \\ &= \mathbf{w}^T \mathbf{U}_r^T \mathbf{C} \mathbf{U}_r \mathbf{w} - 2\mathbf{w}^T \mathbf{U}_r^T \mathbf{p} + 1. \end{aligned} \tag{2.15}$$

Derivative of MSE_r with respect to $\mathbf{w}$ is obtained as

$$\frac{\partial (MSE_r)}{\partial \mathbf{w}} = 2\mathbf{U}_r^T \mathbf{C} \mathbf{U}_r \mathbf{w} - 2\mathbf{U}_r^T \mathbf{p}. \tag{2.16}$$

Letting it be equal to the **0** vector, we get

$$\mathbf{w} = (\mathbf{U}_r^T \mathbf{C} \mathbf{U}_r)^{-1} \mathbf{U}_r \mathbf{p} = \Lambda_r^{-1} \mathbf{U}_r \mathbf{p}. \tag{2.17}$$

Here we use the fact that the eigenvectors are orthonormal. Then the rank-r MMSE detector in (2.13) follows. By substituting $\mathbf{w}$ in (2.17) into (2.15), we get the mean-squared error in (2.14). □

Rank r MMSE detector can also be obtained as follows. The projection matrix for the range space of $\mathbf{U}_r$ is $\mathbf{P}_r = \mathbf{U}_r \mathbf{U}_r^T$. The projection of the received signal to the range of $\mathbf{U}_r$ is $\mathbf{r}_1 = \mathbf{P}_r \mathbf{r}$. Then linear MMSE detector based on $\mathbf{r}_1$ is $\mathbf{c}_{r_1} = \mathbf{C}_1^{-1} \mathbf{p}_1$, where $\mathbf{C}_1$ is the covariance matrix of $\mathbf{r}_1$ and $\mathbf{p}_1$ is the cross-correlation between $\mathbf{r}_1$ and b_1. It is easily shown that $\mathbf{c}_{r_1}$ is the same as $\mathbf{c}_r$ in (2.13).

Comparing (2.14) and (2.12), we can see that the mean-squared error of the reduced-rank detector is not less than that of the rank-K detector. Since the signal to interference ratio for the MMSE detector is given by $SIR = 1/MMSE - 1$ [61], the reduced-rank detector cannot perform better than the full-rank detector. But typically the K user powers are different. Then the desired user may lie in a lower dimensional subspace of the signal space. In this case, if we choose $\mathbf{U}_r$ such that the desired user is in the range of $\mathbf{U}_r$, then the reduced-rank detector has the same performance as the rank-K detector. If the desired user lies in the whole signal space, the reduced-rank detector will perform worse than the rank-K detector. For a given rank, we can choose the subspace in which the reduced-rank MMSE detector lies such that the loss of the performance is minimized. Let us define a quantity Q_i as

$$Q_i = \frac{\mathbf{s}_1^T \mathbf{u}_i \mathbf{u}_i^T \mathbf{s}_1^T}{\lambda_i} = \frac{\| \mathbf{s}_1^T \mathbf{u}_i \|^2}{\lambda_i}. \tag{2.18}$$

Q_i can be viewed as the normalized energy of user 1 projected onto the ith base. Then MMSE in (12) can also be expressed as

$$MSE = 1 - A_1^2 \sum_{i=1}^{K} Q_i. \tag{2.19}$$

Therefore, given the rank of the detector, r, the optimal rank-r MMSE detector is obtained by forcing the detector to lie in the subspace spanned by the r basis corresponding to r largest Q_i. Note that the proposed subspace selection makes use of the signature of the desired user. This method of choosing subspace is similar to the cross spectral metric (CSM) approach [26] for subspace selection in the context of a generalized sidelobe canceler.

In practice, the covariance matrix $\mathbf{C}$ is unknown. It is estimated from the received signal. A commonly used estimation is the sample covariance matrix that is the maximum likelihood estimate of the covariance matrix under the Gaussian assumption. The eigenvectors and eigenvalues of the estimated covariance matrix are different from those of the true covariance matrix. The MMSE detector is obtained from the estimated eigenvectors and eigenvalues. We will see later that the reduced-rank MMSE detector lying in proper subspace performs better than both the rank-K detector and the full-rank detector. This is the major advantage of the reduced-rank MMSE detector.

2.1.2 Performance Analysis

In this section, we analyze the performance of the reduced-rank MMSE detectors in terms of the mean-squared error at the output of the detectors. The reduced-rank MMSE detectors are obtained from the estimated covariance matrix. We first briefly review the asymptotic statistics of the eigenvalues and eigenvectors computed from the sample covariance matrix. When M samples of data vector $\{\mathbf{r}_m, m = 1, \ldots, M\}$ are available, the covariance matrix can be estimated by

$$\hat{\mathbf{C}} = \frac{1}{M} \sum_{m=1}^{M} \mathbf{r}_m \mathbf{r}_m^T \tag{2.20}$$

Let $\hat{\lambda}_i$ and $\hat{\mathbf{u}}_i$ denote the ith eigenvalue and corresponding eigenvector computed from the sample covariance matrix $\hat{\mathbf{C}}$. We defined $\Delta\lambda_i = \hat{\lambda}_i - \lambda_i$ and $\Delta\mathbf{u}_i = \hat{\mathbf{u}}_i - \mathbf{u}_i$. Assuming that all elements of $\{\Delta\lambda_i, i = 1, \ldots, K\}$ are distinct. We know from

[3] that $\{\Delta\lambda_i, \Delta\mathbf{u}_i, i = 1, \ldots, K\}$ is asymptotically normal with zero mean, and $\{\Delta\lambda_i, i = 1, \ldots, K\}$ is asymptotically independent of $\{\Delta\mathbf{u}_i, i = 1, \ldots, K\}$. Elements of $\{\Delta\lambda_i, i = 1, \ldots, K\}$ are mutually independent. The variance of $\Delta\lambda_i$ is $\sigma_i^2 = 2\lambda_i^2/M$. The covariances of $\{\Delta\mathbf{u}_i, i = 1, \ldots, K\}$ in the limiting distribution are given by [3]

$$\mathbf{E}_{ij} = Cov(\Delta\mathbf{u}_i, \Delta\mathbf{u}_j) = \begin{cases} \frac{1}{M}\sum_{\substack{n=1 \\ n\neq i}}^{N} \frac{\lambda_i\lambda_n}{(\lambda_i - \lambda_n)^2}\mathbf{u}_n\mathbf{u}_n^T & i = j \\ -\frac{\lambda_i\lambda_j}{M(\lambda_i-\lambda_j)^2}\mathbf{u}_j\mathbf{u}_i^T & i \neq j \end{cases} \tag{2.21}$$

Let us denote the rank-r MMSE detector obtained from the estimated covariance matrix as $\hat{\mathbf{c}}_r$. It is a random vector depending on the estimated eigenvalues and eigenvectors. And the mean-squared error conditioned on $\hat{\mathbf{c}}_r$ is also a random variable. Our objective is to get the mean of the conditioned mean-squared error. The approach is based on a second-order Taylor series expansion of the conditional mean-squared error.

The mean-squared error conditioned on $\hat{\mathbf{c}}_r$ is given by

$$\widehat{MSE}_r = 1 + \hat{\mathbf{c}}_r^T\mathbf{C}\hat{\mathbf{c}}_r - 2\hat{\mathbf{c}}_r^T\mathbf{p}. \tag{2.22}$$

The second-order Taylor series expansion of $\widehat{MSE}_r$ around the point P=$\{\mathbf{u}_i, \lambda_i, i = 1, \ldots, r\}$ is given by

$$\begin{aligned} \widehat{MSE}_r \;=\; & MSE_r + \sum_{i=1}^{r}\Delta\mathbf{u}_i^T\mathbf{g}_i + \sum_{i=1}^{r}\Delta\lambda_i f_i + \frac{1}{2}\sum_{i=1}^{r}\sum_{j=1}^{r}\Delta\lambda_i\Delta\mathbf{u}_i^T\mathbf{h}_{ij} + \\ & \frac{1}{2}\sum_{i=1}^{r}\sum_{j=1}^{r}\Delta\lambda_i\Delta\lambda_j F_{ij} + \frac{1}{2}\sum_{i=1}^{r}\sum_{j=1}^{r}\Delta\mathbf{u}_i^T\mathbf{H}_{ij}\Delta\mathbf{u}_j. \end{aligned} \tag{2.23}$$

where vector $\mathbf{g}_i$ is the gradient of $\widehat{MSE}_r$ along $\hat{\mathbf{u}}_i$ at point P; f_i is the first partial derivative of $\widehat{MSE}_r$ with respect to $\hat{\lambda}_i$ at point P; F_{ij} is the second partial derivative of $\widehat{MSE}_r$ with respect to $\hat{\lambda}_i$ and $\hat{\lambda}_j$ at point P; and the elements of the vector $\mathbf{h}_{ij}$ and matrix $\mathbf{H}_{ij}$ are given by

$$[\mathbf{h}_{ij}]_m = \frac{\partial^2\widehat{MSE}_r}{\partial\hat{\lambda}_i\partial\hat{\mathbf{u}}_j(m)}|_P, \tag{2.24}$$

$$[\mathbf{H}_{ij}]_{mn} = \frac{\partial^2 \widehat{MSE}_r}{\partial \hat{\mathbf{u}}_i(m) \partial \hat{\mathbf{u}}_j(n)}|_P. \tag{2.25}$$

Take expectation of $\widehat{MSE}_r$ with respect to $\{\Delta\lambda_i, \Delta\mathbf{u}_i, i = 1, \ldots, r\}$, we have

$$\widetilde{MSE}_r = MSE_r + \frac{1}{2}\sum_{i=1}^{r} \sigma_i^2 F_{ii} + \frac{1}{2}\sum_{i=1}^{r}\sum_{j=1}^{r} tr(\mathbf{H}_{ij}\mathbf{E}_{ji}) \tag{2.26}$$

where $tr(\cdot)$ denotes the trace of the matrix in the parenthesis. Here we use the fact that the means of $\Delta\lambda_i$ and $\Delta\mathbf{u}_i$ are zero and the elements of $\{\Delta\lambda_i, i = 1, \ldots, r\}$ are mutually independent and $\{\Delta\lambda_i, i = 1, \ldots, r\}$ is independent of $\{\Delta\mathbf{u}_i, i = 1, \ldots, r\}$. F_{ii} and $\mathbf{H}_{ij}$ can be found as

$$F_{ii} = \frac{2(p^T\mathbf{u}_i)^2}{\lambda_i^3}, \tag{2.27}$$

$$\mathbf{H}_{ij} = \frac{2}{\lambda_i\lambda_j}\mathbf{X}_i^T\mathbf{C}\mathbf{X}_j \quad i \neq j, \tag{2.28}$$

and

$$\mathbf{H}_{ii} = \frac{2}{\lambda_i^2}\mathbf{X}_i^T\mathbf{C}\mathbf{X}_i + \frac{2}{\lambda_i}[\mathbf{Y}_1\mathbf{C}\mathbf{c}_r, \ldots, \mathbf{Y}_N\mathbf{C}\mathbf{c}_r] - \frac{4}{\lambda_i}\mathbf{W} \tag{2.29}$$

where $\mathbf{X}_i = \mathbf{u}_i\mathbf{p}^T + \mathbf{p}^T\mathbf{u}_i\mathbf{I}_N$, $\mathbf{Y}_j = \mathbf{P}_j + \mathbf{p}(j)\mathbf{I}_N$ and the ith column of matrix $\mathbf{W}$ is $\mathbf{p}(i)\mathbf{p}$. Derivation of F_{ii} and $\mathbf{H}_{ij}$ is given in Appendix A.

2.1.3 Adaptive Reduced-Rank MMSE Receiver Based on a Subspace-Tracking Algorithm

To implement the low-rank MMSE detector, we need to estimate the eigenvectors of the covariance matrix corresponding to the signal space and the corresponding eigenvalues. This can be achieved by using singular value decomposition (SVD) or eigenvalue decomposition (EVD) of the data sample covariance matrix. Classical batch EVD and batch SVD algorithms [28] are computationally demanding. In order to overcome this difficulty, a number of adaptive algorithms for subspace tracking has been developed [18, 80, 113]. In [101], the projection approximation subspace tracking (PASTd) algorithm in [113] is used for blind adaptive multiuser detection. The PASTd algorithm has low computational complexity ($O(NK)$).

However, its convergence speed is very slow. To choose the optimal rank for the proposed low-rank MMSE detector, we need the orthogonal eigenvectors. However, the basis for the signal subspace tracked by PASTd are not orthogonal. In this work, we use the subspace tracking algorithm in the low-rank adaptive filter named LORAF 1 in [80]. The subspace tracking algorithm in LORAF 1 has computational complexity of $O(NK^2)$. There is another lower complexity ($O(NK)$) subspace tracking algorithm in LORAF 3 in [80]. However, we observed in simulations that it has very low convergence speed. In contrast, the subspace tracking algorithm in LORAF 1 converges fast in simulations. In a CDMA system, users enter or leave the system randomly. Therefore, the signal space changes. We need a fast convergence algorithm to track variations of the signal space. The subspace tracking algorithm in LORAF 1 assumes a known signal space dimension. It cannot track the rank of the signal covariance matrix. In this work, we combine the rank tracking method in [112] into the subspace tracking algorithm in LORAF 1. We next briefly review the adaptive algorithm for both rank and subspace tracking.

Denote covariance matrix at time t as $\mathbf{C}_t$. Define an $N \times K$ matrix $\mathbf{U}_0$ with orthonormal columns. The following orthogonal iteration [28] generates a sequence of matrix $\{\mathbf{U}_t\}$:

$$\mathbf{A}_t = \mathbf{C}_t\mathbf{U}_{t-1} \tag{2.30}$$

$$\mathbf{A}_t = \mathbf{U}_t\mathbf{R}_t \tag{2.31}$$

where $\mathbf{U}_t$ and $\mathbf{R}_t$ are the factors of a skinny QR decomposition of matrix $\mathbf{A}_t$. Assuming that $\mathbf{C}_t$ does not change in time, one can show [28] that the sequence of recursion matrix $\{\mathbf{U}_t\}$ will converge towards the matrix of dominant eigenvectors. Likewise, the sequence of the triangular matrix $\{\mathbf{R}_t\}$ will converge towards the diagonal matrix of dominant eigenvalues. In our case, $\mathbf{C}_t$ is defined by $\mathbf{C}_t = \sum_{i=1}^{t} \beta^{t-i}\mathbf{r}_i\mathbf{r}_i^T$ where $0 < \beta \leq 1$. $\mathbf{C}_t$ is updated recursively according to $\mathbf{C}_t =$

$\beta \mathbf{C}_{t-1} + \mathbf{r}_t \mathbf{r}_t^T$. A key step [80] towards the fast subspace tracking algorithm is the orthogonal projection of the actual recursion matrix $\mathbf{U}_t$ onto the previous subspace spanned by the columns of $\mathbf{U}_{t-1}$. Thus, we have

$$\mathbf{U}_t = \mathbf{U}_{t-1}\Theta_t + \Delta_t \tag{2.32}$$

where $\Theta_t = \mathbf{U}_{t-1}^T \mathbf{U}_t$ and Δ_t is orthogonal to the column space of $\mathbf{U}_{t-1}$. The update equation (40) become

$$\mathbf{A}_t = \beta \mathbf{A}_{t-1}\Theta_{t-1} + \mathbf{r}_t \mathbf{z}_t^T + \beta \mathbf{C}_{t-1}\Delta_{t-1} \tag{2.33}$$

where $\mathbf{z}_t^T = \mathbf{U}_{t-1}^T \mathbf{r}_t$. Only the last term requires $O(N^2K)$ operations but it can be neglected without any performance penalty [80]. This results in the $O(Nr^2)$ recursion for a direct updating of matrix $\mathbf{A}_t$:

$$\mathbf{A}_t = \beta \mathbf{A}_{t-1}\Theta_{t-1} + \mathbf{r}_t \mathbf{z}_t^T \tag{2.34}$$

The fast subspace tracking algorithm consists of equations (2.31) and (2.34). We can modify this algorithm to track both the rank and the signal space as follows. Suppose that the rank is K, and we track $K+1$ dominant eigenvectors and eigenvalues. Based on the estimated eigenvalues, one can estimate the rank of the signal space using information-theoretic criteria such as the Akaike information criterion (AIC)[103]. Suppose the estimated rank is r. If $r < K$, remove the last $K - r$ columns from matrix $\mathbf{U}_t$. If $r > K$, add a vector $\mathbf{x}$ to matrix $\mathbf{U}_t$ as its last column. Vector $\mathbf{x}$ can be obtained by projecting the data vector $\mathbf{r}_t$ onto orthogonal subspace of column span of $\mathbf{U}_t$. The quantity AIC is defined as follows:

$$AIC(k) = (N-k)L\ ln(\alpha(k)) + k(2N-k) \tag{2.35}$$

where $L = 1/(1-\beta)$ and $\alpha(k)$ is defined as

$$\alpha(k) = \frac{(\sum_{i=k+1}^{N} \hat{\lambda}_i)/(N-k)}{(\prod_{i=k+1}^{N} \hat{\lambda}_i)^{1/(N-k)}} \tag{2.36}$$

The estimate of rank is given by the value of k that minimizes the quantity (2.35).

After the eigenvectors and corresponding eigenvalues are estimated, we can construct the optimal low-rank MMSE detector. Assume that the receiver knows the signature of the desired user, $\mathbf{s}_1$, the estimate of quantity $\hat{Q}_i$ in (2.18) is $\hat{Q}_i = \frac{\|\mathbf{s}_1^T \hat{\mathbf{u}}_i\|^2}{\hat{\lambda}_i}$. The optimal rank-$r$ MMSE detector, $\hat{\mathbf{c}}_r$, is obtained using the r eigenvectors and eigenvalues corresponding to r largest $\hat{Q}_i$. Applying the previous data to each of K low-rank detectors, $\{\hat{\mathbf{c}}_i, i = 1, \ldots, K\}$, we can estimate the mean-squared error at the output of each low-rank detector. The optimal low-rank MMSE detector is the one having the smallest mean-squared error. When we estimate the mean-squared error, the detector can operate either in the training mode or the decision-directed mode. Finally, the proposed adaptive algorithm for the low-rank MMSE detector is summarized in Table I.

2.1.4 Numerical and Simulation Results

In this section, we provide some simulation examples to demonstrate the performance of the reduced-rank MMSE detector developed in section 2.1.1. Rank-r MMSE detector lies in the subspace spanned by r eigenvectors corresponding to r largest Q_i (Q_i is defined in (2.18)). We also give the analytical results using the technique developed in section 2.1.2. We use Gold sequence as the spreading sequence. The desired user is user 1. The performance measure for simulation is the signal to interference ratio (SIR) versus the rank of the MMSE detectors. Since the distribution of the output of the linear MMSE detector is approximately Gaussian [69], the output SIR translates easily into an equivalent error probability. For the fixed data bits of the desired user, SIR is defined as $SIR = E^2\{\mathbf{c}_r^T \mathbf{r}\}/Var\{\mathbf{c}_r^T \mathbf{r}\}$, where the expectation is with respect to the data bits of MAI's and the noise. When the covariance matrix is known, i.e. the signatures and the amplitudes of all the users are known, SIR is

Table 2.1 The Adaptive Algorithm for the Reduced-Rank MMSE Detector

Initialize the algorithm: $\mathbf{U}_0 = [\frac{\mathbf{I}}{\mathbf{0}}]; \theta_0 = \mathbf{I}; \mathbf{A} = \mathbf{0}; K_0 = N; \beta = 0.995; \sigma_0^2 = 0; N_{mse} = 10$

Update the eigenvalues and eigenvectors of signal subspace $\{\lambda_k\}_{k=1}^{K(t)}$ and $\mathbf{U}(t)$

$\mathbf{h}_t = \mathbf{U}_{t-1}^T \mathbf{r}_t$
$\mathbf{A}_t = \beta \mathbf{A}_{t-1} \theta_{t-1} + \mathbf{r}_t \mathbf{h}_t^T$
$\mathbf{A}_t = \mathbf{U}_t \mathbf{R}_t$: QR factorization
$\theta_t = \mathbf{U}_{t-1}^T \mathbf{U}_t$
$\mathbf{x} = \mathbf{r}_t - \mathbf{U}_t \mathbf{U}_t^T \mathbf{r}_t$
$\sigma_t^2 = \beta \sigma_{t-1}^2 + \mathbf{x}^T \mathbf{x}/(N - K_{t-1})$

Update the rank of signal subspace K_t

FOR $k = 1 : K_{t-1}$ DO
  $\alpha(k) = [\sum_{i=k+1}^{N} \lambda_i^t/N - k]/(\prod_{i=k+1}^{N} \lambda_i^t)^{\frac{1}{N-k}}$
  $AIC(k) = (N-k) ln[\alpha(k)]/(1-\beta) + k(2N-k)$
END
  K_t=arg $\min_{0 \le k \le N-1} AIC(k) + 1$
IF $K_t < K_{t-1}$ THEN
  $\mathbf{U}_t = \mathbf{U}_t(:, 1:r)$
  $\mathbf{A}_t = \mathbf{A}_t(:, 1:r)$
  $\theta_t = \theta_t(1:r, 1:r)$
ELSE IF $K_t > K_{t-1}$ THEN
  $K_t = K_{t-1} + 1$
  $\mathbf{U}_t = [\mathbf{U}_t, \mathbf{x}/\sigma_t^2]$
  $\mathbf{A}_t = [\mathbf{A}_t, \mathbf{x}]$
  $\theta_t = [\frac{\theta_t}{\mathbf{0}} \frac{\mathbf{0}}{1}]$
END

Choose the best reduced-rank MMSE detector $\mathbf{c}_l$

calculate $\{Q_i\}_{i=1}^{K_{t-1}}$, generate a matrix $\mathbf{V}$ whose first column is $\mathbf{u}_i$ corresponding to the largest $\{Q_i\}_{i=1}^{K_{t-1}}$ and second column is $\mathbf{u}_i$ corresponding to the second largest $\{Q_i\}_{i=1}^{K_{t-1}}$ and so on. η_i is the eigenvalue corresponding to $\mathbf{v}_i$
$\mathbf{c}_0 = \mathbf{0}$
FOR $k = 1 : K_t - 1$ DO
  $\mathbf{c}_k = \mathbf{c}_{k-1} + \mathbf{V}(:, k) \mathbf{V}(:, k)^T \mathbf{p}/\eta_k$
  $MSE(k) = 0$
  FOR $i = 1 : N_{mse}$ DO
    $MSE(k) = MSE(k) + (\hat{b}(t-i) - \mathbf{c}_k^T \mathbf{r}_{t-i})^2$
  END
END
$\mathbf{c}_l$=arg $\min_{\{\mathbf{c_k}\}} MSE(k)$
$\hat{b}(t) = sgn(\mathbf{c}_l^T \mathbf{r}_t)$

given by

$$SIR = \frac{(A_1 \mathbf{c}_r^T \mathbf{s}_1)^2}{\sigma^2 \parallel \mathbf{c}_r \parallel^2 + \sum_{i=2}^{K} (A_i \mathbf{c}_r^T \mathbf{s}_i)^2}. \tag{2.37}$$

In simulations, the expectation operation is replaced by the time averaging operation. In analysis, the performance measure is mean-squared error (MSE) versus the rank of the detectors. The input SNR (SNR is defined as A_1^2/σ^2) of the desired user is $20dB$.

Example 1: Simulation of a single user system

We first consider the single user case. The processing gain is $N = 31$. The simulated performance is plotted in Fig. 2.1. The data plotted are averaged over 400 independent simulations. Since the noise-free signal has rank 1, performances of all the detectors with different ranks are the same when the covariance matrix is known. When the covariance matrix is estimated, we see that the rank-1 detector has the best performance. If we use more basis other than the one corresponding to the largest $Q_i, i = 1, \ldots, N$ to construct the detector, we get more noise than the desired signal at the output of the detector. Therefore, the performance degrades. We can also see that the number of samples, M, used to estimate the covariance matrix affects the performance of the rank-r ($r > 1$) detector. For example, when $M = 400$, SIR at the full-rank detector output is $11.1dB$. When $M = 1000$, it is about $14dB$.

Example 2: Simulation of 10 user systems

We next consider 10 user cases. The processing gain is $N = 31$. The data plotted are the average over 400 independent simulations. In Fig. 2.2, nine interference users' SNRs are 10dB. This may be the case in which there is only one user in the cell but there exist inter-cell interferences. The signature of the desired user lies in a subspace whose dimension is 2 and most of its energy is in a one-dimensional subspace. Therefore, when the covariance matrix is estimated, the rank-1 detector

has the best performance. In Fig. 2.3, there are five weak interferences and four strong interferences. The rank-2 detector has the best performance. Fig. 2.4 is for the perfect power control case where nine interference users have the same power as the desired user. In this case, rank-K detector has the best performance since the signature of the desired user is in the whole signal space. All of the simulations show that the detectors whose rank is greater than K perform worse than the optimal reduced-rank detector.

Example 3: Comparison of simulation and analytical results

In this example, we compare the simulation results with the analytical results. The processing gain is $N = 31$. There are 10 users in the system. The number of samples used to estimate the covariance matrix is 1000. SNRs of different users are chosen to be different in order to make the ten largest eigenvalues of the covariance matrix be different which is necessary in analysis. The simulation results are the average over 2000 independent runs. In Fig. 2.5 and Fig. 2.6, most of the energy of the desired user is in a low dimensional subspace. Hence, when the detector is obtained from the estimated covariance matrix, both the simulation results and the analytical results show a reduced-rank detector has better performance than the rank-K detector. But when covariance matrix is known, rank-K has the best performance as expected. This shows the advantage of the reduced-rank MMSE detector when the covariance matrix is unknown. In Fig. 2.7, interferences' powers are close to that of the desired user. The signature of the desired user is in the whole signal space. Therefore, the rank-K detector has the best performance.

Example 4: Performance simulation of the adaptive reduced-rank MMSE detector

Finally, we use the adaptive algorithm developed in Section 4 to simulate the performance of the adaptive reduced-rank detector in a dynamic multiple-access channel. The simulation results are displayed in Fig. 2.8. At $t = 0$, there are 10

users in the channel. The desired user's SNR is 20 dB. There are six 10-dB users, one 20-dB user, one 30-dB user, one 40-dB user. At $t = 2000$, a 40-dB user enters the channel; at $t = 4000$, the two 40-dB users exit the channel. The processing gain is $N = 31$. The forgetting factor is $\beta = 0.995$. The data plotted are the average over 400 independent simulations. The first 100 iterations are in the training mode and the rest are in the decision directed mode. The ten previous bits are used to estimate the mean-squared error. We see that the optimal reduced-rank detector has approximate 2dB advantage over the rank-K detector. The adaptive algorithm has a fast convergence speed.

2.2 Reduced-Rank Minimum Variance Receiver

In this section, we consider the reduced-rank minimum variance (MV) receiver. The advantage of minimum variance receiver relative to the MMSE receiver is that the MV receiver can be implemented blindly. The MV receiver only needs know the signature and the timing of the desired user. Its performance is close to the MMSE receiver. In adaptive implementation of the optimal minimum variance receiver [90], the optimal constraint vector is difficult to track. Furthermore, in complex multipath channels, there is a phase ambiguity in the optimal constraint vector. Therefore, the transmitted data should be differentially encoded. The phase ambiguity can be resolved by differential decoding. In this section, we propose a RAKE receiver followed by an equal gain combiner. The impulse response of the filter in each finger is obtained by the minimum variance criterion. The noise at the output of the RAKE receiver is approximately white. The transmitted data are differentially encoded. Thus, we can use a simple equal gain combiner to collect all the energy of the desired user. Every finger of the RAKE receiver is implemented adaptively with the same structure as a GSC. A subspace tracker tracks the signal space of the data in the low-branch of the GSC. Based on the tracked signal space, every finger of the RAKE

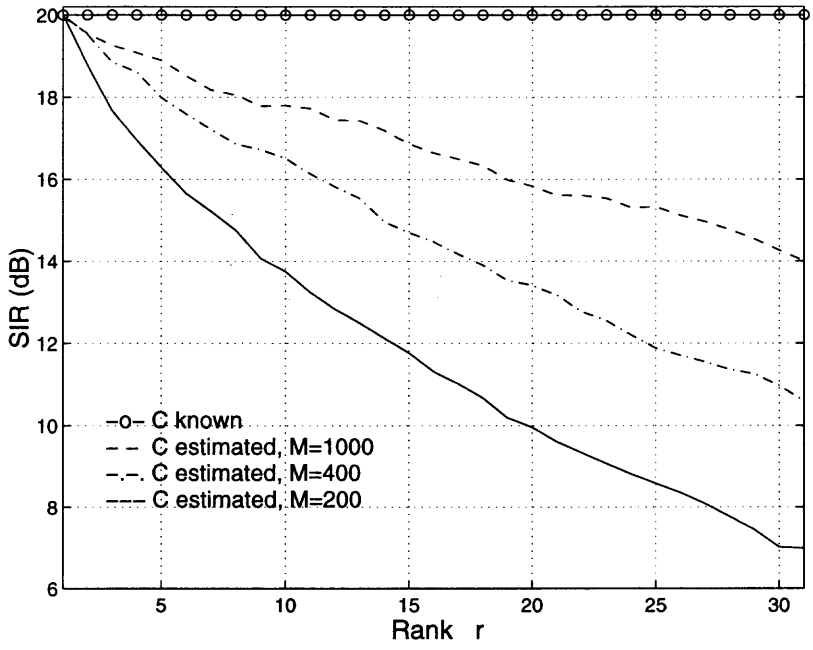

Figure 2.1 SIR of the MMSE detectors. N=31, K=1, SNR=20dB.

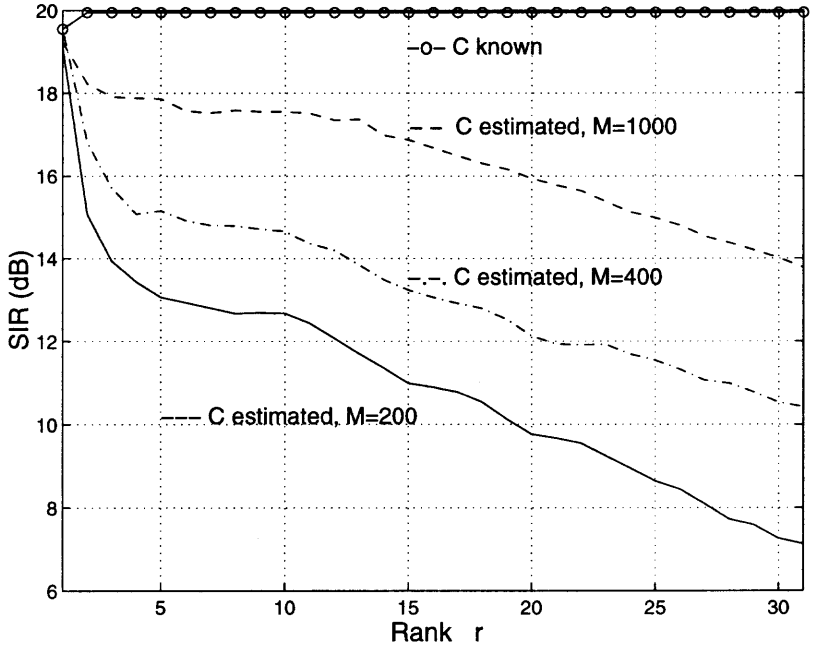

Figure 2.2 SIR of the MMSE detectors. N=31, K=10, SNR=20dB, (K-1) interferences' SNRs 10dB .

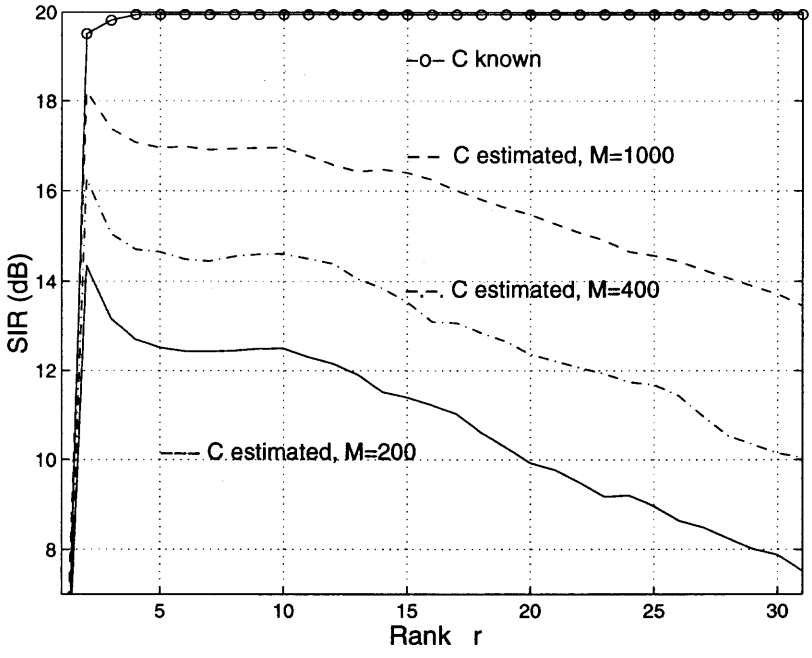

Figure 2.3 SIR of the MMSE detectors. N=31, K=10, SNR=20dB, (K-1) interferences' SNRs are 10dB, 10dB, 10dB, 10dB, 10dB, 20dB, 30dB, 30dB, 40dB.

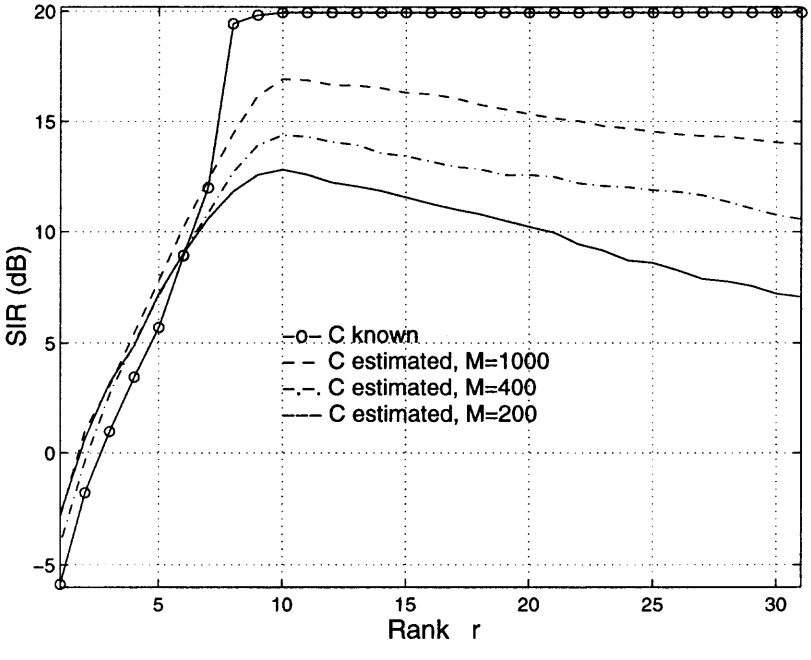

Figure 2.4 SIR of the MMSE detectors. N=15, K=10, SNR=20dB, (K-1) interferences' SNRs are 20dBs.

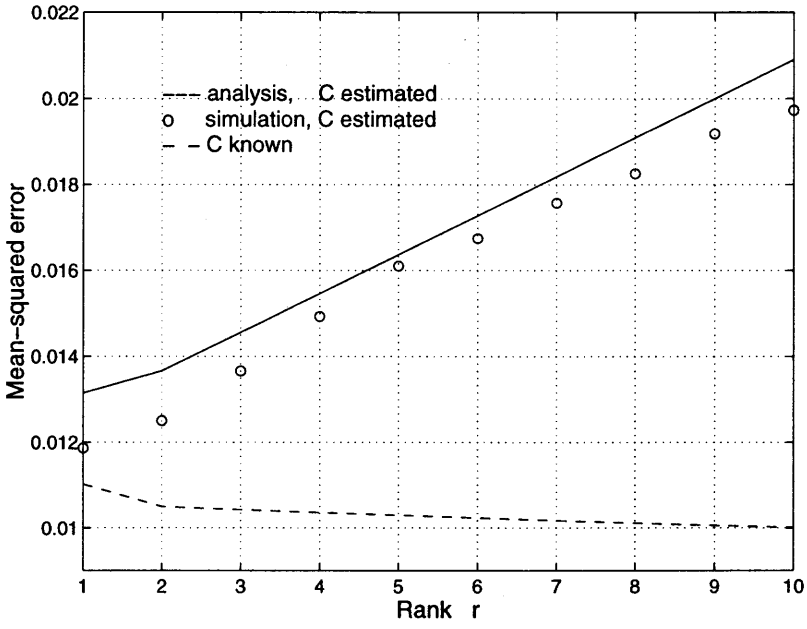

Figure 2.5 MSE of the MMSE detectors. N=31, K=10, SNR=20dB. K-1 interference users' SNRs are 8.4dB, 8.8dB, 9.2dB, 9.6dB, 10dB, 10.4dB, 10.8dB, 11.2dB, 11.6dB.

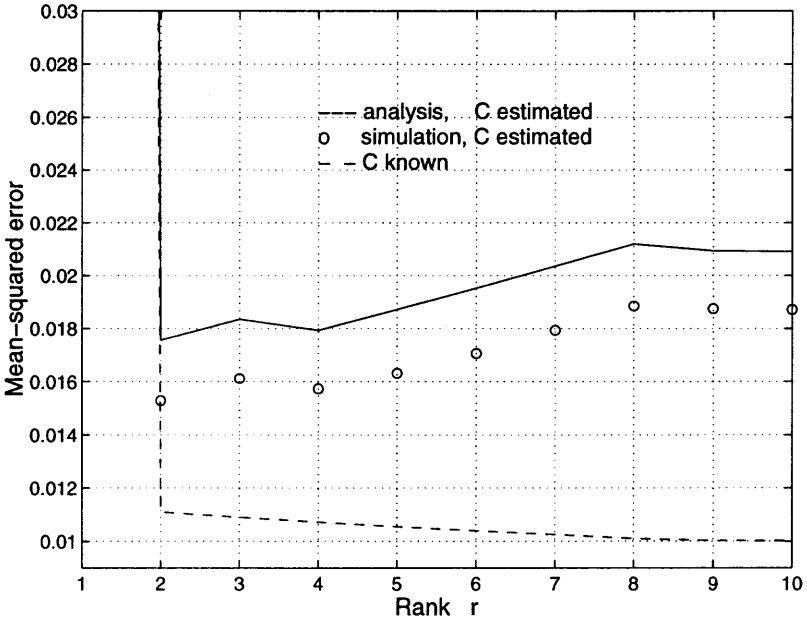

Figure 2.6 MSE of the MMSE detectors. N=31, K=10, SNR=20dB. K-1 interference users' SNRs are 8dB, 9dB, 10dB, 11dB, 12dB, 20dB, 30dB, 31dB, 40dB.

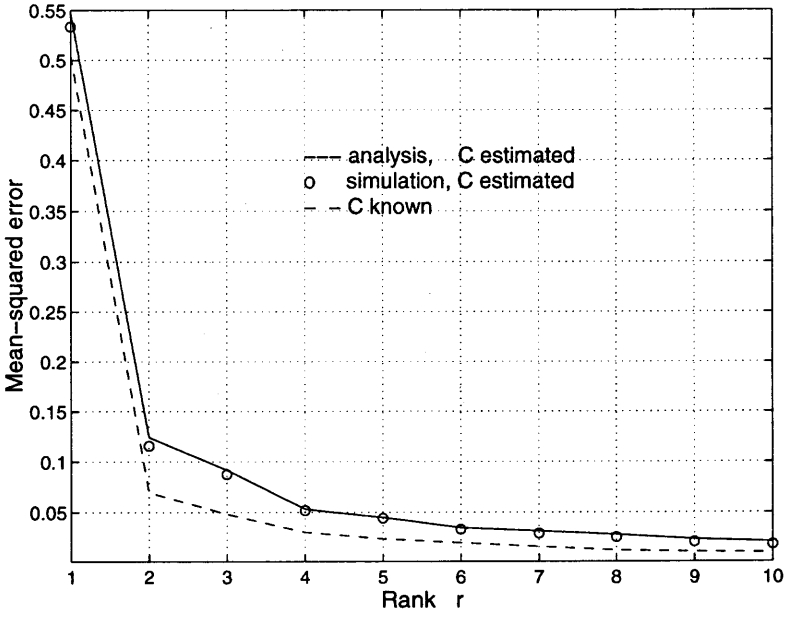

Figure 2.7 MSE of the MMSE detectors. N=31, K=10, SNR=20dB, K-1 interference users' SNRs are 16dB, 17dB, 18dB, 19dB, 20dB, 21dB, 22dB, 23dB, 24dB.

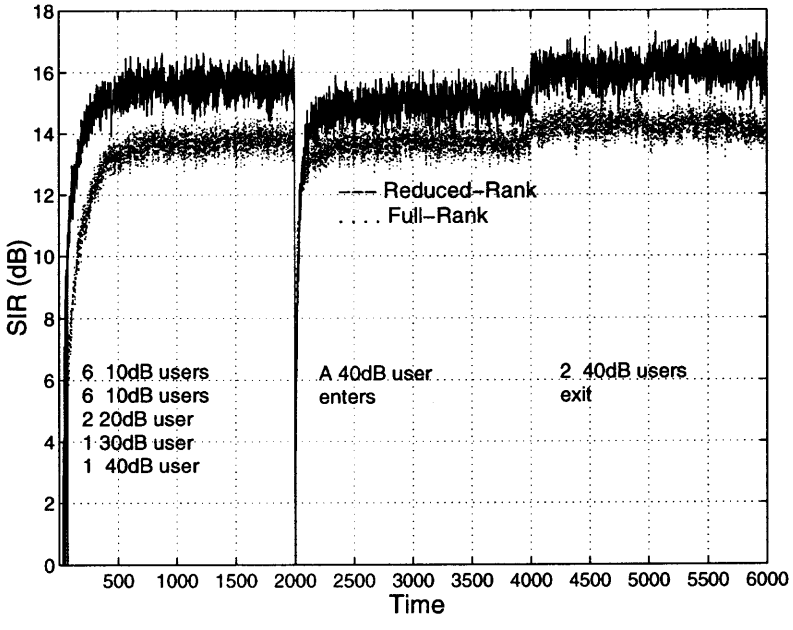

Figure 2.8 Performance of the adaptive reduced-rank MMSE detector in a dynamic multiple-access channel The processing gain is N=15. The forgetting factor is $\beta = 0.995$.

T

receiver chooses a subspace of the signal space to form the reduced-rank receiver. Since we need only one subspace tracker for all the fingers and constraint vectors are fixed, the computation complexity of the proposed receiver is much lower than that of the minimum variance receiver with the optimal constraints. Simulations demonstrate that the performance of the proposed receiver is almost the same as that of the minimum variance receiver with the optimal constraints. When the covariance matrix is estimated, the optimal reduced-rank receiver outperforms the full-rank receiver.

2.2.1 A Low-Complexity Minimum Variance Receiver

We consider a DS-CDMA system with K users simultaneously transmitting through their respective multipath channels with additive white Gaussian noise (AWGN). The transmitted signal due to the kth user is given by

$$x_k(t) = \sum_{i=-\infty}^{\infty} b_k[i] A_k s_k(t - iT - \tau_k) \tag{2.38}$$

where A_k is the signal amplitude, T is the symbol duration, τ_k is relative delay with respect to the receiver, and $s_k(t)$ is the normalized spreading waveform given in (2.2).

The kth user's signal propagates through a multipath channel with the complex impulse response $g_k(t)$. At the receiver, the received signal is first filtered by a chip matched filter and then sampled at the chip rate. Thus impulse response of the composite channel is $\bar{g}_k(t) = \psi(t - \tau_k) * g_k(t) * \psi(t)$ and the discrete-time channel is $\bar{g}_k[n] = \bar{g}_k(nT_c), n = 0, \ldots, q-1$, where q is the length of the channel impulse response. Let $h_k[n] = \sum_{i=-\infty}^{\infty} s_k[i] * \bar{g}_k[n-i]$. The lth sample of the signal component due to the kth user is

$$y_k[l] = \sum_{i=-\infty}^{\infty} b_k[i] h_k[l - iN]. \tag{2.39}$$

For making a decision on the nth symbol of the desired user, we consider a vector $\mathbf{y}[n] \in C^{N+q}$ corresponding to the nth observation interval. Let $d_k = \lfloor \tau_k / T_c \rfloor$

where $\lfloor x \rfloor$ denotes the largest integer that is smaller than x. As in [60], let $\mathbf{T}_L$ denote the acyclic left shift operator, and $\mathbf{T}_R$ denote the acyclic right shift operator, both on vectors of length $N+q$. Thus, for a vector $\mathbf{x} = [x_0, \ldots, x_{N+q-1}]^T$, we have $\mathbf{T}_L\mathbf{x} = [x_1, \ldots, x_{N+q-1}, 0]^T$ and $\mathbf{T}_R\mathbf{x} = [0, x_0, \ldots, x_{N+q-2}]^T$. Let $\mathbf{T}_L^n$, $\mathbf{T}_R^n$, denote n applications of these operators, resulting in left and right shifts by n, respectively. Let $\mathbf{h}_k[0] = \mathbf{T}_R^{d_k}\mathbf{h}_k$, $\mathbf{h}_k[-1] = \mathbf{T}_L^{N-d_k}\mathbf{h}_k$ and $\mathbf{h}_k[+1] = \mathbf{T}_R^{N+d_k}\mathbf{h}_k$. Then the signal vector due to the *kth* user is

$$\mathbf{y}_k = b_k[n]\mathbf{h}_k[0] + b_k[n-1]\mathbf{h}_k[-1] + b_k[n+1]\mathbf{h}_k[+1]. \tag{2.40}$$

The total signal vector is given by

$$\mathbf{y}[n] = \sum_{k=1}^{K} \mathbf{y}_k[n] + \mathbf{u}, \tag{2.41}$$

where $\mathbf{u}$ is a complex AWGN vector with covariance $\sigma^2\mathbf{I}$.

A linear receiver is a correlator $\mathbf{w}$ that produces the following statistic for the nth symbol: $z[n] = \mathbf{w}^T\mathbf{y}[n]$. The minimum variance approach selects the correlator $\mathbf{w}$ by minimizing the output power $E\{z^2[n]\}$ subject to a set of constraints [44] :

$$min\ \mathbf{w}^H\mathbf{R}_y\mathbf{w} \quad subject\ to \quad \mathbf{C}\mathbf{w} = \mathbf{f} \tag{2.42}$$

where $\mathbf{R}_y = E\{\mathbf{y}[n]\mathbf{y}^H[n]\}$ is the data covariance matrix. $\mathbf{C}$ is a matrix whose rows specify the constraints, $\mathbf{f}$ is the constraint vector. As shown in [44], the optimal solution to this problem is $\mathbf{w}_o = \mathbf{R}_y^{-1}\mathbf{C}^H(\mathbf{C}\mathbf{R}_y^{-1}\mathbf{C}^H)^{-1}\mathbf{f}$.

Suppose that the desired user is user 1, the $q \times (N+q)$ constraint matrix $\mathbf{C}$ is given by

$$\mathbf{C} = \begin{bmatrix} s_1[0] & \ldots & s_1[N-1] & 0 \\ \ddots & & & \ddots \\ 0 & s_1[0] & \ldots & s_1[N-1] \end{bmatrix}. \tag{2.43}$$

The optimal vector $\mathbf{f}$ is found as the eigenvector of $\mathbf{C}\mathbf{R}_y^{-1}\mathbf{C}^H$ corresponding to the minimum eigenvalue [90]. In adaptive implementation, the optimal vector $\mathbf{f}$ is difficult to track. In [88], vector $\mathbf{f}$ is chosen as $\mathbf{f} = [1, 0, \ldots, 0]^T$. By doing so, the

receiver collects the signal energy in the first path but discards the energy in other paths. To exploit all the energy, Liu *et al.* [57] proposed a decorrelating RAKE receiver. The impulse response of the filter in the ith finger of the RAKE receiver is obtained by above constrained optimization with the vector $\mathbf{f}_i = \mathbf{e}_i$, where $\mathbf{e}_i$ is the unit vector with all elements 0's except 1 at the ith position. The outputs from the fingers of the RAKE receiver are coherently combined. The combining vector is found as the principal eigenvector of the covariance matrix of the output of the RAKE receiver. It is noticed that there are phase ambiguities in the optimal vector $\mathbf{f}$ in Tsatsanis' receiver [90] and in the combing vector in Liu's decorrelating RAKE receiver [57]. Therefore, transmitted data should be differentially encoded. To reduce the complexity of the receiver further, we propose a simple equal gain combiner after Liu's decorrelating RAKE receiver in combination with differential encoding/decoding. First, we discuss the following fact.

Fact: The noise at the output of the RAKE receiver is approximately white. Let vector $\mathbf{v}[n] \in C^q$ denote the noise at the output of the RAKE receiver. The covariance matrix of $\mathbf{v}$ is $\mathbf{R}_v = \sigma^2(\mathbf{C}\mathbf{R}_y^{-1}\mathbf{C}^H)^{-1}\mathbf{C}\mathbf{R}_y^{-1}\mathbf{R}_y^{-1}\mathbf{C}^H(\mathbf{C}\mathbf{R}_y^{-1}\mathbf{C}^H)^{-1}$ Suppose that there is a matrix $\mathbf{A}$ such that $\mathbf{C}^H\mathbf{A}\mathbf{C} = \mathbf{I}$, then $\mathbf{R}_v = \sigma^2\mathbf{A}$. From the relations that $\mathbf{C}\mathbf{C}^H\mathbf{A}\mathbf{C}\mathbf{C}^H = \mathbf{C}\mathbf{C}^H$ and $\mathbf{C}\mathbf{C}^H \approx \mathbf{I}$, we have $\mathbf{A} \approx \mathbf{I}$. Thus $\mathbf{v}$ is approximately white.

Denotes vector $\mathbf{z}[n] \in C^q$ as the output of the RAKE receiver. Suppose that there is no residual interference in $\mathbf{z}[n]$, the optimum decision variable [94] for the differentially encoded data is $U[n] = \mathbf{z}[n-1]^H\mathbf{R}_v^{-1}\mathbf{z}[n]$. Since noise is approximately white, the decision variable can be obtained from an equal gain combiner. It is given by $U[n] = \mathbf{z}[n-1]^H\mathbf{z}[n]$. In practice, the residual interference may not be negligible. Nevertheless, we still use this simple combiner. We will see later in simulations that this low-complexity receiver has almost the same performance as Tsatsanis' minimum variance receiver with optimal cons traits.

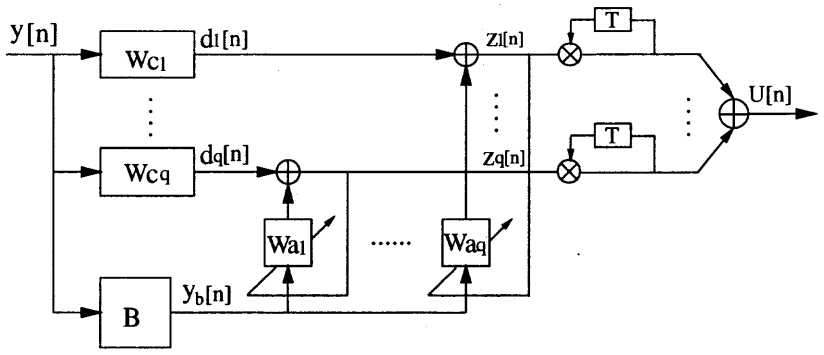

Figure 2.9 Minimum variance receiver

2.2.2 Reduced-Rank Minimum Variance Receiver

The minimum variance receiver can be implemented in a partitioned form termed a generalized sidelobe canceler (GSC) [44], as shown in Fig.2.9. The vector $\mathbf{w}_{ci}$ in the ith finger in the upper branch can be expressed as $\mathbf{w}_{ci} = \mathbf{C}^H(\mathbf{C}\mathbf{C}^H)^{-1}\mathbf{e}_i$. Blocking matrix $\mathbf{B}$ in the lower branch is chosen to satisfy $\mathbf{B}\mathbf{C}^H = 0$ and often has dimensions of $N \times (N+q)$. The optimal adaptive weights $\mathbf{w}_{ai}$ can be found as [44]:

$$\mathbf{w}_{ai} = \mathbf{R}_{y_b}^{-1}\mathbf{r}_{y_b d_i} \tag{2.44}$$

where $\mathbf{R}_{y_b} = E\{\mathbf{y}_b[n]\mathbf{y}_b^H[n]\}$ is the covariance matrix of the lower branch data, and $\mathbf{r}_{y_b d_i} = E\{\mathbf{y}_b[n]d_i[n]\}$ is the cross-correlation between the lower branch data and output of the ith finger in the upper branch.

The covariance matrix $\mathbf{R}_{y_b}$ can also be expressed in terms of its singular value decomposition

$$\mathbf{R}_{y_b} = \mathbf{U}\Lambda\mathbf{U}^H = [\mathbf{U}_s \ \mathbf{U}_n]\begin{bmatrix} \Lambda_s & \\ & \Lambda_n \end{bmatrix}\begin{bmatrix} \mathbf{U}_s^H \\ \mathbf{U}_n^H \end{bmatrix} \tag{2.45}$$

where $\mathbf{U} = [\mathbf{U}_s \ \mathbf{U}_n]$, $\Lambda = diag(\Lambda_s, \Lambda_n)$; $\Lambda_s = diag(\lambda_1, \ldots, \lambda_D)$ contains the D (D depends on users' delays, $min(2K, N) \leq D \leq min(3K+1, N)$) largest eigenvalues of $\mathbf{R}_{y_b}$ in descending order and $\mathbf{U}_s = [\mathbf{u}_1 \ \ldots \mathbf{u}_D]$ contains the corresponding orthonormal eigenvectors; $\Lambda_n = \sigma^2\mathbf{I}_{N-D}$ and $\mathbf{U}_n$ contains the $N-D$ orthonormal

eigenvectors with the eigenvalue σ^2. The range space of $\mathbf{U}_s$ is called the signal space. The range of $\mathbf{U}_n$ is called the noise space.

The full-rank solution in (2.44) is a vector in the signal space. The reduced-rank solution to $\mathbf{w}_{ai}$ is a vector in a subspace of the signal space. Suppose $\mathbf{w}_{ai}^r$ is in the range of matrix $\mathbf{U}_r$ where $\mathbf{U}_r$ contains r columns of the matrix $\mathbf{U}_s$ and the diagonal matrix Λ_r contains corresponding eigenvalues. Then $\mathbf{w}_{ai}^r$ is given by

$$\mathbf{w}_{ai}^r = \mathbf{U}_r \Lambda_r^{-1} \mathbf{U}_r^H \mathbf{r}_{y_b d_i} \tag{2.46}$$

Let $Q_{im} \triangleq \frac{|\mathbf{u}_m^H \mathbf{r}_{y_b d_i}|^2}{\lambda_m}, m = 1, \ldots, D$, where $\mathbf{u}_m$ is the mth column of the matrix $\mathbf{U}_s$. For a given rank r, to minimize the output power, the optimal $\mathbf{w}_{ai}^r$ chooses r eigenvectors corresponding to r largest values of Q_{im}. When $\mathbf{R}_{y_b}$ and $\mathbf{r}_{y_b d_i}$ are known, the output power of the reduced-rank receiver cannot be less than that of the full-rank receiver. Therefore, any reduced-rank receiver performs worse than the full-rank receiver. In a practical system, the covariance matrix, $\mathbf{R}_{y_b}$, and the cross-correlation, $\mathbf{r}_{y_b d_i}$, are estimated. The estimates are $\hat{\mathbf{R}}_{y_b} = 1/M \sum_{n=1}^{M} \mathbf{y}_b[n] \mathbf{y}_b^H[n]$ and $\hat{\mathbf{r}}_{y_b d_i} = 1/M \sum_{n=1}^{M} \mathbf{y}_b[n] d_i[n]$. When the receiver is obtained from the estimated covariance matrix and cross-correlation, simulations demonstrate that the rank-D receiver always outperforms the full-rank receiver. Since the estimated signal space and noise space are different with the true ones, the reduced-rank receiver with the rank less than D may have better performance than the rank-D receiver. This is also verified in simulations. Therefore, we can choose a proper subspace for every finger such that the reduced-rank receiver achieves the best performance. An intuitive way of choosing the subspace is to select the one such that the square of the output is minimized. However, the reduced-rank receiver obtained using this method has lower signal to interference ratio (SIR) than the full-rank receiver in simulations. We thus propose another method for choosing reduced-rank receiver as follows. For every rank, r $(1 \leq r \leq D)$, we can get an optimal $\mathbf{w}_{ai}^r$. Suppose $\{\mathbf{u}_m, m \in I\}$ is the set of the eigenvectors that $\mathbf{w}_{ai}^r$ chooses. Calculate the quantities $Q_i^r = \sum_{m \in I} Q_{im}$

and $Q_i = \sum_{m=1}^{D} Q_{im}$. Then the reduced-rank $\mathbf{w}_{ai}^r$ is the one that has the smallest rank such that $Q_i^r/Q_i > t_s$, where t_s is a threshold that is close to 1. This method avoids using the eigenvectors that are close to the noise space. In simulations, the reduced-rank receiver that is chosen using this method performs at least as well as the rank-D receiver.

The recursive least-squares (RLS) algorithm can be used for the weight adaptation for the full-rank receiver. To implement the reduced-rank receiver, we need to estimate the eigenvectors of the covariance matrix corresponding to the signal space and the corresponding eigenvalues. Here, we use the subspace tracking algorithm in [80] to track the eigenvectors and eigenvalues of the covariance matrix that is defines as $\mathbf{R}_{y_b}[n] = \sum_{i=1}^{n} \beta^{n-i} \mathbf{y}_b[i]\mathbf{y}_b^H[i]$ where β is the forgetting factor. The algorithm in [80] cannot track the rank of the signal covariance matrix. In a CDMA system, users leave or enter the system randomly. Therefore, the signal space changes. We need to track the variations of the signal space. The rank tracking method in [112] is combined into the subspace tracking algorithm. The cross-correlation can be updated recursively according to $\mathbf{r}_{y_b d_i}[n] = \beta \mathbf{r}_{y_b d_i}[n-1] + d_i[n]\mathbf{y}_b[n]$.

2.2.3 Simulation Results

In this section, simulation results are presented to demonstrate the performance of the proposed algorithm. The performance measure for simulations is the averaged SIR obtained by 400 independent runs. The input SNR of the desired user is $20dB$. The processing gain is $N = 31$. The spreading sequences are the Gold sequences. Multipath channels have three taps. Every tap is randomly generated from a complex Gaussian distribution. Delays are also randomly generated. Channels and delays are fixed in every run. The output SIR versus the rank of the receiver for the equal power case and the near-far case are displayed in Fig. 2.10, Fig. 2.11 respectively. We observe that the proposed low-complexity receiver has almost the same performance

as Tsatsanis's minimum variance receiver with the optimal constraints. When the covariance matrix is known, reduced-rank receivers cannot outperform the full-rank receiver. However, when the covariance matrix is estimated, the optimal reduced-rank receiver has larger SIR than the full-rank receiver. For example, in equal power case displayed in Fig. 2.10, the output SIR of the rank-15 receiver is 2dB larger than that of the full-rank receiver when $M = 400$. The reason is explained as follows. When the covariance matrix is known, the noise space is also known. The noise space is orthogonal to the cross-correlation vector. Thus, the full-rank receiver is in the signal space. Therefore, the full-rank receiver has the same performance as the rank-D receiver. However, when the covariance matrix is estimated, the estimated noise space is not orthogonal to the cross-correlation vector anymore. As a result, the full-rank receiver has a component in the noise space. There is more noise at the output of the full-rank receiver than a proper reduced-rank receiver. Therefore, its output SIR degrades. The simulation results for the adaptive version of the proposed reduced-rank and full-rank minimum variance receivers are demonstrated in Fig. 2.12. The RLS algorithm is used for the full-rank receiver. In reduced-rank receiver, the threshold for subspace selection is $t_s = 0.99$. At $t = 0$, there are eight users in the channel. SNRs of all the users are 20dB. At $t = 2000$, two 30-dB users and one 40-dB user enter the channel; at $t = 4000$, the 40-dB user, two 30-dB users and two 20-dB users exit the channel. We see the advantage of the reduced-rank receiver over the full-rank receiver.

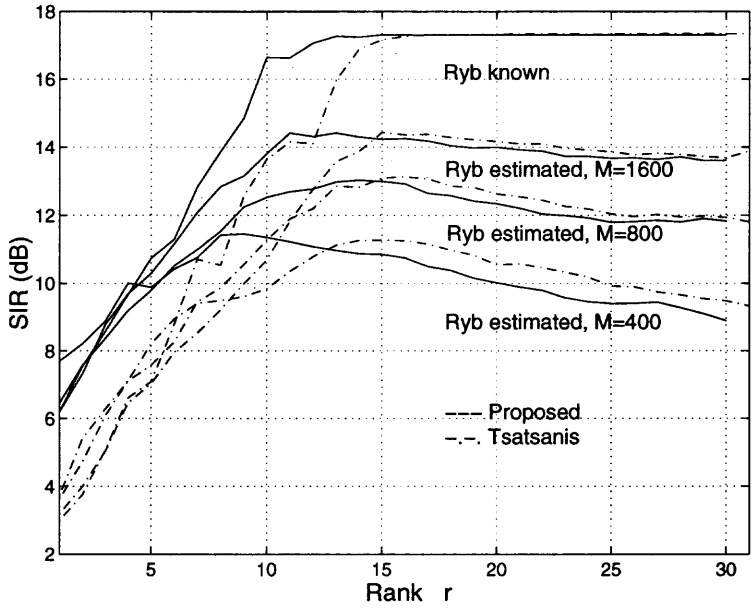

Figure 2.10 Output SIR comparison for different ranks. N=31, K=8, SNR=20dB, (K-1) interferences' SNRs are 20dBs.

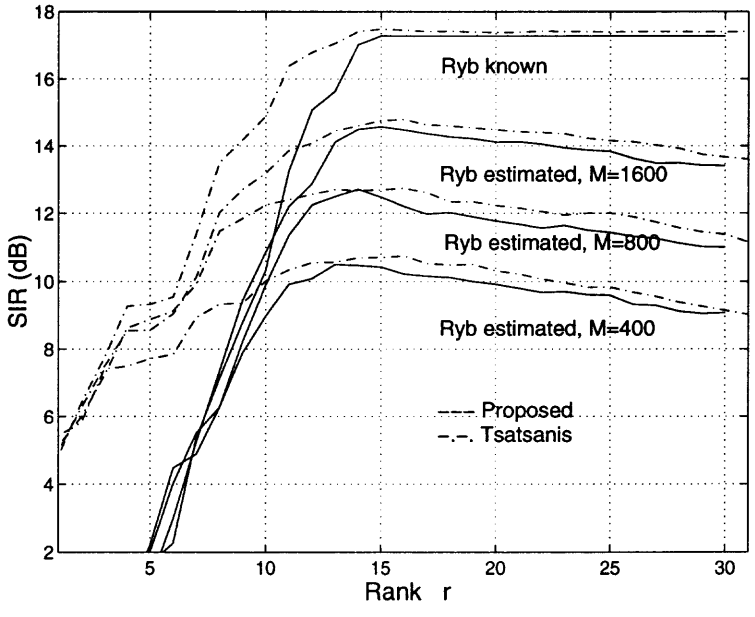

Figure 2.11 Output SIR comparison for different ranks. N=31, K=8, SNR=20dB, (K-1) interferences' SNRs are 30dBs.

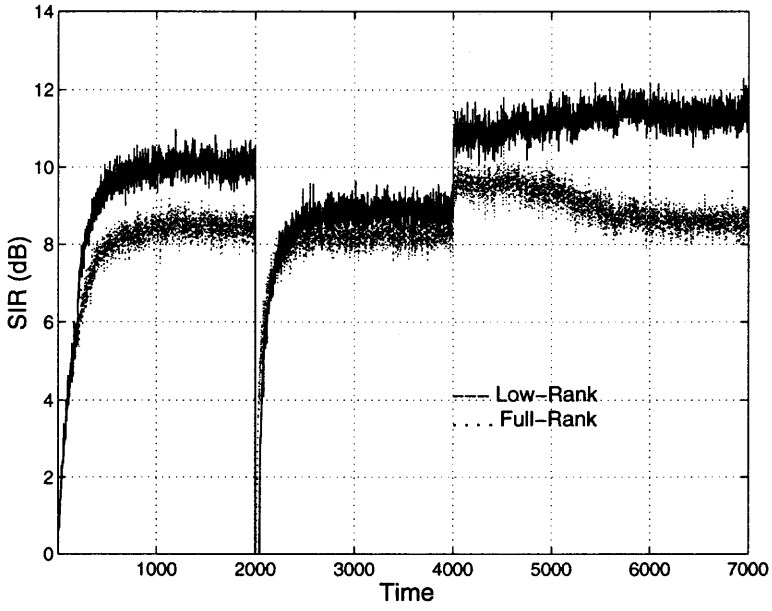

Figure 2.12 Performance of the adaptive reduced-rank MMSE detector in a dynamic multiple-access channel.

2.3 Probability Density Function of Conditioned SNRs of Linear MMSE Estimators

To further understand the performance of the reduced-rank receivers developed in last two sections, we study the probability density function of the output SNR of linear MMSE estimators when the covariance matrix is estimated. A related problem is to detect a known signal with random phase in the presence of complex Gaussian noise using an adaptive array. The optimum detector was given in [21]. The probability density function of SNR at the output of the detector that is obtained using the sample covariance matrix was derived by Reed, *et al* [73] and Hanumara [33]. When the underlying noise covariance matrix is not full-rank, reduced-rank detectors [68, 48] provide performance advantage over the full-rank approach.

2.3.1 Probability Density Function of Conditioned SNRs of Full-Rank and Reduced-Rank MMSE Estimators

Consider a general linear data model [47] given by

$$\begin{aligned} \mathbf{x} &= \boldsymbol{H}\boldsymbol{\theta} + \mathbf{n} \\ &= \mathbf{h}_1\theta_1 + \tilde{\boldsymbol{H}}\tilde{\boldsymbol{\theta}} + \mathbf{n}. \end{aligned} \tag{2.47}$$

where $\mathbf{x}$ is an $N \times 1$ vector of observations, $\mathbf{H} = [\mathbf{h}_1, \ldots, \mathbf{h}_p] = [\mathbf{h}_1, \tilde{\mathbf{H}}]$ is an $N \times p$ matrix (with $N > p$) of rank p, $\boldsymbol{\theta} = [\theta_1, \ldots, \theta_p]^T = [\theta_1, \tilde{\boldsymbol{\theta}}^T]^T$ is a $p \times 1$ vector of random parameters, and $\mathbf{n}$ is an $N \times 1$ Gaussian noise vector with zero mean and covariance matrix $\sigma^2\mathbf{I}$. Suppose that a realization of θ_1 is to be estimated. $\mathbf{h}_1$ and variance of θ_1 (say σ_1^2) are assumed to be known. Other parameters are assumed to be nuisance parameters or interferences to θ_1. The matrix $\tilde{\mathbf{H}}$ and the variance of nuisance parameters and noise are assumed to be unknown to the estimator. This data model is often used in digital communications. For example, in a multiuser communication system with linear modulation, let $\boldsymbol{\theta}$ be the information-bearing data of p users and $\mathbf{H}$ be the modulated waveform. The signal of user 1 is of interest and others are interferences. Then the received signal can be modeled with above data model.

For convenience of analysis, we further assume that the elements of $\boldsymbol{\theta}$ are independent Gaussian random variables with zero mean and that the variance of each element is not necessary the same. Under the Gaussian assumptions, the linear MMSE estimator is actually a true MMSE estimator. The filter weights, $\mathbf{w}$, that yield the linear MMSE estimator for θ_1, are given by

$$\mathbf{w} = \sigma_1^2\mathbf{R}^{-1}\mathbf{h}_1, \tag{2.48}$$

where $\mathbf{R}$ is the covariance matrix of $\mathbf{x}$. The estimate of θ_1 is $\hat{\theta}_1 = \mathbf{w}^H\mathbf{x}$. The output SNR is given by

$$S = \frac{E\{|\mathbf{w}^H\mathbf{h}_1\theta_1|^2\}}{E\{|\mathbf{w}^H(\tilde{\boldsymbol{H}}\tilde{\boldsymbol{\theta}} + \mathbf{n})|^2\}} \tag{2.49}$$

$$= \frac{\sigma_1^2 \mathbf{h}_1^H \mathbf{R}^{-1} \mathbf{h}_1}{1 - \sigma_1^2 \mathbf{h}_1^H \mathbf{R}^{-1} \mathbf{h}_1}$$

The optimal detector that detects signal $\mathbf{h}_1$ is $\mathbf{w}_d = \tilde{\mathbf{R}}^{-1}\mathbf{h}_1$ [73], where $\tilde{\mathbf{R}}$ is the covariance matrix of interferences plus noise. It can be shown that the weight vector of the optimal detector is proportional to that of the MMSE estimator. Therefore, the output SNR of the optimal detector is the same as that of the MMSE estimator. However, when the weight vectors are obtained from the estimated covariance matrix, we will see that the density functions of the output SNRs are different.

For many applications, the covariance matrix is unknown. Therefore, estimated covariance matrix is used in calculating the weight vector $\mathbf{w}$. Let us assume that M independent data snapshots $\{\mathbf{x}_m\}$ are observed. Under the Gaussian assumption, the maximum-likelihood estimate of the covariance is the sample covariance matrix that is given by

$$\hat{\mathbf{R}} = \frac{1}{M} \sum_{i=1}^{M} \mathbf{x}_m \mathbf{x}_m^H. \tag{2.50}$$

Thus, the weight vector is found as

$$\hat{\mathbf{w}} = \sigma_1^2 \hat{\mathbf{R}}^{-1} \mathbf{h}_1. \tag{2.51}$$

This method of calculating the weight vector is called the sample matrix inverse (SMI) method. Note that the weight vector $\hat{\mathbf{w}}$ is a random vector. The output SNR conditioned on $\hat{\mathbf{w}}$ is

$$\hat{S} = \frac{\sigma_1^2 (\mathbf{h}_1^H \hat{\mathbf{R}}^{-1} \mathbf{h}_1)^2}{\mathbf{h}_1^H \hat{\mathbf{R}}^{-1} \tilde{\mathbf{R}} \hat{\mathbf{R}}^{-1} \mathbf{h}_1}. \tag{2.52}$$

The conditioned SNR is upper bounded by the maximum achievable SNR expressed in (2.49). We normalize the conditioned SNR with respect to its upper bound. Denote this normalized SNR by ρ_s. Denote $r \triangleq \frac{S}{1+S} = \sigma_1^2 \mathbf{h}_1^H \mathbf{R}^{-1} \mathbf{h}_1$, $\hat{r} \triangleq \frac{\hat{S}}{1+\hat{S}} = \frac{\sigma_1^2 (\mathbf{h}_1^H \hat{\mathbf{R}}^{-1} \mathbf{h}_1)^2}{\mathbf{h}_1^H \hat{\mathbf{R}}^{-1} \mathbf{R} \hat{\mathbf{R}}^{-1} \mathbf{h}_1}$ and $\rho \triangleq \frac{\hat{r}}{r}$. We notice that ρ has the same formula as the normalized output SNR of the detector based on the SMI method in [73]. Because the data have

a Gaussian distribution, the density of ρ is given by [73]

$$f(\rho) = \frac{M!}{(M-N+1)!(N-2)!}\rho^{M+1-N}(1-\rho)^{N-2}, \tag{2.53}$$

where $0 \leq \rho \leq 1$ and $M \geq N$. ρ and ρ_s have the following relation

$$\rho = \frac{(1+S)\rho_s}{1+S\rho_s}, \tag{2.54}$$

and we have

$$\frac{d\rho_s}{d\rho} = \frac{(1+S\rho_s)^2}{1+S}. \tag{2.55}$$

Thus, the density of ρ_s is found as

$$p(\rho_s) = \frac{f(\rho)}{|\frac{d\rho_s}{d\rho}|} = \frac{1+S}{(1+S\rho_s)^2} f(\frac{(1+S)\rho_s}{1+S\rho_s}). \tag{2.56}$$

Substitute (2.53) into (2.56), we have

$$\begin{aligned} p(\rho_s) &= \frac{M!}{(M-N+1)!(N-2)!} \times \\ &\quad \frac{(1+S)^{M+2-N}\rho_s^{M+1-N}(1-\rho_s)^{N-2}}{(1+S\rho_s)^{M+1}}. \end{aligned} \tag{2.57}$$

Unlike the normalized SNR of the optimal detector in [73], the normalized SNR of the MMSE estimator depends on the maximum achievable SNR. In [73], it is found that at least $M = 2N - 3$ samples of data are needed for the detector to maintain an average output SNR loss of better than 3 dB. Since the expectation of ρ_s is a hypergeometric function, there is no closed-form for the number of samples required for the MMSE estimator to achieve an average performance level. However, given the maximum achievable SNR, length of the data vector N and the performance loss relative to the maximum achievable SNR, one can compute the number of the samples by using numerical integration. We can also approximately calculate the number of samples as follows. When $N > 2$, the function $p(\rho_s)$ has one and only one maximum point on the interval $(0, 1)$. It can be found as $\rho_s = (NS + M - 1 - \sqrt{(NS+M-1)^2 - 8S(M+1-N)})/(4S)$. When $N = 2$, the function $p(\rho_s)$ has an

maximum point at $\rho_s = (M-1)/(2S)$. If the maximum point is at $\rho_s = 0.5$, the probability that ρ_s is greater than 0.5 is approximately equal to 0.5. We can find that $M = 2N - 3 + (N-1)S$ so that $p(\rho_s)$ achieves maximum value at $\rho_s = 0.5$. This is a useful "rule-of-thumb" requirement on the number of data samples for the estimator's performance loss to be less than 3dB. Note that the number of data samples is proportional to the maximum output SNR and the length of the data vector.

When $\mathbf{R}$ is estimated using sample covariance matrix in (2.50), we perform the SVD on the estimated covariance matrix $\hat{\mathbf{R}}$. The reduced-rank MMSE estimators are constructed from the estimated eigenvectors and eigenvalues. When p principal eigenvalues are different, these eigenvalues and their corresponding eigenvectors have asymptotic Gaussian distributions [46]. Their mean and covariance can be found in [46]. However, it is difficult to derive the density of the output SNR of the reduced-rank estimators from the distributions of the eigenvalues and eigenvectors. We consider the reduced-rank estimator using p estimated eigenvectors corresponding to the p largest eigenvalues, which is given by

$$\hat{\mathbf{w}} = \sigma_1^2 \hat{\mathbf{U}}_s \hat{\Lambda}_s^{-1} \hat{\mathbf{U}}_s^H \mathbf{h}_1. \tag{2.58}$$

This method of calculating the weight vector is called the principal component inverse (PCI) method. We will give an asymptotic formula for the PCI estimator. Based on the formula, we get the asymptotic density of the output SNR.

Suppose that we have a vector

$$\tilde{\mathbf{w}} = \sigma_1^2 \mathbf{U}_s (\mathbf{U}_s^H \hat{\mathbf{R}} \mathbf{U}_s)^{-1} \mathbf{U}_s^H \mathbf{h}_1. \tag{2.59}$$

It is known that $\hat{\mathbf{R}} \xrightarrow{\text{P}} \mathbf{R}$ as $M \to \infty$, where $\xrightarrow{\text{P}}$ denotes convergence in probability. Hence, we have $\hat{\mathbf{w}} \xrightarrow{\text{P}} \mathbf{w}$ and $\tilde{\mathbf{w}} \xrightarrow{\text{P}} \mathbf{w}$. Therefore, $\hat{\mathbf{w}} - \tilde{\mathbf{w}}$ converges to the zero vector in probability. Since the output SNR is a continuous function of the weight vector, we have $\hat{S} - \tilde{S} \xrightarrow{\text{P}} 0$. In general, the convergence of the difference of two

random sequences to zero in probability doesn't necessarily imply that their densities converge. However, in simulation, we observe that the density functions of the output SNR of the estimators using above two formula are almost same. It is easy to get the theoretic density of the output SNR of the estimator $\tilde{\mathbf{w}}$.

The estimator $\tilde{\mathbf{w}}$ in (2.59) can be obtained as follows. Apply the linear transform $\mathbf{T} = \mathbf{U}_s$ to the $N \times 1$ data vector $\mathbf{x}$, we get a $p \times 1$ vector $\mathbf{t} = \mathbf{T}^H\mathbf{x}$. Based on the transformed data $\mathbf{t}$, we can use the SMI method to get the estimator. The linear transform preserves the Gaussian distribution of the data. Thus, the probability density function of the normalized output SNR of estimator $\tilde{\mathbf{w}}$ is the same function as in (11) with the parameter N replaced by p. Since the density of output SNR of estimator $\hat{\mathbf{w}}$ is approximately the same as that of estimator $\tilde{\mathbf{w}}$ as $M \to \infty$, we get an asymptotic density of the normalized output SNR for the PCI estimator $\hat{\mathbf{w}}$.

2.3.2 Numerical Results

Consider a case in which the columns of matrix $\mathbf{H}$ are Gold sequences (spreading sequences used in direct sequence spread-spectrum code-division multiple-access). Theoretic curves and simulation curves for the pdf of the output SNR are shown in Fig. 2.13, Fig. 2.14, Fig. 2.15 and Fig. 2.16. In these figures, solid line is theoretic curve, dash line is simulation curve and dot line is simulation for PCI estimator using asymptotic formula. When $N = 31$, $p = 4$, $M = 400$, the probability density functions are displayed in Fig. 2.13 and Fig. 2.14 for SNR=15dB and SNR=20dB respectively. SNR is defined as σ_1^2/σ^2. The interferences have the same power as the desired signal. Simulated density functions are obtained from the histogram of 10000 independent runs. We observe that the PCI estimators using the exact formula and using the asymptotic formula have almost the same density curve. Comparing Fig. 2.13 with Fig. 2.14, we see that the estimator needs more data samples to

have the same normalized output SNR when the input SNR is higher. From Fig. 2.13 and Fig. 2.14, we also see that with much higher probability, the PCI method yields higher output SNR than SMI method. Equivalently, to achieve the same level of performance, the PCI method needs less number of data samples than the SMI method. For example, in the case in Fig. 2.13, we can use the "rule of thumb" in section 2 to get $M \approx 1000$ for the SMI estimator and $M \approx 100$ for the PCI estimator to achieve a performance within 3dB of the maximum output SNR. When M is large and p is close to N, the performance gap between the SMI estimator and the PCI estimator becomes smaller. This is demonstrated in Fig. 2.15 and Fig. 2.16.

2.4 Summary

In this chapter, we study the reduced-rank MMSE and minimum variance CDMA receivers. It is demonstrated that the reduced-rank MMSE receiver outperforms the conventional full-rank MMSE receiver when the desired signal is in a low-dimensional subspace and the covariance matrix is estimated. The minimum variance receiver can be blindly implemented using the structure of generalized sidelobe canceler. The proposed low-complexity minimum variance receiver has almost the same performance as the high-complexity optimal minimum variance receiver. The reduced-rank minimum variance receiver again get the better performance compared with the full-rank minimum variance receiver. To further verify that the reduced-rank receiver does have advantage over the full-rank receiver, we study the probability density function of the conditioned SNR of liner MMSE estimators. Under the Gaussian assumption, we derive the pdf of the full-rank MMSE estimator based on the sample matrix inverse method. The pdf of the asymptotic reduced-rank MMSE estimator based on the principal component inverse method is also obtain. From those pdfs we conclude that the reduced-rank estimators do outperform the full-rank estimator.

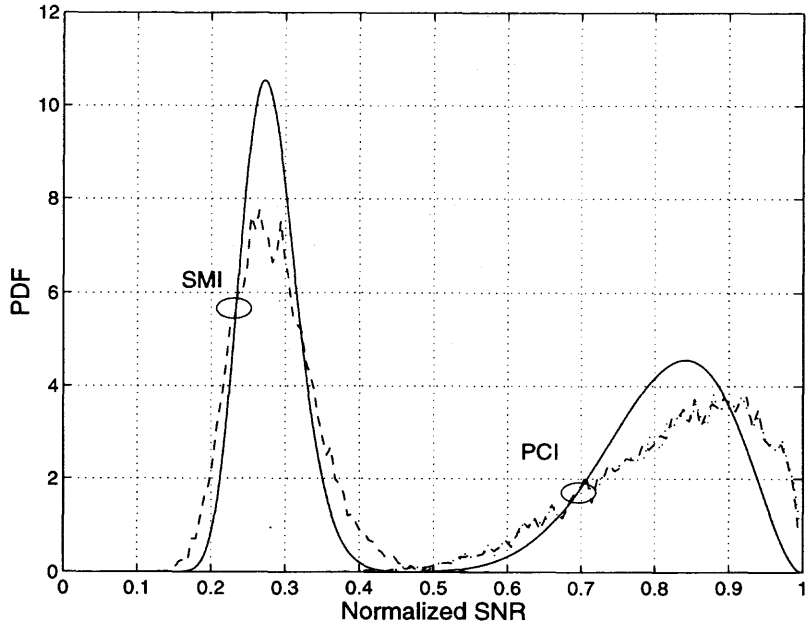

Figure 2.13 Density function of normalized output SNR, input SNR=15dB, M=400, N=31, p=4.

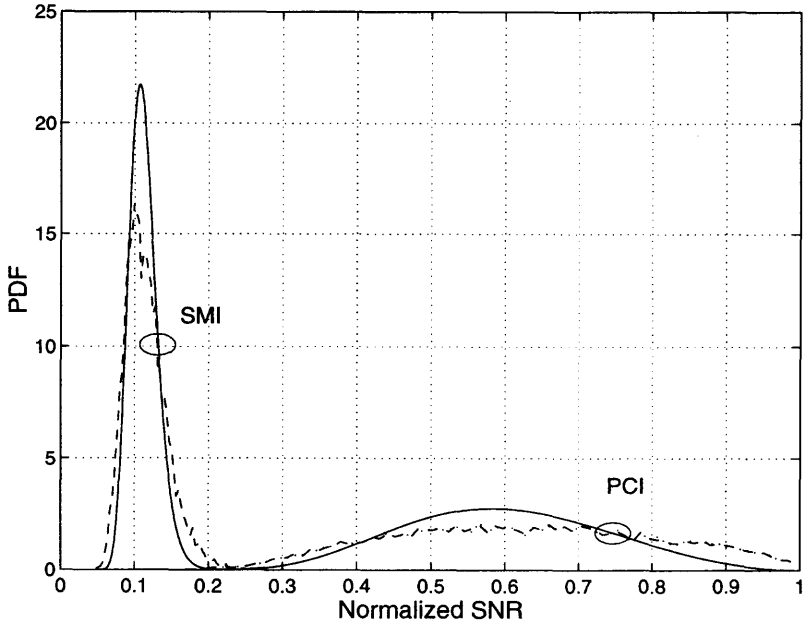

Figure 2.14 Density function of normalized output SNR, input SNR=20dB, M=400, N=31, p=4.

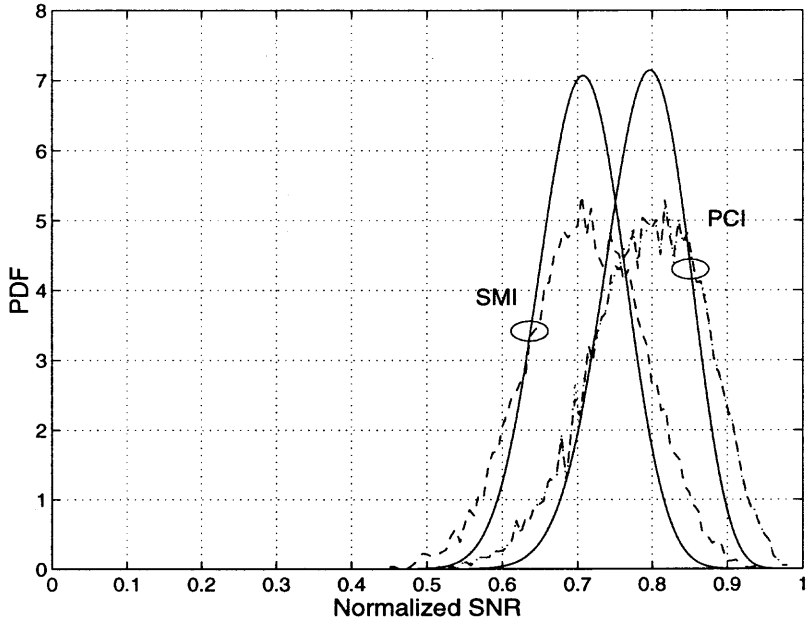

Figure 2.15 Density function of normalized output SNR, input SNR=15dB, M=1000, N=15, p=10.

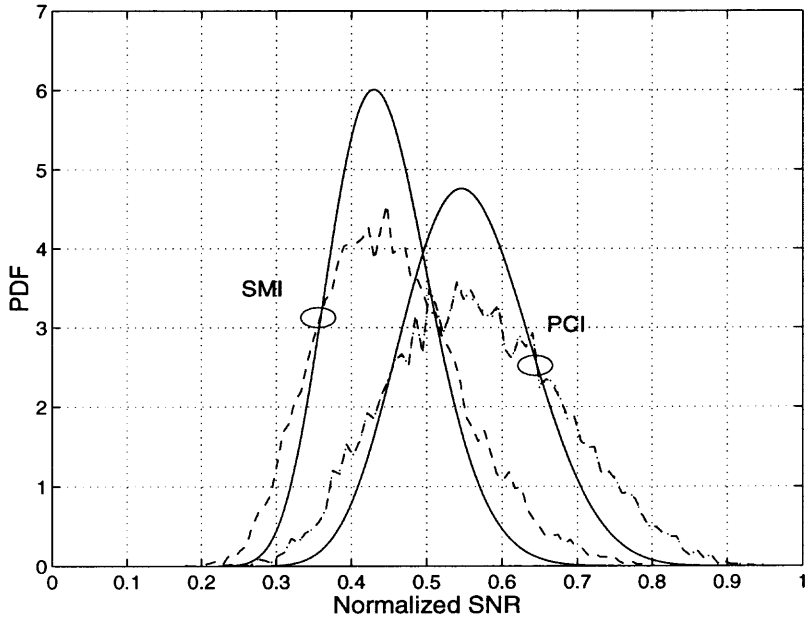

Figure 2.16 Density function of normalized output SNR, input SNR=20dB, M=1000, N=15, p=10.

CHAPTER 3
MULTICARRIER CDMA SYSTEMS WITH TRANSMIT DIVERSITY

Antenna diversity is a practical, effective technique for reducing the detrimental effects in wireless fading channels. The classical antenna diversity that uses multiple antennas at the receiver increases the cost, size, and power of the remote units. It is more feasible and economical to have multiple antennas at the base station rather than the remote units. Recently, transmit diversity has been studied to combat the fading channels.

In [108, 109], linear filtering is introduced at the transmitter so that the waveform at every transmit antenna is orthogonal to each other. At the receiver, due to the orthogonality among signals from different antennas, an optimal combiner can be used to collect all the energy form different antennas. An orthogonal signaling for transmit diversity in CDMA system is studied in [104]. Delay transmit diversity that is a special case of orthogonal filtering is studied in [77, 107]. A linear or nonlinear equalizer should be used at the receiver in the delay diversity scheme. In [35, 53], phase sweeping is used at the transmitter so that the received signal is a fast fading signal even the channel is slow fading. Combined with coding, this technique transfers the space diversity to time diversity. All these techniques approached transmit diversity from a signal processing point of view. Space-time codes [87, 85] combine signal processing at the receiver with coding techniques provides significant gain over the diversity gain introduced by signal processing at the transmitter.

Multicarrier CDMA [34] has been proposed for the wideband multiuser systems. It is shown [34] that MC-CDMA can effectively combine all the received signal energy scattered in the frequency domain whereas DS-CDMA cannot always employ the energy scattered in the time domain. Therefore, MC-CDMA has better performance in frequency-selective fading channel than the DS-CDMA. Since each subcarrier in

MC-CDMA undergoes flat fading, we can naturally combine the space-time coding with MC-CDMA to get transmit diversity for a wideband system.

3.1 Space-Time Coding

Space-time trellis coding is proposed in [87, 86]. It is demonstrated that specific space-time trellis codes designed for 2-4 transmit antennas perform extremely well in slow-fading channel environment. However, when the number of transmit antennas is fixed, the decoding complexity of space-time trellis codes increases exponentially with transmission rate. In [1, 85], orthogonal block codes are proposed for narrowband fading channels. It was shown that the space-time block codes can achieve the maximum diversity order for a given number of transmit and receive antennas, and its encoding and decoding scheme has very little complexity. The general theory of constructing space-time codes for PSK modulation is given in [32]. To decode the space-time codes, the receiver needs the channel state information. However, another family of the space-time codes named unitary space-time modulation [36] performs very well even though the receiver has no knowledge of the channel state information. A space-time code is defined as [32]:

Definition 3.1 An $L \times n$ space-time code $\mathcal{C}$ of size M consists of an (Ln, M) error control code C and a spatial parser σ that maps each codeword vector $\bar{c} \in C$ to an $L \times n$ matrices $\mathbf{c}$ whose entries are a rearrangement of those of $\bar{c}$. The space-time code $\mathcal{C}$ is said to be linear if both C and σ are linear.

Suppose that there are L_t transmit antennas. the standard parser maps

$$\bar{c} = (c_1^1, c_1^2, \ldots, c_1^{L_t}, c_2^1, c_2^2, \ldots, c_2^{L_t}, \ldots, c_n^1, c_n^2, \ldots, c_n^{L_t}) \in C \tag{3.1}$$

to the matrix

$$\mathbf{c}_m = \begin{bmatrix} c_1^1 & c_2^1 & \ldots & c_n^1 \\ c_1^2 & c_2^2 & \ldots & c_n^2 \\ \vdots & \vdots & \ddots & \vdots \\ c_1^{L_t} & c_2^{L_t} & \ldots & c_n^{L_t} \end{bmatrix}, \tag{3.2}$$

where c_t^i is the code symbol assigned to transmit i at time t.

Suppose that the symbol alphabet of the codewords is $\mathcal{Y}$. The encoded symbols are mapped by the modulator into constellation points from the discrete complex-valued signaling constellation Ω. Let $f : \mathcal{Y} \rightarrow \Omega$ be the modulator mapping function. Then $\mathbf{s} = f(\mathbf{c})$ is the baseband version of the codewords as transmitted through the channel. Suppose that the rank of the matrix $\mathbf{B} = f(\mathbf{c}) - f(\mathbf{e})$ is r and the eigenvalues of the matrix $\mathbf{A} = \mathbf{B}\mathbf{B}^H$ are $\{\lambda_i\}_1^r$, where $\mathbf{c}$ and $\mathbf{e}$ are any pair of distinct codewords. Then we have the design criteria for space-time codes [87]:

1. *Rank Criterion:* Maximize the rank r over all pairs of distinct codewords to achieve the maximum diversity

2. *Product Distance Criterion:* Maximize the coding advantage $\eta = (\lambda_1 \lambda_2 \ldots \lambda_r)^{1/r}$ over all pairs of distinct codewords.

Since the decoding method for the block space-time codes is very simple, we will use them for the MC-CDMA system. We are particularly interested in the block space-time codes for transmission using two and four transmit antennas, which are given by

$$\mathbf{c}_2 = \begin{bmatrix} c_1 & -c_2^* \\ c_2 & c_1^* \end{bmatrix}, \tag{3.3}$$

and

$$\mathbf{c}_2 = \begin{bmatrix} c_1 & -c_2 & -c_3 & -c_4 & c_1^* & -c_2^* & -c_3^* & -c_4^* \\ c_2 & c_1 & c_4 & -c_3 & c_2^* & c_1^* & c_4^* & -c_3^* \\ c_3 & -c_4 & c_1 & c_2 & c_3^* & -c_4^* & c_1^* & c_2^* \\ c_4 & c_3 & -c_2 & c_1 & c_4^* & c_3^* & -c_2^* & c_1^* \end{bmatrix}. \tag{3.4}$$

3.2 MC-CDMA with Transmit Diversity

A MC-CDMA transmitter with space-time coding is shown in Fig.3.1. We assume that there are two transmit antennas and the processing gain N is equal to the number of carriers. The simplest space-time block code in [1, 85] is used for the two transmit antenna case. The outputs of the space-time encoder are copied to

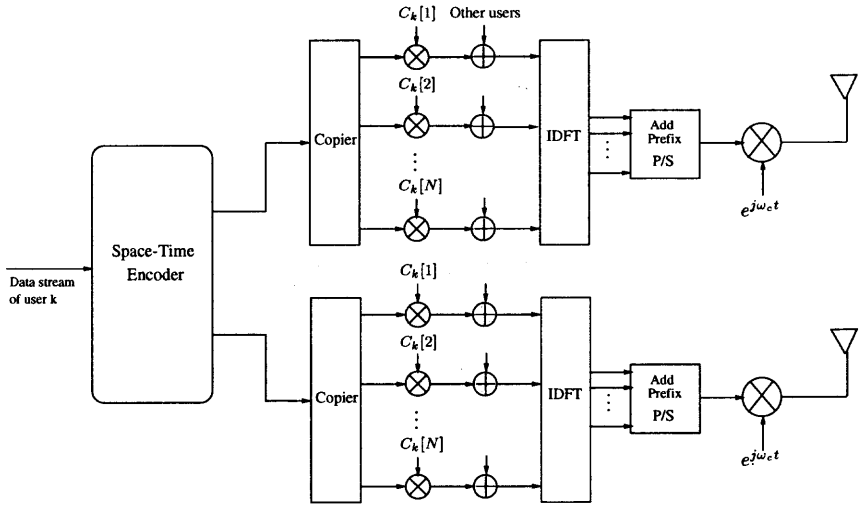

Figure 3.1 A MC-CDMA transmitter with transmit diversity

different carriers. The bit over different carrier is multiplied by a chip of the spreading code. Inverse discrete Fourier transform (IDFT) is used to implement multicarrier modulation. After the cyclic prefix is added, the signal is transmitted from one of the antennas. At the receiver, the RF signal is first converted to baseband signal. After the portion of the signal corresponding to the prefix is removed, discrete Fourier transform (DFT) is performed on the signal samples.

3.2.1 Signal Model

Assume that the length of the cyclic prefix is longer than the length of the channel impulse response, then there is no interblock interference (IBI). It is sufficient to consider the received signal in two consecutive blocks, say block 0 and block 1. After DFT is performed, the data at *nth* carrier in block 0 and block 1 can be written as

$$\begin{aligned} r_0[n] &= \sum_{k=1}^{K}(H_0[n]\mathbf{s}_k[n]b_k[0] + H_1[n]\mathbf{s}_k[n]b_k[1])A_k \\ &\quad +N_0[n] \end{aligned} \tag{3.5}$$

$$\begin{aligned} r_1[n] &= \sum_{k=1}^{K}(-H_0[n]\mathbf{s}_k^*[n]b_k^*[1] + H_1[n]\mathbf{s}_k^*[n]b_k^*[0])A_k \\ &\quad +N_1[n], \end{aligned} \tag{3.6}$$

where K is the number of active users, $\mathbf{s}_k[n]$ is the nth chip of the kth user's spreading code, A_k is the amplitude of the kth user's signal, $N_0[n]$ and $N_1[n]$ are additive white Gaussian noise with variance σ^2, and $H_0[n]$ and $H_1[n]$ are channel response from two transmit antennas to the receiver at the nth carrier. We assume that the channel is the slow fading channel, that is, the channel responses are the same in block 0 and block 1. Denote $\underline{r}_0 = [r_0[0], r_0[1], \ldots, r_0[N-1]]^T$, $\underline{r}_1 = [r_1[0], r_1[1], \ldots, r_1[N-1]]^H$. Let $N_0 = [N_0[0], N_0[1], \ldots, N_0[N-1]]^T$, $N_1 = [N_1[0], N_1[1], \ldots, N_1[N-1]]^T$. We have

$$\underline{r}_0 = H_0\mathbf{S}Ab_0 + H_1\mathbf{S}Ab_1 + N_0 \tag{3.7}$$

$$\underline{r}_1 = H_1^*\mathbf{S}Ab_0 - H_0^*\mathbf{S}Ab_1 + N_1, \tag{3.8}$$

where H_0 is a diagonal matrix with $[H_0]_{nn} = H_0[n]$, H_1 is a diagonal matrix with $[H_1]_{nn} = H_1[n]$, $\mathbf{S} = [\mathbf{s}_1, \mathbf{s}_2, \ldots, \mathbf{s}_K]$ with C_k be the spreading code of user k, $A = diag(A_1, \ldots, A_K)$, $b_0 = [b_1[0], b_2[0], \ldots, b_K[0]]^T$ and $b_1 = [b_1[1], b_2[1], \ldots, b_K[1]]^T$. Let $\mathbf{r} = [\underline{r}_1^T\ \underline{r}_2^T]^T$. The signal vector $\mathbf{r}$ is given by

$$\mathbf{r} = \mathcal{H}\mathcal{S}\mathcal{A}\mathbf{b} + \mathcal{N}, \tag{3.9}$$

where $\mathcal{N} = [N_0^T, N_1^H]^T$, $\mathbf{b} = [b_0^T, b_1^T]^T$, $\mathcal{S} = diag(\mathbf{S}, \mathbf{S})$, $\mathcal{A} = diag(A, A)$, and matrix $\mathcal{H}$ is defined as

$$\mathcal{H} = \begin{bmatrix} H_0 & H_1 \\ H_1^* & -H_0^* \end{bmatrix}. \tag{3.10}$$

3.2.2 Interference Suppression and Decoding

If there is only one user in the system, the maximum likelihood decoder is simply a maximum ratio combiner [85]. However, when there are more than one users in the system, it is difficult to employ a maximum likelihood decoder because the receiver has no knowledge of the spreading codes of all the active users. We shall consider four schemes that detect the information bearing bits of the desired user while suppressing other user's interference. These four schemes are maximum ratio combiner (MRC),

orthogonality restoring combiner (ORC), minimum mean square error combiner (MMSEC) and minimum mean square error multiuser detector(MMSEMUD).

1) Maximum ratio combiner:

The outputs of the MRC are given by

$$y_0 = \sum_{n=0}^{N-1}(H_0[n]^*\mathbf{s}_1[n]r_0[n] + H_1[n]\mathbf{s}_1[n]r_1^*[n]) \tag{3.11}$$

$$y_1 = \sum_{n=0}^{N-1}(H_1^*[n]\mathbf{s}_1[n]r_0[n] - H_0[n]\mathbf{s}_1[n]r_1^*[n]). \tag{3.12}$$

It can be shown that

$$y_0 = \sum_{n=0}^{N-1}(|H_0[n]|^2 + |H_1[n]|^2)b_1[0] + I_0 + \tilde{N}_0 \tag{3.13}$$

$$y_1 = \sum_{n=0}^{N-1}(|H_0[n]|^2 + |H_1[n]|^2)b_1[1] + I_1 + \tilde{N}_1 \tag{3.14}$$

where I_0 and I_1 are interference from the other users, and $\tilde{N}_0$ and $\tilde{N}_1$ are Gaussian noise. It is seen from (3.13) and (3.14) that MRC coherently combine the signals from two transmit antennas. The decisions for two bits are $\hat{b}_1[0] = sgn(\sum_{n=0}^{N-1} y_0[n])$, $\hat{b}_1[1] = sgn(\sum_{n=0}^{N-1} y_1[n])$.

2) Orthogonality restoring combiner:

The orthogonality among the signals of different users is lost after the transmitted signal passes through the channel. If the orthogonality can be restored, the interference can be completely eliminated. The inverse of matrix $\mathcal{H}$ can be found as

$$\mathcal{H}^{-1} = \begin{bmatrix} \tilde{H}_0^* & \tilde{H}_1 \\ \tilde{H}_1^* & -\tilde{H}_0 \end{bmatrix}, \tag{3.15}$$

where $\tilde{H}_0$ is a diagonal matrix with $[\tilde{H}_0]_{nn} = \frac{H_0[n]}{|H_0[n]|^2+|H_1[n]|^2}$ and $\tilde{H}_1$ is a diagonal matrix with $[\tilde{H}_1]_{nn} = \frac{H_1[n]}{|H_0[n]|^2+|H_1[n]|^2}$. Here we assume that $|H_0[n]|^2+|H_1[n]|^2 \neq 0, \forall n$. If the matrix $\mathcal{H}$ is singular, a psuedoinverse of $\mathcal{H}$ can be found. Suppose that the matrix $\mathcal{H}$ is not singular, the outputs of the ORC are given by

$$y_0 = \sum_{n=0}^{N-1}([\tilde{H}_0]_{nn}^*\mathbf{s}_1[n]r_0[n] + [\tilde{H}_1]_{nn}\mathbf{s}_1[n]r_1^*[n])$$

$$= A_1 b_1[0] + \tilde{N}_0 \tag{3.16}$$

$$y_1 = \sum_{n=0}^{N-1} ([\tilde{H}_1]^*_{nn} \mathbf{s}_1[n] r_0[n] - [\tilde{H}_0]_{nn} \mathbf{s}_1[n] r_1^*[n])$$

$$= A_1 b_1[1] + \tilde{N}_1. \tag{3.17}$$

where $\tilde{N}_0$ and $\tilde{N}_1$ are Gaussian noise with variance $\sigma^2 \sum_{n=0}^{N-1} \frac{1}{|H_0[n]|^2 + |H_1[n]|^2}$. While ORC cancels all the interference, it enhances the noise. When the channel responses at a carrier are small, the SNR at the output of ORC will be very low.

3) *Minimum mean square error combiner:*

In MMSEC, an MMSE estimate of the signal of the desired user at each carrier is first obtained. The estimates of the signal is then correlated with the spreading code of the desired user to obtain the decision statistic. The weights $w_{00}[n]$ and $w_{01}[n]$ that minimize the mean square error $E|\mathbf{s}_1[n]b_1[0] - w_{00}[n] * r_0[n] - w_{01}[n] * r_1^*[n]|^2$ can be found as

$$w_{00}[n] = \frac{H_0^*[n]}{(|H_0[n]|^2 + |H_1[n]|^2) \sum_{k=1}^{K} A_k^2 + \sigma^2} \tag{3.18}$$

$$w_{01}[n] = \frac{H_1[n]}{(|H_0[n]|^2 + |H_1[n]|^2) \sum_{k=1}^{K} A_k^2 + \sigma^2}. \tag{3.19}$$

Similarly, the weights $w_{10}[n]$ and $w_{11}[n]$ that minimize the mean square error $E|\mathbf{s}_1[n]b_1[1] - w_{10}[n] * r_0[n] - w_{11}[n] * r_1^*[n]|^2$ is given by

$$w_{10}[n] = \frac{H_1^*[n]}{(|H_0[n]|^2 + |H_1[n]|^2) \sum_{k=1}^{K} A_k^2 + \sigma^2} \tag{3.20}$$

$$w_{11}[n] = \frac{-H_0[n]}{(|H_0[n]|^2 + |H_1[n]|^2) \sum_{k=1}^{K} A_k^2 + \sigma^2}. \tag{3.21}$$

Denote $y_0[n] = w_{00}[n] * r_0[n] + w_{01}[n] * r_1^*[n]$ and $y_1[n] = w_{10}[n] * r_0[n] + w_{11}[n] * r_1^*[n]$. The decision variables for $b_1[0]$ and $[b_1[1]$ are given by

$$y_0 = \sum_{n=0}^{N-1} (\mathbf{s}_1[n] * y_0[n]) \tag{3.22}$$

$$y_1 = \sum_{n=0}^{N-1} (\mathbf{s}_1[n] * y_1[n]). \tag{3.23}$$

MMSEC tries to restore the orthogonality as much as possible but not to enhance the noise as in ORC. It needs the knowledge of the noise variance.

4) *Minimum mean square error multiuser detector:*

In above three schemes, the structure of the other users' spreading codes is not explored by the receiver to suppress the interference. MMSEMUD uses this structure to achieve better performance. MMSEMUD finds the $2N \times 2$ weight matrix $\mathbf{W}$ to minimize the mean square error $E(\| \mathbf{W}^H\mathbf{r} - \underline{b}_1 \|^2)$, where $\underline{b}_1 = [b_1[0]\ b_1[1]]^T$. We assume that $b_1[0]$ and $b_1[1]$ are uncorrelated. Matrix $\mathbf{W}$ can be found as $\mathbf{W} = \mathbf{R}^{-1}\mathbf{P}$, where $\mathbf{R} = E(\mathbf{r}\mathbf{r}^H) = \mathcal{H}\mathcal{S}\mathcal{A}^2\mathcal{S}^H\mathcal{H}^H + \sigma^2\mathbf{I}$. The first column of $\mathbf{P}$ is given by $\mathbf{P}(:,1) = [H_0[1]\mathbf{s}_1[0], \ldots, H_0[N-1]\mathbf{s}_1[N-1], H_1^*[0]\mathbf{s}_1[0], \ldots, H_1^*[N-1]\mathbf{s}_1[N-1]]^T$ and the second column of of $\mathbf{P}$ is given by $\mathbf{P}(:,2) = [H_1[1]\mathbf{s}_1[0], \ldots, H_1[N-1]\mathbf{s}_1[N-1], -H_0^*[0]\mathbf{s}_1[0], \ldots, 1H_0^*[N-1]\mathbf{s}_1[N-1]]^T$. When the fading is slow, the covariance matrix $\mathbf{R}$ can be estimated using available data. We can see that the complexity of the MMSEMUD is much higher than the other three schemes because it needs to invert a $2N \times 2N$ matrix.

In all these schemes, the receiver needs to know the channel state information. In practice, each antenna can employ a pilot channel. The receiver uses the pilot channel to estimate the channel state. Alternatively, some pilot symbols can be inserted in the users' transmitted signals. The pilot symbols enable the receiver to estimate the channel.

3.2.3 Simulation Results

Simulations demonstrate the performance of the MC-CDMA with transmit diversity in a downlink multipath fading channel. Walsh-Hadamard codes are chosen as the spreading codes. Processing gain is $N = 32$. The fading channel has 3 independent taps and its multipath intensity profile is exponential. The delay spread is $T_m = 3T_c$ where T_c is the chip duration of the DS-CDMA that has the same bandwidth as

the MC-CDMA. We assume that the receiver know the channel perfectly. Fig. 3.2 shows the bit error rate of the DS-CDMA, MC-CDMA with single transmit antenna and with two transmit antennas. The DS-CDMA system uses a three finger RAKE receiver with maximum ratio combiner. The MC-CDMA systems use maximum ratio combiners. The number of users is 10. It is seen that the MC-CDMA with transmit diversity has the best performance. Fig. 3.3 and Fig. 3.4 compare the bit error rate of MC-CDMA systems with different combing schemes. MMSE combiner has the same BER as MMSE multiuser detector when K=32 and has slightly higher BER than MMSEMUD when K=10. Because MMSEMUD has much higher complexity than MMSEC, MMSEC is preferred in a practical system. In Fig. 3.5, The performance of the MC-CDMA systems with and without transmit diversity is compared. The MMSE combiner is used. It is seen again that the transmit diversity improve the system performance no matter how many users are in the system.

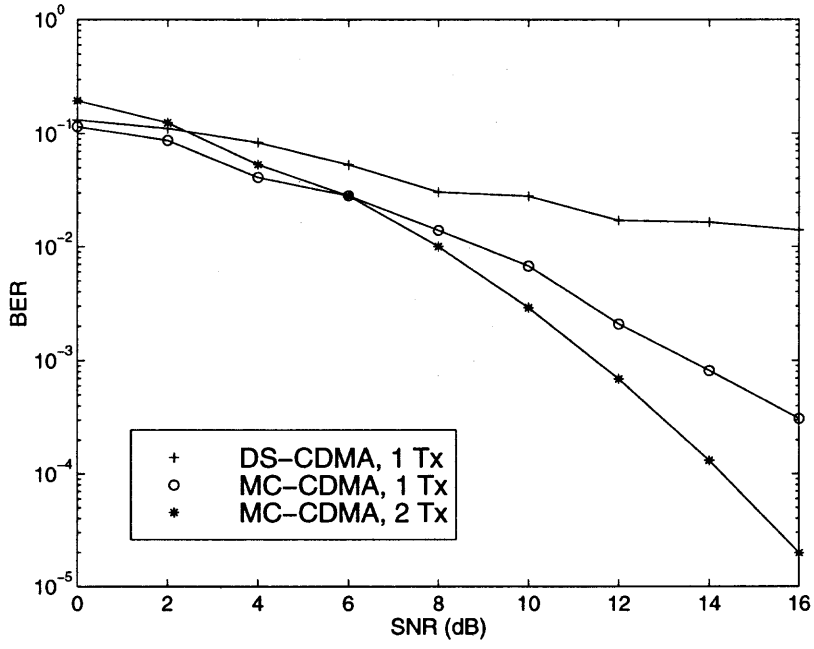

Figure 3.2 BER versus SNR for DS-CDMA, MC-CDMA with one antenna and with two antennas, K=10

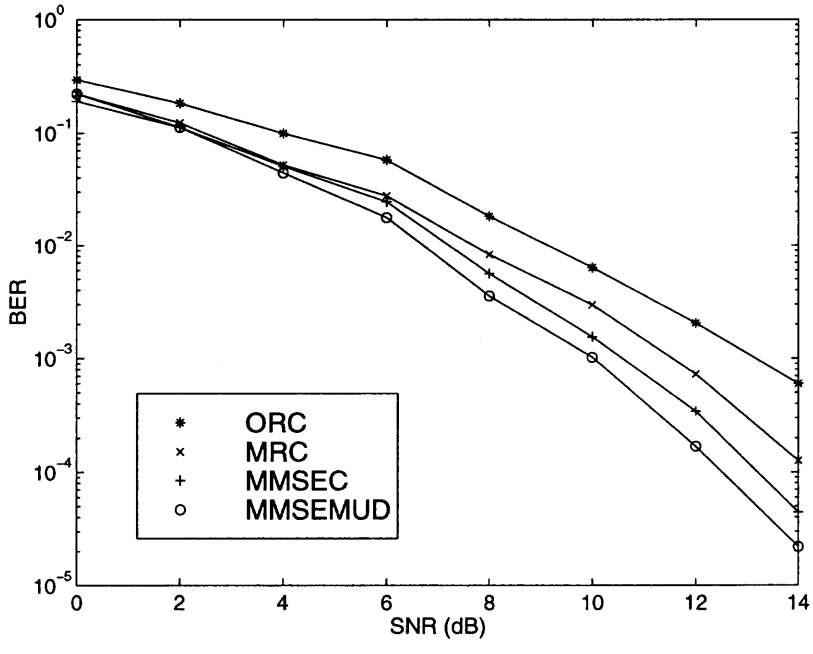

Figure 3.3 BER versus SNR for MC-CDMA with transmit diversity, K=10

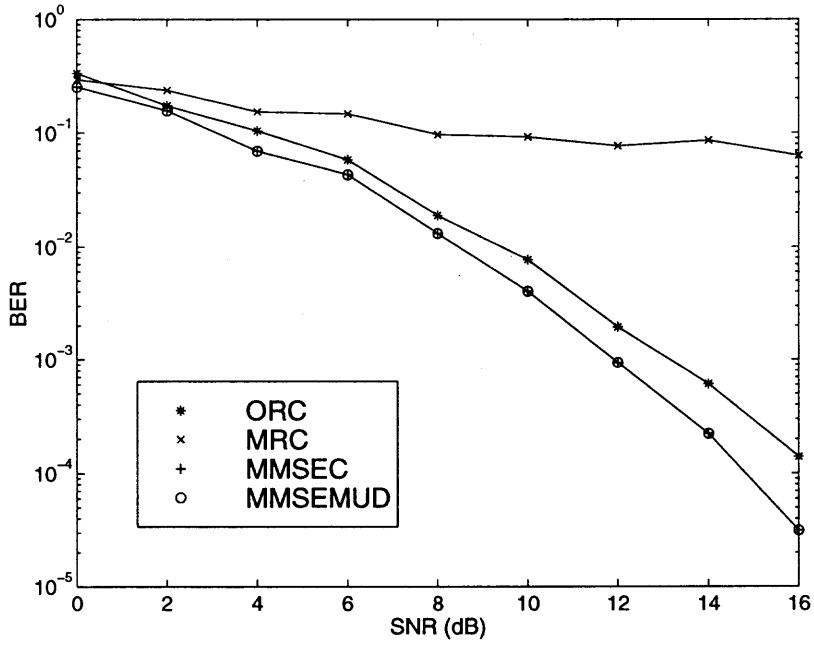

Figure 3.4 BER versus SNR for MC-CDMA with transmit diversity, K=32

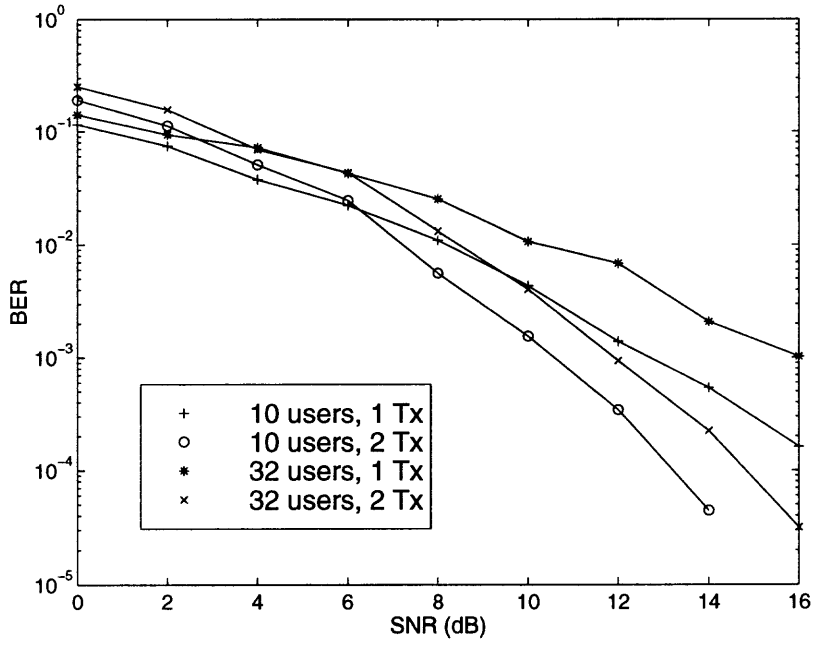

Figure 3.5 BER versus SNR for MC-CDMA with transmit diversity, MMSE per carrier combiner

3.3 Channel Estimation

In the receiver design in section 3.2, the channel state information is assumed to be known. In practice, the receiver has to estimate the channel response. The reference signal is needed for the receiver to estimate the channel. To provide with the reference signal for the receiver, the transmitter can transmit pilot signals. In a CDMA system, the pilot signal can be transmitted using a particular spreading code, that is the pilot signal is transmitted by pilot channel. In downlink, the common pilot channel can be used by all the mobile users. The pilot signal can also be time-multiplexed [11, 12, 56] with a user's data and spread by the user's spreading code [23, 55]. In this case, each user uses its particular pilot symbols to estimate the channel. Since the pilot symbols are not transmitted continuously, the receiver has to interpolate the estimated channel to do demodulation. In next sections, after briefly introduce the wide-sense-stationary and uncorrelated scattering (WSSUS) channel model for the wireless communication channel, we shall study the performance of the MC-CDMA system with space-time coding when the channel is estimated using either pilot channels or pilot symbols.

3.3.1 Wide-Sense-Stationary and Uncorrelated Scattering Channel Model

In wireless communication systems, the received signal experiences significant power fluctuation due to fading. Signal fading is caused by multipath propagation in the form of scattering, reflection, and refraction. The propagation path or paths change with the movement of the mobile unit and/or the movement of its surroundings in the propagation environment.

A fading multipath channel is generally characterized as a linear, time-varying system having an impulse response $c(\tau; t)$ which is a wide-sense stationary random in the t-variable. By assuming that the multipath signals propagating through the channel at different delays are uncorrelated, the channel is modeled as a wide-sense

stationary uncorrelated scattering, or WSSUS, channel [6, 70]. When there are a large number of scatters in the channel that contribute to the signal at the receiver, as is the case in ionospheric or tropospheric signal propagation, the central limit theorem can be applied. In this case, the time-variant impulse response $c(\tau;t)$ is a complex-valued Gaussian random process in the t variable. If the process is zero-mean, then the envelope of the channel impulse response at any time instant has a Rayleigh probability distribution and the phase is uniformly distributed in the interval $(0, 2\pi)$). Time variations in the channel impulse can be characterized by the autocorrelation function of $c(\tau;t)$ as

$$\phi_c(\tau_1, \tau_2; \triangle t) = \frac{1}{2} E[c^*(\tau_1; t) c(\tau_2; t + \triangle t)]. \tag{3.24}$$

Since the scattering at two different delays is uncorrelated, we have

$$\phi_c(\tau_1, \tau_2; \triangle t) = \phi_c(\tau_1; \triangle t)\delta(\tau_1 - \tau_2). \tag{3.25}$$

The typical autocorrelation function for mobile communication channel is given by [42]

$$\phi_c(\tau; \triangle t) = J_0(2\pi f_d \triangle t), \tag{3.26}$$

where $J_0(x)$ is the zeroth-order Bessel function of the first kind, f_d is Doppler frequency. If we let $\triangle t = 0$, the resulting autocorrelation function $\phi_c(\tau) \triangleq \phi_c(\tau; 0)$ is simply the average power output of the channel as a function of the time delay τ. $\phi_c(\tau)$ is called the delay power spectrum or the multipath intensity profile.

Time variations in the channel impulse response or frequency response result in frequency spreading, generally called Doppler spreading, of the signal transmitted through the channel. Multipath propagation results in spreading the transmitted signal in time. Consequently, a fading multipath channel may be generally characterized as a doubly spread channel in time and frequency. A doubly spread channel may be characterized by the scattering function $S(\tau; \lambda)$, which is given by the Fourier

transform of $\phi_c(\tau; \triangle t)$ in the $\triangle t$ variable. That is,

$$S(\tau; \lambda) = \int_{-\infty}^{\infty} \phi_c(\tau; \triangle t) e^{-j2\pi\lambda\triangle t} d\triangle t. \tag{3.27}$$

Scattering function is a measure of the power spectrum of the channel at delay τ and frequency offset λ. From the scattering function, we obtain the delay power spectrum of the channel by simply averaging $S(\tau; \lambda)$ over λ, i.e.,

$$\phi_c(\tau) = \int_{-\infty}^{\infty} S(\tau; \lambda) d\lambda. \tag{3.28}$$

Similarly, the Doppler power spectrum is

$$S_c(\lambda) = \int_{0}^{\infty} S(\tau; \lambda) d\tau. \tag{3.29}$$

The range of values over which the delay power spectrum $\phi_c(\tau)$ is nonzero is defined as the multipath spread T_m of the channel. The channel coherence bandwidth B_{coh} is defined as the reciprocal of the multipath spread, i.e. $B_{coh} = 1/T_m$. B_{coh} provides us with a measure of the width of the frequency band over which the fading is highly correlated. Similarly, the range of values over which the Doppler power spectrum $S_c(\lambda)$ is nonzero is defined as the Doppler spread B_d of the channel. The value of the Doppler spread B_d provides a measure of how rapidly the channel impulse varies in time. The channel coherence time T_{coh} is defined as the reciprocal of the Doppler spread, i.e. $T_{coh} = 1/B_d$.

When the bandwidth W of the transmitted signal is much smaller than the coherence bandwidth of the channel, i.e., $W \ll B_{coh}$, all the frequency components in the transmitted signal undergo the same attenuation and phase shift in transmission through the channel. Such a channel is called *frequency-nonselective* or *flat fading.* A frequency-nonselective fading channel has a time-varying multiplicative effect on the transmitted signal. When the transmitted signal has a bandwidth W greater than the coherence bandwidth B_{coh} of the channel, the frequency components of the transmitted signal with frequency separation exceeding B_{coh} are subjected to

different gains and phase shift. In such a case, the channel is said to be *frequency-selective.* When $W \gg B_{coh}$, the multipath components in the channel response that are separated in delay by at least $1/W$ are resolvable. In this case, if we use the sampling theorem to represent the resolvable received signal components, the time-varying channel response can be represented as[70]

$$c(\tau;t) = \sum_{l=1}^{L} h_l(t)\delta(\tau - l/W), \tag{3.30}$$

where $h_l(t)$ is the complex-valued channel gain of the lth multipath component and L is the number of resolvable multipath components. L is given by $L = \lfloor T_m W \rfloor + 1$. The tap gains $\{h_l(t)\}$ are modeled as wide-sense stationary mutually uncorrelated random processes.

3.3.2 Channel Estimation Using Pilot Channels

In IS-95 and CDMA2000, there is pilot channel in the downlink. The receiver at mobile can use the pilot channel to estimate the channel state and do coherent demodulation. In the MC-CDMA system with transmit diversity, each transmit antenna can also uses a pilot channel as in IS-95 and CDMA2000 to enable the receiver to estimate the channel. Denote the channelization codes for transmit antenna 0 and transmit antenna 1 as $\mathbf{s}_{p0}$ and $\mathbf{s}_{p1}$. Let $\mathbf{s}'_k$ and $\mathbf{s}'_{pi}$ be the inverse Fourier transform of the spreading code of user k and the code of the pilot channel of antenna i respectively. Let $\tilde{\mathbf{s}}_k$ and $\tilde{\mathbf{s}}_{pi}$ be the code vectors that add a cyclic prefix of length P to the spreading codes $\mathbf{s}'_k$ and $\mathbf{s}'_{pi}$. The transmitted signal is the superposition of the pilot signal and K users' signal. The transmitted signals in block $2n$ and block $2n+1$ at transmit antenna 0 are given by

$$\begin{aligned} \mathbf{x}_0[2n] &= A_p\tilde{\mathbf{s}}_{p0} + \sum_{k=1}^{K} A_k\tilde{\mathbf{s}}_k b_k[2n] \\ \mathbf{x}_0[2n+1] &= -A_p\tilde{\mathbf{s}}_{p1} - \sum_{k=1}^{K} A_k\tilde{\mathbf{s}}_k b_k[2n+1] \end{aligned} \tag{3.31}$$

The transmitted signals in block $2n$ and block $2n+1$ at transmit antenna 1 are given by

$$\begin{aligned} \mathbf{x}_1[2n] &= A_p\tilde{\mathbf{s}}_{p1} + \sum_{k=1}^{K} A_k\tilde{\mathbf{s}}_k b_k[2n+1] \\ \mathbf{x}_1[2n+1] &= -A_p\tilde{\mathbf{s}}_{p0} - \sum_{k=1}^{K} A_k\tilde{\mathbf{s}}_k b_k[2n] \end{aligned} \tag{3.32}$$

Assume that the channel is slow fading so that the channel impulse response in two consecutive data block is essentially the same. Denote the impulse response of the channel from transmit antenna $i, i = 0, 1$ in block $2n$ and block $2n+1$ as $\mathbf{h}_i[n] = [h_{i1}[n]\ h_{i2}[n],\ \ldots,\ h_{iL}[n]]^T, i = 1, 2$. The $N \times 1$ received signal vectors in block $2n$ and block $2n+1$ after removing the signal corresponding to the cyclic prefix is given by

$$\begin{aligned} \mathbf{r}[2n] &= \mathbf{H}_{0n}\mathbf{x}_0[2n] + \mathbf{H}_{1n}\mathbf{x}_1[2n] + \mathbf{v}[2n] \\ \mathbf{r}[2n+1] &= \mathbf{H}_{0n}\mathbf{x}_0[2n+1] + \mathbf{H}_{1n}\mathbf{x}_1[2n+1] + \mathbf{v}[2n+1], \end{aligned} \tag{3.33}$$

where $\mathbf{v}[2n]$ and $\mathbf{v}[2n+1]$ are white Gaussian noise and matrix $\mathbf{H}_{0n}$ is given by

$$\mathbf{H}_{0n} = \begin{bmatrix} h_{01}[n] & \ldots & h_{0L}[n] & 0 \\ \ddots & & & \ddots \\ 0 & h_{01}[n] & \ldots & h_{0L}[n] \end{bmatrix}, \tag{3.34}$$

and matrix $\mathbf{H}_{1n}$ is defined in a similar manner. Define matrix $\tilde{\mathbf{C}}_{p0}$ as

$$\tilde{\mathbf{C}}_{p0} = \begin{bmatrix} \tilde{\mathbf{s}}_{p0}[L] & \ldots & \tilde{\mathbf{s}}_{p0}[2] & \tilde{\mathbf{s}}_{p0}[1] \\ \tilde{\mathbf{s}}_{p0}[L+1] & \ldots & \tilde{\mathbf{s}}_{p0}[3] & \tilde{\mathbf{s}}_{p0}[2] \\ \vdots & & \vdots & \vdots \\ \tilde{\mathbf{s}}_{p0}[N-L+1] & \ldots & \tilde{\mathbf{s}}_{p0}[N-1] & \tilde{\mathbf{s}}_{p0}[N] \end{bmatrix}, \tag{3.35}$$

and define matrix $\tilde{\mathbf{C}}_{p1}$ in a similar way as $\tilde{\mathbf{C}}_{p0}$. The received signal vector in (3.33) can also be expressed as

$$\begin{aligned} \mathbf{r}[2n] &= A_p\tilde{\mathbf{C}}_{p0}\mathbf{h}_0[n] + A_p\tilde{\mathbf{C}}_{p1}\mathbf{h}_1[n] + \mathbf{I}[2n] + \mathbf{v}[2n] \\ \mathbf{r}[2n+1] &= -A_p\tilde{\mathbf{C}}_{p1}\mathbf{h}_0[n] + A_p\tilde{\mathbf{C}}_{p0}\mathbf{h}_1[n] + \mathbf{I}[2n+1] + \mathbf{v}[2n+1], \end{aligned} \tag{3.36}$$

where $\mathbf{I}[2n]$ and $\mathbf{I}[2n+1]$ are signals of K users which are considered as the interference to the pilot signal when the receiver estimates the channel. Let $\tilde{\mathbf{r}}[n] = [\mathbf{r}[2n]^T\ \mathbf{r}[2n+1]^T]^T$ $\mathbf{h}[n] = [\mathbf{h}_0[n]^T, \mathbf{h}_1[n]^T]^T$, and

$$\tilde{\mathbf{C}} = \begin{bmatrix} \tilde{\mathbf{C}}_{p0} & \tilde{\mathbf{C}}_{p1} \\ -\tilde{\mathbf{C}}_{p1} & \tilde{\mathbf{C}}_{p0} \end{bmatrix}. \tag{3.37}$$

Then, we have

$$\tilde{\mathbf{r}}[n] = A_p\tilde{\mathbf{C}}\mathbf{h}[n] + \tilde{\mathbf{I}}[n] + \tilde{\mathbf{v}}[n], \tag{3.38}$$

where $\tilde{\mathbf{I}}[n] = [\mathbf{I}[2n]^T,\ \mathbf{I}[2n+1]^T]^T$ and $\tilde{\mathbf{v}}[n] = [\mathbf{v}[2n]^T,\ \mathbf{v}[2n+1]^T]^T$. Suppose $4Q+2$ blocks of received data from block $2(n-Q)$ to block $2(n+Q)+1$ are available. Let $\mathbf{r} = [\mathbf{r}[2(n-Q)]\ \mathbf{r}[2(n-Q)+1]\ \ldots\ \mathbf{r}[2n]\ \mathbf{r}[2n+1]\ \ldots\ \mathbf{r}[2(n+Q)]\ \mathbf{r}[2(n+Q)+1]]^T$. The receiver uses these $4Q+2$ blocks of data to estimated the channel.

A. MMSE channel estimator

The MMSE channel estimator for channel coefficients $\mathbf{h}$[n] is given by

$$\mathbf{w} = \mathbf{R}^{-1}\mathbf{p}, \tag{3.39}$$

where $\mathbf{R} = E(\mathbf{r}\mathbf{r}^H)$ is the covariance matrix of $\mathbf{r}$ and $\mathbf{p} = E(\mathbf{r}\mathbf{h}^H(n))$ is the crosscorrelation between the data vector and the channel coefficients. To calculate $\mathbf{R}$ and $\mathbf{p}$, the receiver needs the knowledge of the all the spreading codes of the active users, the amplitudes of the users' signal, the autocorrelation function and the multipath intensity profile. While the MMSE channel estimator is optimal linear estimator that minimizes the mean squared error between the channel coefficients and the estimate of the channel, it needs to invert the covariance matrix of size $(4Q+2)N \times (4Q+2)N$, which requires much computation.

B. LSE channel channel estimator

LSE channel estimator first obtains instantaneous estimates of the channel coefficients using least square error criterion, then use a linear filter to smooth the instantaneous estimates of the channel coefficients. The instantaneous estimate of the

channel is given by

$$\hat{\mathbf{h}}[n] = (\tilde{\mathbf{C}}^H\tilde{\mathbf{C}})^{-1}\tilde{\mathbf{C}}^H\tilde{\mathbf{r}}[n]. \tag{3.40}$$

Since the receiver knows the spreading codes of the pilot channels, the matrix $(\tilde{\mathbf{C}}^H\tilde{\mathbf{C}})^{-1}\tilde{\mathbf{C}}^H$ can be calculated off-line. Therefore, to obtain an instantaneous estimate of the channel, the receiver only need to multiply the received data vector by a $2L \times 2N$ matrix. If the channel autocorrelation function, or equivalently, the Doppler spectrum is known, the optimal MMSE linear filter to smooth the instantaneous estimates is the Wiener filter that has a frequency response equal to the square root of the Doppler spectrum. To reduce the delay of the channel estimation, a FIR MMSE filter can be used instead of the optimal Wiener filter, which can be obtained as follows. Denote the ith element of $\hat{\mathbf{h}}[n]$ as $\hat{\mathbf{h}}_i[n]$. If $2Q+1$ instantaneous estimates are available, we define a vector $\hat{\mathbf{h}}_i = [\hat{\mathbf{h}}_i[n-Q], \ldots, \hat{\mathbf{h}}_i[n], \ldots, \hat{\mathbf{h}}_i[n+Q]]^T$. We can use the channel autocorrelation function to calculate the covariance matrix of vector $\hat{\mathbf{h}}_i$, $\mathbf{R}_h$, and the crosscorrelation between $\mathbf{h}_i[n]$ and $\hat{\mathbf{h}}_i$, $\mathbf{p}_h$. Then the FIR MMSE filter is $\mathbf{w}_i = \mathbf{R}_h^{-1}\mathbf{p}_h$.

In general, the Doppler spectrum is not known, or it may even change with time. The best knowledge of the Doppler spectrum is that is a lowpass spectrum with a maximum Doppler frequency f_d. Therefore, we can use an ideal low pass filter with a cut-off frequency equal to or greater than f_d as the filter to smooth the instantaneous estimate of the channel. The nth tap of impulse response of the ideal lowpass filter is given by

$$f(n) = 2f_d sinc(2\pi n f_d T), \tag{3.41}$$

where $sinc(x) = \frac{sin(\pi x)}{\pi x}$ and T is the duration of a data block. In practice, to reduce the delay and memory, the lowpass filter can be truncated to a FIR filter.

3.3.3 Channel Estimation Using Pilot Symbols

If we use the pilot channel to estimate the channel state, each antenna needs one spreading code. When the number of transmit antennas increases, the receiver needs more spreading codes which reduces the number of codes available to the users. Furthermore, when the base station uses transmit beamformer to reduce the interference between the users at different locations, the users at different locations should be assigned different spreading codes for the pilot channels, which further reduce the number of spreading codes available and limit the number of users in a cell. This problem can be avoided if each mobile uses time multiplexed pilot symbols to estimate the channel.

Suppose that in every $2M$ data blocks, two blocks of the pilot symbols are inserted. The pilot signal is unmodulated spreading code. Assume that the desired user is user 1. The transmitted signals at antenna 0 in nth the pilot data blocks of user 1 are given by

$$\begin{aligned} \mathbf{x}_0[2nM] &= A_1\tilde{\mathbf{s}}_1 + \sum_{k=2}^{K} A_k\tilde{\mathbf{s}}_k b_k[2n] \\ \mathbf{x}_0[2nM+1] &= -A_1\tilde{\mathbf{s}}_1 - \sum_{k=2}^{K} A_k\tilde{\mathbf{s}}_k b_k[2n+1] \end{aligned} \tag{3.42}$$

The transmitted signals at antenna 1 in the nth pilot data blocks are given by

$$\begin{aligned} \mathbf{x}_1[2nM] &= A_1\tilde{\mathbf{s}}_1 + \sum_{k=2}^{K} A_k\tilde{\mathbf{s}}_k b_k[2n] \\ \mathbf{x}_1[2nM+1] &= A_1\tilde{\mathbf{s}}_1 + \sum_{k=2}^{K} A_k\tilde{\mathbf{s}}_k b_k[2n+1] \end{aligned} \tag{3.43}$$

Define a matrix $\tilde{\mathbf{C}}_1$ in the same manner as $\tilde{\mathbf{C}}_{p0}$ in (3.35), the received signal is given by

$$\begin{aligned} \mathbf{r}[2nM] &= A_1\tilde{\mathbf{C}}_1\mathbf{h}_0[nM] + A_1\tilde{\mathbf{C}}_1\mathbf{h}_1[nM] + \mathbf{I}[2nM] + \mathbf{v}[2nM] \\ \mathbf{r}[2nM+1] &= -A_1\tilde{\mathbf{C}}_1\mathbf{h}_0[nM] + A_1\tilde{\mathbf{C}}_1\mathbf{h}_1[nM] + \mathbf{I}[2nM+1] \\ &\quad +\mathbf{v}[2nM+1], \end{aligned} \tag{3.44}$$

where $\mathbf{I}(2nM)$ and $\mathbf{I}(2nM+1)$ are interference users' signals, $\mathbf{v}(2nM)$ and $\mathbf{v}(2nM+1)$ are white Gaussian noise.

Suppose that $4Q$ data blocks corresponding to the pilot signals, $\mathbf{r}[2(n+m)M]$ $\mathbf{r}[2(n+m)M+1]$, $m=-Q+1,\ldots,-1,0,1,Q$, are available. The receiver can use these data to estimate the channel impulse response in the $(nM+i)$th, $i=2,\ldots,M-1$ block. The MMSE channel estimator can be found if the channel autocorrelation function, multipath intensity profile, all the users' codes and transmitted power and the noise variance are known. The MMSE channel estimator should invert a $4NQ\times 4NQ$ matrix, which needs too much computation for a practical system. Thus, as in the previous section, we can first use least squared error criterion to obtain the instantaneous channel estimates, then smooth the instantaneous estimates to reduce the variance of the estimate errors. Let $\tilde{\mathbf{r}}[nM]=[\mathbf{r}[2nM]^T\ \mathbf{r}[2nM+1]^T]^T$ $\mathbf{h}[nM]=[\mathbf{h}_0[nM]^T,\mathbf{h}_1[nM]^T]^T$, and

$$\tilde{\mathbf{C}}=\begin{bmatrix}\tilde{\mathbf{C}}_1 & \tilde{\mathbf{C}}_1\\ -\tilde{\mathbf{C}}_1 & \tilde{\mathbf{C}}_1\end{bmatrix}. \tag{3.45}$$

Then, we have

$$\tilde{\mathbf{r}}[nM]=A_1\tilde{\mathbf{C}}\mathbf{h}[nM]+\tilde{\mathbf{I}}[nM]+\tilde{\mathbf{v}}[nM], \tag{3.46}$$

where $\tilde{\mathbf{I}}[nM]=[\mathbf{I}[2nM]^T,\ \mathbf{I}[2nM+1]^T]^T$ and $\tilde{\mathbf{v}}[nM]=[\mathbf{v}[2nM]^T,\ \mathbf{v}[2nM+1]^T]^T$. As in (3.40), the LSE estimate of the channel is given by

$$\hat{\mathbf{h}}[nM]=(\tilde{\mathbf{C}}^H\tilde{\mathbf{C}})^{-1}\tilde{\mathbf{C}}^H\tilde{\mathbf{r}}[nM]. \tag{3.47}$$

Since the Doppler spectrum is usually not known, the optimal smoothing filter is difficult to find. We then can use a ideal lowpass linear filter to interpolate the instantaneous channel estimates to obtain final channel estimates. The nth tap of impulse response of the ideal interpolating filter for $\mathbf{h}[nM+i]$, $i=2,\ldots,M-1$ blocks given by

$$f_i(n)=2f_d sinc(2\pi(nM-i)f_dT), i=2,\ldots,M-1, \tag{3.48}$$

where T is the duration of a data block.

3.3.4 Simulation Results

In this section, we use simulation results to compare the system performance under different channel conditions when either pilot channels or pilot symbols is used to estimate the channel. In simulation, a two path WSSUS channel is generated by using the Monte Carlo method [114]. The delay spread is uniformly distributed in the guard interval whose length is assmued to be 1/4 of the data block. Two paths have the same variance σ_h^2. the average squared error of the channel estimates when pilot channels are used. All the users have the same power. Define the ratio of the power of pilot channel and the power of the data as $P = A_p^2/A_1^2$. In Fig. 3.6 P is $P = 0dB$ for $f_dT_b = 0.001$ and $P = 6dB$ for $f_dT_b = 0.005$. We see that high power of the pilot channel is needed for the channel estimator to maintain good performance when the Doppler frequency is large. In Fig. 3.7, Fig. 3.8, Fig. 3.9 and Fig. 3.10, the bit error rate under different channel conditions are shown. It is observed that performance degrades slightly when the channel is estimated. Fig. 3.11 demonstrates average squared error of the channel estimate when pilot symbols are used. Compared with the estimator using pilot channels, the channel estimator using pilot symbols needs higher power to compensate the less number of the instantaneous channel estimates available to smooth the channel estimates. When powers of all the users' pilot symbols are raised, interference level is also raised. Therefore, channel estimate error is large when the Doppler frequency is high. Bit error rates of the system for different number of users when $f_dT_b = 0.01$ are demonstrated in Fig. 3.12 and Fig. 3.13. Since the channel estimate error is small, the BER is slightly larger when the estimated channels are used. In Fig. 3.14 and Fig. 3.15, BER is shown for $f_dT_b = 0.005$. In this case, interference degrades the performance of the channel estimator, especially when the number of the active users is large. Therefore, bit error rate using the estimated channel is much larger than the ideal case.

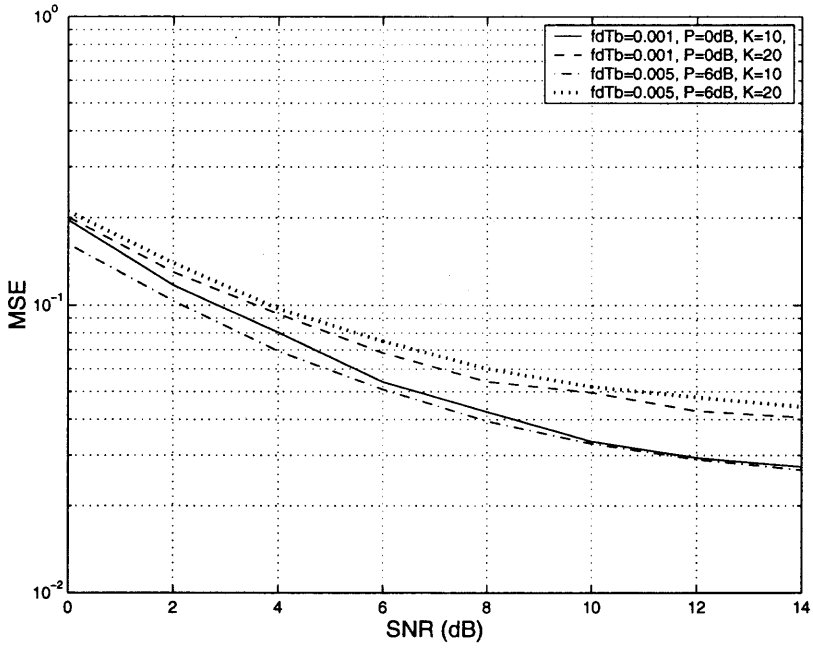

Figure 3.6 Mean squared-error of the channel estimator using pilot channels.

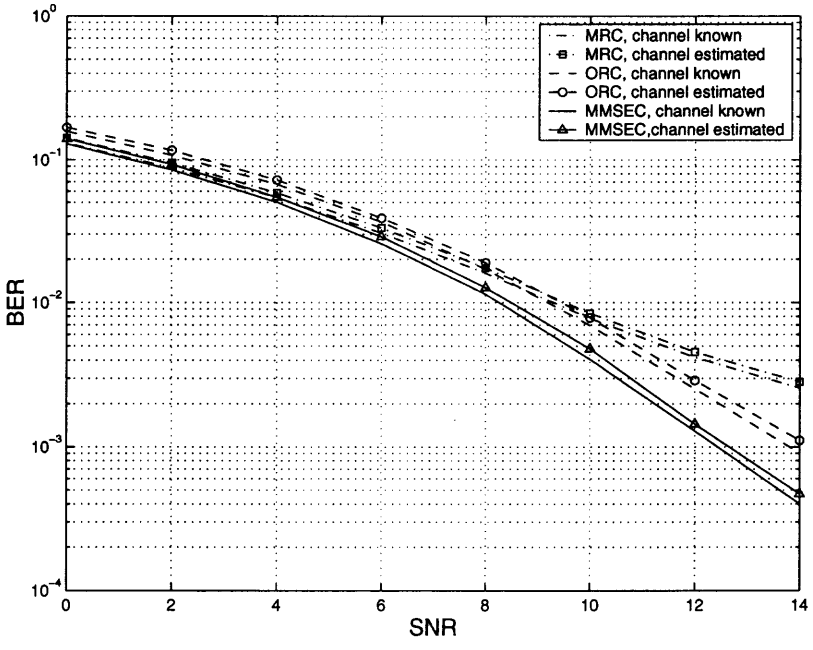

Figure 3.7 Bit error rate of MC-CDMA with pilot channels. $f_d T_b = 0.001$, K=10, P=0dB.

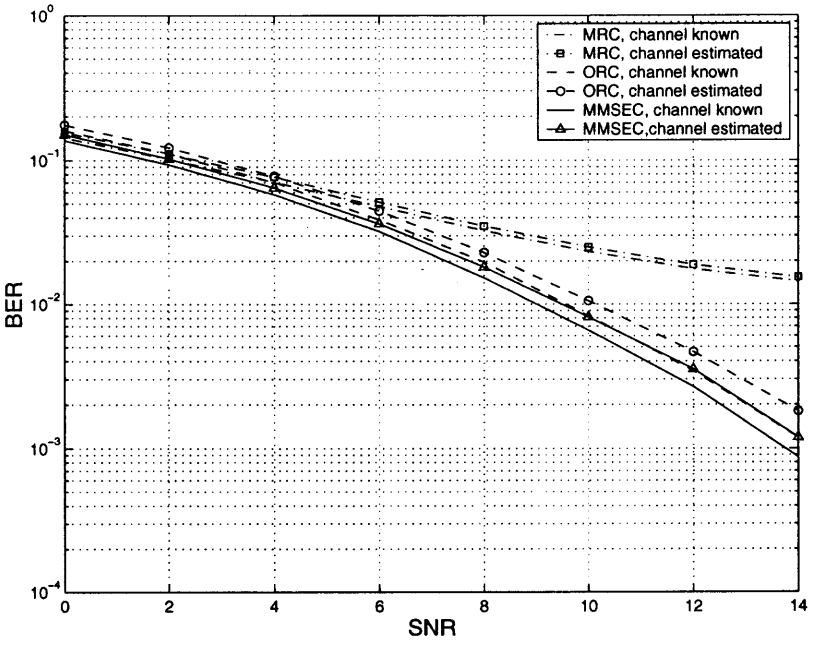

Figure 3.8 Bit error rate of MC-CDMA with pilot channels. $f_d T_b = 0.001$, K=20, P=0dB.

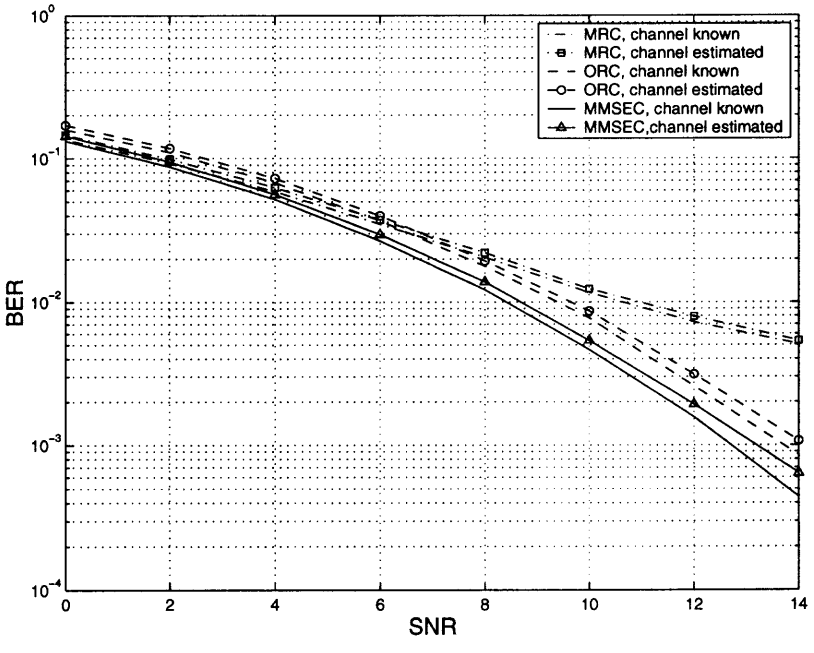

Figure 3.9 Bit error rate of MC-CDMA with pilot channels. $f_d T_b = 0.005$, K=10, P=6dB.

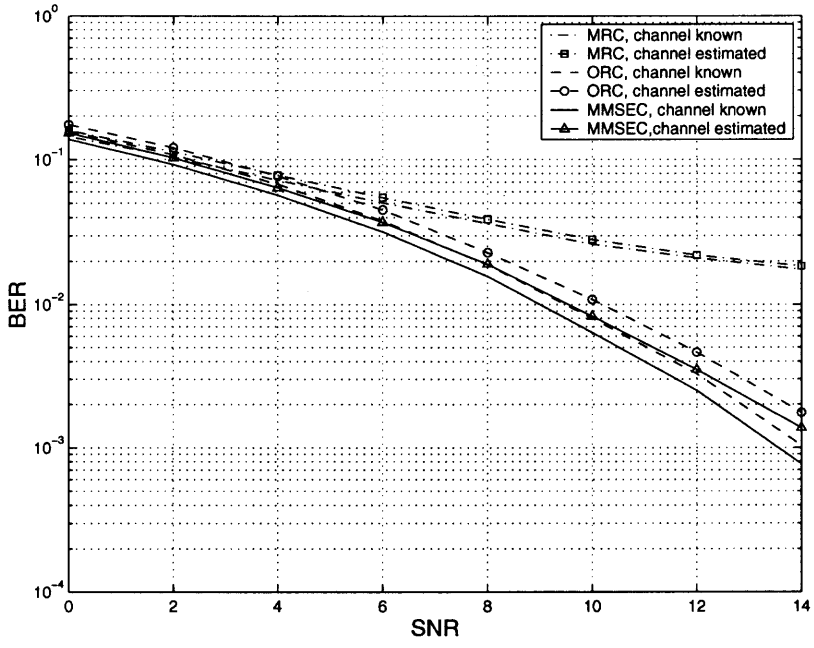

Figure 3.10 Bit error rate of MC-CDMA with pilot channels. $f_d T_b = 0.005$, K=20, P=6dB.

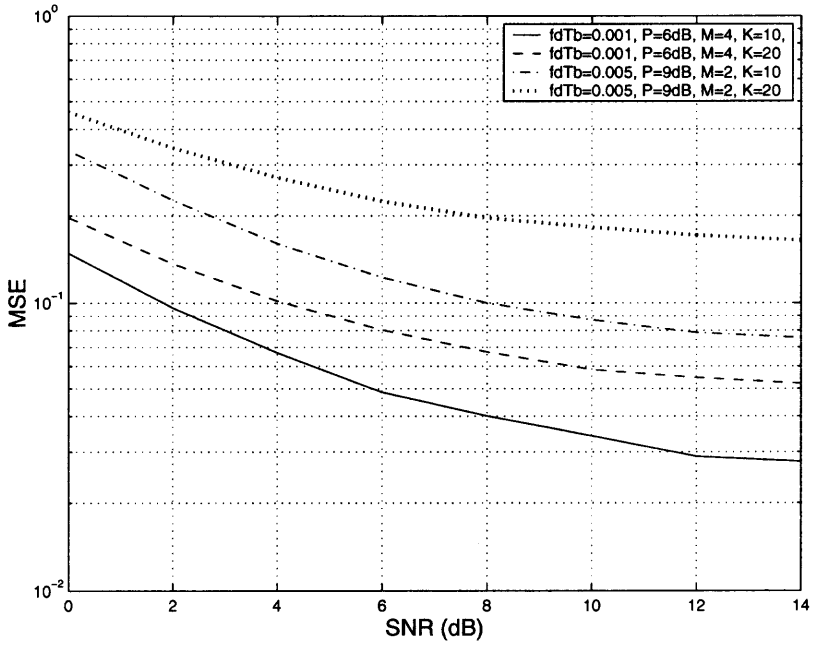

Figure 3.11 Mean squared-error of the channel estimator using pilot symbols.

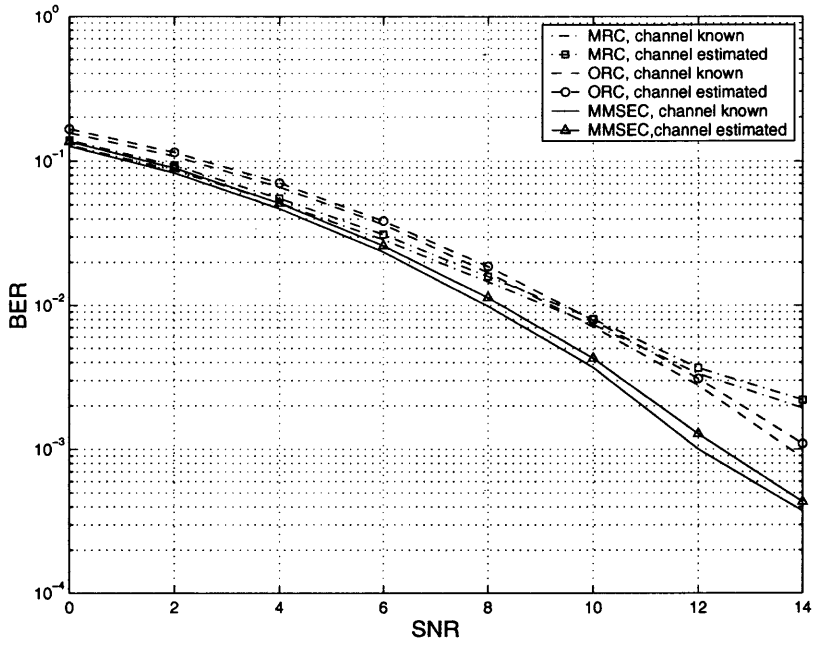

Figure 3.12 Bit error rate of MC-CDMA with pilot symbols. $f_dT_b = 0.001$, K=10, P=6dB, M=4

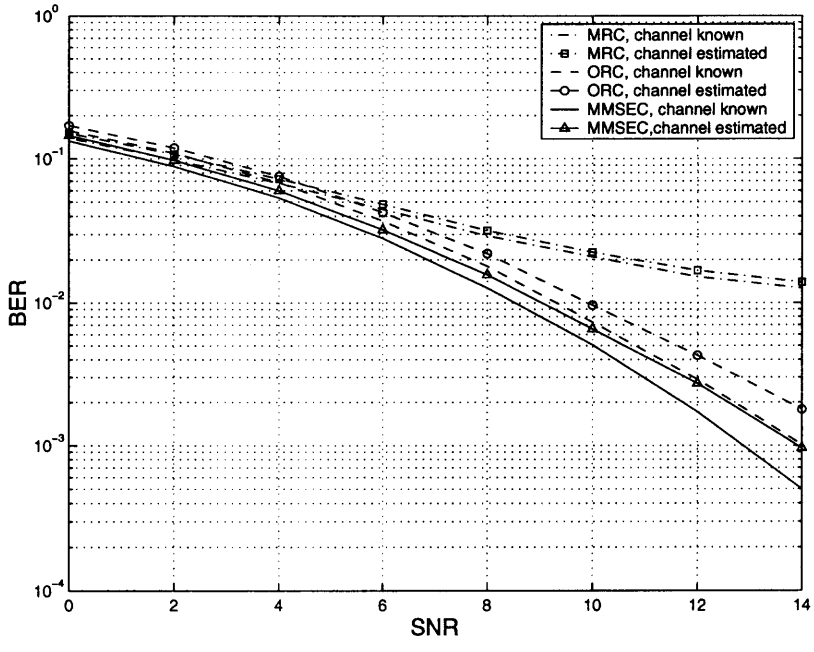

Figure 3.13 Bit error rate of MC-CDMA with pilot symbols. $f_dT_b = 0.001$, K=20, P=6dB, M=4

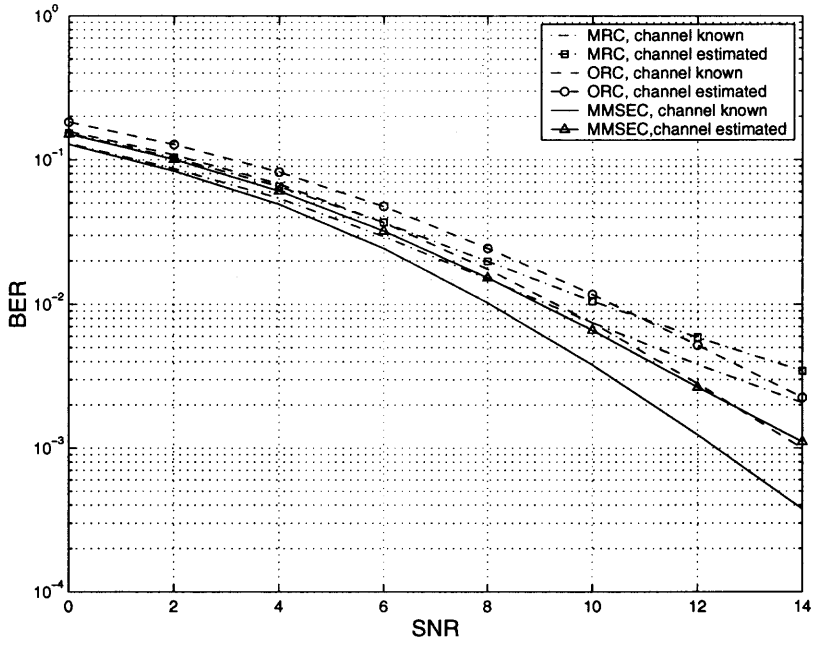

Figure 3.14 Bit error rate of MC-CDMA with pilot symbols. $f_dT_b = 0.005$, K=10, P=9dB, M=2

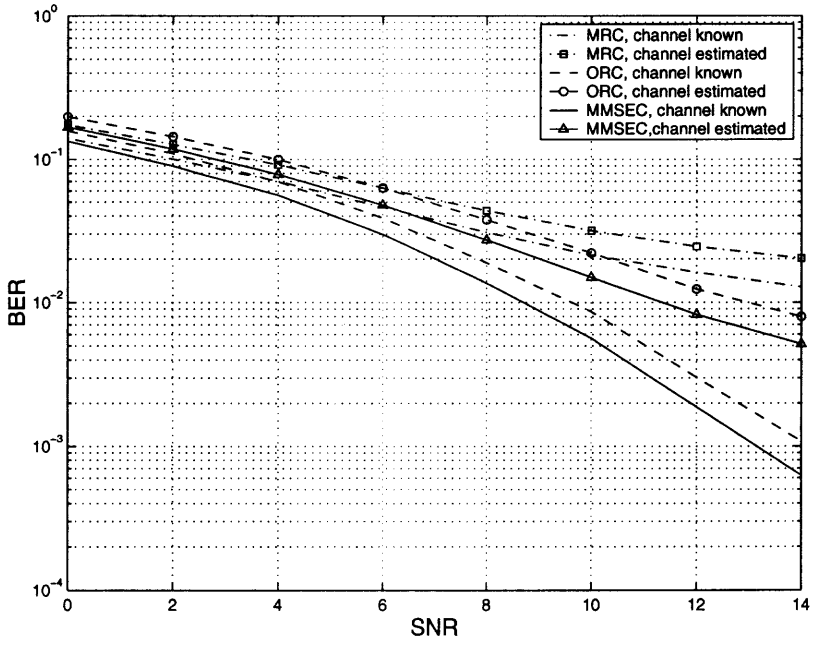

Figure 3.15 Bit error rate of MC-CDMA with pilot symbols. $f_dT_b = 0.005$, K=20, P=9dB, M=2

3.4 Summary

In this chapter, we apply the block space-time codes that is originally proposed for a narrow-band system to wideband multicarrier CDMA systems. Our emphasis is on designing receiver that can jointly decode the space-time codes and suppress multiple access interference. Among the proposed four receivers, MMSE combiner is the best trade-off between the performance and the complexity. The channel estimation using pilot channels and pilot symbols is studied for the MC-CDMA with space-time coding. While the channel estimator using pilot channels has better performance, it is not suitable for a system with many transmitted antennas or with transmit beamformer. On the other hand, since the channel estimator using pilot symbols does not using extra channels, more spreading codes are available for mobile users, thereby more users can be accommodated in a cell. However, in a fading channel with relative large Doppler frequency, a sufficient number of pilot symbols is required for estimating the channel, which reduces the frequency efficiency.

CHAPTER 4

PACKET-SWITCHED CDMA RANDOM ACCESS SYSTEMS WITH PACKET COMBINING

Direct sequence code division multiple access (DS-CDMA) has been investigated to provide packet multiple access and high data rates in wireless communications [52]. In a random access packet switched CDMA system, two or more users can simultaneously transmit data packets (with some error rate); while in other ALOHA random access systems, if two or more transmissions occur, all the packets are destroyed. Therefore, CDMA random access systems have the potential for improving on the capacity of ALOHA. The performance of the CDMA random access systems was analyzed in [72] with the assumption that the multiple-access interference (MAI) is the dominant cause of errors. The throughput analyses of the CDMA random access systems in additive white Gaussian noise (AWGN) channels were presented in [16, 66, 75, 79]. It was shown that the CDMA system with error correction coding has the same or lightly better throughput performance compared to a multichannel narrow-band ALOHA system with the same total bandwidth [16]. The CDMA random access systems studied in [16, 66, 75, 79] employ matched filter receivers that limit their interference suppression capability, therefore, their throughput is limited. Recently, increased attention has been paid to CDMA random access systems with multiuser detection [63, 71, 74]. It is shown that multiuser detection significantly improve the system throughput.

Automatic repeat request (ARQ) schemes are commonly used in a communication system with feedback channels [106]. In the pure and type-I hybrid ARQ schemes, packets in error that must be retransmitted are discarded and replaced by their copies. In the type-II hybrid ARQ scheme, packets that must be retransmitted are not discarded, but are combined with their repeated copies. Code combing [13, 45] and diversity combing [106] are two commonly used packet combing schemes. In

code combing, the packets are concatenated to form code words from increasingly longer and low-rate codes. In diversity combing, packets are combined at the bit level, i.e., the individual bits from multiple, identical copies of a packet are combined to create a single packet [105]. Packet combing has been applied to CDMA random access systems to improve the system performance [4, 5, 9, 78, 99]. Average diversity combiner was analyzed for a CDMA system with convolutional coding [78]. In [9], both diversity combining and code combining are analyzed for CDMA random access systems without and with forward error correction (FEC) in AWGN channel. In [4, 5], a lower bound and an upper bound of the throughput of the CDMA random access system with diversity combing in fading channel are presented. The stability of the CDMA random access system with diversity combing was investigated in [99]. These packet combing schemes improve the performance, but they cannot effectively suppress the interference since the matched filter outputs are used as the input to the combiner. In [81, 82, 83, 84], optimum multiuser detector and linear multiuser detectors that use all the copies of the transmitted packets are proposed. The bit error rate (BER) and the network performance are analyzed for AWGN channel.

In this work, we study the performance of the DS-CDMA random access system with linear multiuser receivers and diversity combing in fading channels. Our performance analysis is performed for large systems with each user using random spreading sequences. We assume that the average arrival rate of the traffic and the processing gain tend to infinity but their ratio is fixed. Large system approach was used for analyzing the Erlang capacity of different teletraffic systems [41, 62]. In a large CDMA system in which the number of the active user K and the processing gain N tends to infinity and their ratio is fixed, it was shown [15, 98] that the output signal to noise ratio (SNR) converges to a deterministic limit in probability. While performance analysis for a CDMA random access system of finite size with diversity combing is very difficult (if possible), the asymptotic analysis for a large system is

tractable. Furthermore, the asymptotic results can predict the behavior of a system with moderate size and we can gain some insights into the system performance from the asymptotic results. The large systems we are interested in here are perhaps more relevant to future wireless systems. We shall analyze both slotted and unslotted CDMA random access systems. In general, analysis of unslotted CDMA systems is complicated because the multiuser interference experience by a packet varies continuously due to asynchronous packet arrivals and departures. However, in a large system no matter it is slotted or unslotted, the output SNR of linear receiver converges to a deterministic limit. Therefore, we can put the analysis of slotted and unslotted systems in one frame work. If the receiver combines the current retransmitted packet with all its previous transmitted copies, the bit error rate (BER) dramatically decreases with the number of transmissions increasing. Suppose that the receiver combines J identical copies of the desired user's packet. Compared to the receiver that discards all the packets fail in transmissions, we get a diversity gain plus an increased interference and noise suppression gain of J. Each retransmission has a random delay. If the delay is longer than the coherent time of the fading channel, each retransmitted packet undergoes independent fading, which provides diversity gain. In general, the interference users' information bits at each retransmission of the desired user's packet are uncorrelated and the noise are also uncorrelated. Therefore, we can coherently combine the desired user's signal but average out the interference and noise, which provides the interference and noise suppression gain. The packet success probability increases with the number of transmissions increasing, which in turn improves the system throughput.

4.1 System Description

We consider a DS-CDMA random access system consisting of a single base station and a total of M mobile wireless users. The users generate data packets and transmit

over a common wideband wireless channel to the base station. Each user uses a random signature sequence with processing gain of N chips per bit. Essentially, the channel access protocol is ALOHA. Each user can be in either one of the two operation modes: origination mode or backlog mode. In the origination mode, the user transmits a newly arriving packet. A user is considered to be in backlog mode when its previously transmitted packet was not successfully received by the base station and a retransmission is requested. We shall consider both the slotted system and the unslotted system with fixed packet length . In a slotted system, each user in the origination mode transmits a newly arriving packet in the first slot after the packet arrival. When the user enters the backlog mode, it retransmits the packet in the next slot with probability p_r. In an unslotted system, the user in the origination mode, upon receiving a new packet, transmits it immediately. If a user is backlogged, it retransmits the packet after a random delay. We assume that packets contain sufficient error detection capability so that the base station can detect all the error packets. The feedback channel is assumed to be error-free. For simplicity of analysis, we assume that the data are not encoded using any forward error correction (FEC) code though the error detection code should be used. This is somewhat unrealistic, but it is easy to extend the analysis in this work to the system with FEC. For the system with FEC, it is possible to retransmit a packet with a different code word. The receiver combines the packets at the code level as in type-II hybrid ARQ [45]. In this work, we assume that the backlogged user transmits a packet identical to the previous transmitted packet. The receiver processes the received data in each transmission at the bit level. The receiver has two ways to process the received packets. One is that it keeps the outputs of the detector and combines them in some ways (optimal or sub-optimal) to get decision statistic. The other way is to keep all the original received data in each transmission and do jointly detection based on these

data. The later method needs more memory and higher computation complexity, but may be able to get lower bit error probability.

In general, the composite arrivals have a steady-state probability distribution [72]. In this work, we assume that the composite arrival distribution is Poisson with arrival rate λ. We define the offered traffic load G as the average number of arriving packets in a packet duration T_p, i.e. $G \triangleq \lambda T_p$. Therefore, the probability that exactly k users transmit in a packet duration is

$$p(k) = \frac{(\lambda T_p)^k}{k!} e^{-\lambda T_p} = \frac{G^k}{k!} e^{-G} \tag{4.1}$$

We are here interested in a large system in which we have $G \to \infty$, $N \to \infty$ and $G/N = \alpha$. The large system essentially has infinite offered traffic load and bandwidth but the offered traffic load normalized by the processing gain is fixed. In a slotted system, it was shown [83] that the number of users K transmitting in a packet duration (also in a bit duration) is infinity and K/N converges to α in probability as $N \to \infty$. A heuristic proof is as follows. Since the number of users K in the system is a random Poisson variable with mean G, we can think K as the sum of N independent Poisson random variables with mean $G/N = \alpha$. By the Weak Law of Large Numbers, K/N converges to α in probability as $N \to \infty$. Unlike in a finite system in which the interference is variant in different transmissions, the effect of the interference to linear receivers in a large system is essentially the same in all the transmissions, which facilitates the performance analysis. One difficulty to analyze the performance of the unslotted CDMA packet network is that the interference in one packet duration is changing due to randomly arrivals and departures. In an unslotted system, We can also show that the number of the active user K in a bit duration normalized by the processing gain N also converges to α in probability as $N \to \infty$. We consider a bit duration from t to $t + T_b$ of the desire user. K_1 users arrived in the duration $(t - T_p,\ t - T_p + T_b]$ leave the system, K_2 users arrived in the duration $(t - T_p + T_b,\ t]$ stay in the system and K_3 users arrive in the system

in this bit duration. The number of active users in this particular bit duration is $K = K_2 + K_3 - K_1$. It is straightforward to show that K/N converges to α in probability as $N \to \infty$. Therefore, it is relative easy to characterize the effect of the interference for such a large unslotted system.

4.2 Bit Error Probability

We shall study the performance of MMSE receiver, decorrelator and matched filter receiver for both slotted and unslotted CDMA random access systems in multipath fading channels. The receivers utilize the statistics of all the received packets in different transmissions.

4.2.1 Slotted CDMA System

Suppose that the desired user failed to transmit a packet in $J-1$ transmissions and is transmitting a packet of its J^{th} time at the current slot. We consider one bit duration of the packet. Sampling the output of the chip-matched filter at the chip rate, we obtain a $N \times 1$ data vector for the j^{th} $(0 < j < J+1)$ transmission of the packet

$$\begin{aligned} \mathbf{y}(j) &= \sum_{l=1}^{L} s_{1l} a_{1l}(j) b_1 + \sum_{k=2}^{K(j)} \sum_{l}^{L} s_{kl}(j) a_{kl}(j) b_k(j) + \mathbf{n}(j) \\ &= S_1 \mathbf{a}_1(j) b_1 + S_2(j) A_2(j) b_2(j) + n(j) \qquad j = 1, \ldots, J, \end{aligned} \tag{4.2}$$

where $S_1 = [\mathbf{s}_{11}, \ldots, \mathbf{s}_{1L}]$, $\mathbf{a}_1(j) = [a_{11}, \ldots, a_{1L}]^T$, $S_2(j) = [\mathbf{s}_2(j), \ldots, \mathbf{s}_{K(j)}(j)]$ with $\mathbf{s}_k = [\mathbf{s}_{k1}(j), \ldots, \mathbf{s}_{kL}(j)]$, $A_2(j) = diag(\mathbf{a}_2(j), \ldots, \mathbf{a}_{K(j)}(j))$ with $\mathbf{a}_k = [a_{k1}, \ldots, a_{kL}]^T$, $\mathbf{b}_2(j) = [b_2(j), \ldots, b_{K(j)}(j)]$. BPSK modulation is used; thus, $b_k(j)$ is an equal-probable ± 1 random variable. We assume that user 1 is the desired user whose information bits are the same in each transmission. The bits $b_k(j), k = 2, \ldots, K(j), j = 1, \ldots, J$ are assumed to be uncorrelated. This is a reasonable assumption when

the retransmission probability in the next packet duration is very small. In this case, when two users both fail in a transmission, the probability that these two users retransmit the same bits in the same packet duration is negligible. $\mathbf{s}_{k1}$ is the spreading signature of user k. Its elements are randomly generated from the set $\{-1/\sqrt{N}, 1/\sqrt{N}\}$ with equal probability. $\mathbf{s}_{kl}, l = 2, \ldots, L$ are the shifted replicas of $\mathbf{s}_{k1}$. To simplify the analysis, we make the assumption as in [22] that $\mathbf{s}_{kl}, l = 0, \ldots, L-1$ are independent with each other. All though this assumption is unrealistic, the analysis results under this assumption fit the simulation results in the shifted case. Basically, in a large system, the shifting provides enough randomness even though there is code replication. $a_{kl}(j)$ is the channel gain for path l of user k in the j^{th} transmission, which is assumed to be uncorrelated. If the random delay of a retransmission is larger than the coherent time of the fading channel, this assumption is reasonable. However, in a practical system, the retransmission delay may not be large enough so that the channel coefficients in different transmissions are uncorrelated. Nevertheless, to simplify the analysis, we still assume that they are uncorrelated. Analysis based on the correlated channel coefficients is possible, but it will not be pursued in this work. In a wireless environment without line-of-sight between base station and mobile, $a_{kl}(j)$ is a zero-mean complex Gaussian random variable whose amplitude has Rayleigh distribution. We also assume that the delay-spread of the channel is small compared to the symbol time so that inter-symbol-interference (ISI) can be neglected. $\mathbf{n}(j)$ is complex white Gaussian noise with variance σ^2.

For the joint detection purpose, we stack J data vectors in (4.2) to obtain a $JN \times 1$ vector

$$\mathbf{y} = \tilde{S}_1 b_1 + S_2 A_2 \mathbf{b}_2 + \mathbf{n}, \tag{4.3}$$

where $\mathbf{y} = [\mathbf{y}(1), \ldots, \mathbf{y}(J)]^T$, $\tilde{S}_1 = [S_1\mathbf{a}_1(1), \ldots, S_1\mathbf{a}_1(J)]^T$, $S_2 = diag(S_2(1), \ldots, S_2(J))$, $A_2 = diag(A_2(1), \ldots, A(J))$, $\mathbf{b}_2 = [\mathbf{b}_2(1), \ldots, \mathbf{b}_2(J)]^T$, $\mathbf{n} = [\mathbf{n}(1), \ldots, \mathbf{n}(J)]^T$.

We first consider the minimum mean squared error (MMSE) receiver. It is well known [61] that the MMSE receiver for the j^{th} transmission is

$$\mathbf{m}(j) = d(j)R_2^{-1}(j)\mathbf{p}(j), \tag{4.4}$$

where $d(j) = 1/(1+\mathbf{a}_1^H(j)S_1^H R_2^{-1}(j)S_1\mathbf{a}_1(j))$, $R_2(j) = S_2(j)A_2(j)A_2^H(j)S_2^H(j)+\sigma^2\mathbf{I}_N$ is the covariance matrix of the interference plus noise, and $\mathbf{p}(j) = S_1\mathbf{a}_1(j)$ is the cross correlation between b_1 and $\mathbf{y}(j)$. The output of the MMSE receiver for the j^{th} transmission is

$$z(j) = d(j)\{\mathbf{a}_1^H(j)S_1^H R_2^{-1}(j)S_1\mathbf{a}_1(j)b_1 + I(j)\}, \tag{4.5}$$

where $I(j)$ is the interference plus the noise. It was shown [69, 115] that $I(j)$ is Gaussian. The mean of $I(j)$ is zero and the variance is $\mathbf{a}_1^H(j)S_1^H)R_2^{-1}(j)S_1\mathbf{a}_1(j)$. The receiver combines outputs of the MMSE receiver for J transmissions to form the decision variable z for b_1. It can be shown that the the optimal weight of the combiner for $z(j)$ is $1/d(j)$. Therefore, the decision variable is

$$z = \sum_{j=1}^{J}\{(\mathbf{a}_1^H(j)S_1^H)R_2^{-1}(j)S_1\mathbf{a}_1(j)\}b_1 + \sum_{j=1}^{J} I(j). \tag{4.6}$$

Consider the limiting regime where we have $N \to \infty$ with $K/N = \alpha$ (with L fixed). If the empirical distribution of the eigenvalues of $A_2(j)A_2^H(j)$ converges to the fixed distribution $F(p)$ in probability, then we known [22] that $S_1^H R_2^{-1}(j)S_1$ converges to $\beta\mathbf{I}_L$ in probability as $N \to \infty$, where β is the unique solution to the equation

$$\beta = \frac{1}{\sigma^2 + \alpha L \int_0^\infty \frac{p}{1+p\beta} dF(p)}. \tag{4.7}$$

Therefore, the decision variable in (4.6) converges to a limit z^* in probability

$$z^* = \beta \sum_{j=1}^{J}\sum_{l=1}^{L} |a_{1l}(j)|^2 b_1 + I, \tag{4.8}$$

The signal to interference ratio (SIR) of z converges to $\beta\sum_{j=1}^{J}\sum_{l=1}^{L}|a_{1l}(j)|^2$ as $N \to \infty$. The decision for b_1 is $\hat{b}_1 = sgn(Real(z))$. Suppose that $a_{1l}(j), l = 1, \ldots, L$ have

the same variance. Define the signal to noise ratio γ as $\gamma \triangleq \frac{\sum_{l=1}^{L} E(|a_{1l}(j)|^2)}{\sigma^2}$. Since the bit error rate P_e is a continuous function of $S_1^H R_2^{-1}(j) S_1$, BER converges to a limit P_{lim} in probability [70]

$$P_{lim} = [(1-\mu)/2]^{JL} \sum_{i=0}^{JL-1} \binom{JL-1+i}{i} [(1+\mu)/2]^i, \tag{4.9}$$

where

$$\mu = \sqrt{\frac{\beta\gamma/L}{1+\beta\gamma/L}}. \tag{4.10}$$

When the variances of $a_{kl}(j)$ are different, we can evaluate BER using the formula in [65]. In this work, we assume that each channel gain has the same variance, and we shall use (4.9) to calculate packet success probability.

We can also do joint MMSE detection based on all the data received in J transmissions. Using the signal model in (4.3), we obtain the MMSE receiver

$$\mathbf{m} = d R_2^{-1} \tilde{S}_1, \tag{4.11}$$

where $d = 1/(1+\tilde{S}_1^H R_2^{-1} \tilde{S}_1)$, $R_2 = S_2 A_2 A_2^H S_2^H + \sigma^2 \mathbf{I}_{JN}$. Since both S_2 and A_2 are block diagonal matrices, it can be shown that $\mathbf{m} = d[\mathbf{m}^T(1)/d(1), \ldots, \mathbf{m}^T(J)/d(J)]^T$. It is observed that the joint detector is actually equivalent to the separate detectors with the optimal combiner. Since we only have to keep the output of individual detector in separate detection, we need less memory for separate detection. Thus, the separate detection with the optimal combiner is preferred in a practical system.

The multipath decorrelating detector is proposed in [116]. Define the signature matrix in the j^{th} transmission $S(j) = [S_1(j)\ S_2(j)]$. The decorrelator is $S^+(j)$ the pseudo-inverse of the signature matrix $S(j)$. When $S(j)$ has full column rank, $S^+(j) = (S(j)^T S(j))^{-1} S(j)^T$. Because we are here interested in user 1, we take the first L outputs of the decorrelator,

$$\mathbf{z}(j) = \mathbf{a}_1(j) b_1 + \mathbf{n}_1(j), \tag{4.12}$$

where $\mathbf{n}_1(j)$ is Gaussian and its covariance matrix $R_{n1}(j)$ is the first $L \times L$ sub-block of $\sigma^2(S(j)^T S(j))^{-1}$. Using an MMSE combiner to combine the outputs of J decorrelators, we have

$$z = \sum_{j=1}^{J} \mathbf{a}_1^H(j) R_{n1}^{-1}(j) \mathbf{z}(j). \tag{4.13}$$

In the case when $\alpha L = LK/N < 1$, we have $R_{n1}(j) \xrightarrow{P} \frac{\sigma^2}{1-\alpha L}\mathbf{I}_L$ as $N \to \infty$ [22], where $\xrightarrow{P}$ denotes the convergence in probability. Thus, we have $z \xrightarrow{P} z^*$, and z^* is given by

$$z^* = \beta \sum_{j=1}^{J} \sum_{l=1}^{L} |a_{1l}(j)|^2 b_1 + I, \tag{4.14}$$

where $\beta = \frac{1-\alpha L}{\sigma^2}$ and I is Gaussian with zero mean and variance $\beta \sum_{j=1}^{J} \sum_{l=1}^{L} |a_{1l}(j)|^2$. We can use (4.9) to evaluate bit error rate for the decorrelator.

When the receiver is the matched filter with an maximum ratio combiner, it is straightforward to get the following result for large systems [22]. The decision variable z converges to z^* in probability

$$z^* = \sum_{j=1}^{J} \sum_{l=1}^{L} |a_{1l}(j)|^2 b_1 + I,$$

where I has the covariance $\beta \sum_{j=1}^{J} \sum_{l=1}^{L} |a_{1l}(j)|^2$ and $\beta = 1/[\sigma^2 + \alpha L \int_0^\infty p dF(p)]$. By central limit theorem, I is Gaussian distributed. Therefore, BER can be calculated by using (4.9).

4.2.2 Unslotted CDMA System

In unslotted CDMA random access systems, users can transmit at any time. Suppose that the receiver knows the timing of the desired user and there are $K(j)$ users transmit in one bit duration with random delays. As in[91], we assume the system to be chip synchronous to make the analysis tractable. The samples of chip matched

filter output form a $N \times 1$ data vector

$$\mathbf{y}(j) = \sum_{l=1}^{L} \mathbf{s}_{1l} a_{1l}(j) b_1 + \sum_{k=2}^{K(j)} \sum_{l}^{L} \mathbf{u}_{kl}(j) a_{kl}(j) b_k^{-1}(j) + \sum_{k=2}^{K(j)} \sum_{l}^{L} \mathbf{v}_{kl}(j) a_{kl}(j) b_k^{0}(j) + \mathbf{n}(j), \tag{4.15}$$

where $b_k^{-1}(j)$, $b_k^0(j)$ are the two consecutive symbols of the kth user which overlap with user 1 in one bit duration. $a_{kl}(j)$ is the channel gain as defined before in slotted systems. $\mathbf{u}_{kl}(j)$ and $\mathbf{v}_{kl}(j)$ are determined by the spreading signature $\mathbf{s}_{kl}(j)$ and the delays relative to user 1. If $d_k \in [0, \ N)$ denotes the relative delay in terms of number of chips of the k^{th} user with respect to user 1, then $\mathbf{u}_{kl}(j)$ has its first d_k elements to be the last d_k elements of $\mathbf{s}_{kl}(j)$ and the rest zeros. Similarly, $\mathbf{v}_{kl}(j)$ has the first d_k elements zero and the last $N - d_k$ elements to be the first $N - d_k$ elements of $\mathbf{s}_{kl}(j)$. Let $\mathbf{a}_k(j) = [a_{k1}(j), \ldots, a_{kL}(j)]^T$, $U_k(j) = [\mathbf{u}_{k1}(j), \ldots, \mathbf{u}_{kL}(j)]$, $V_k(j) = [\mathbf{v}_{k1}(j), \ldots, \mathbf{v}_{kL}(j)]$, and $\mathbf{b}_2(j) = [b_2^{-1}(j), \ldots, b_{K(j)}^{-1}(j), b_2^0(j), \ldots, b_{K(j)}^0(j)]^T$. Denote $A_2(j) = diag(\mathbf{a}_2(j), \ldots, \mathbf{a}_{K(i)}(j))$, $S_1 = [\mathbf{s}_{11}, \ldots, \mathbf{s}_{1L}]$, $S_2(j) = [U_2(j), \ldots, U_{K(j)}, V_2(j), \ldots, V_{K(j)}]$. Then (4.15) can be written as

$$\begin{aligned} \mathbf{y}(j) &= S_1 \mathbf{a}_1(j) b_1 + S_2(j) A_2(j) \mathbf{b}_2(j) + \mathbf{n}(j) \\ &= S_1 \mathbf{a}_1(j) b_1 + \tilde{S}_2(j) \mathbf{b}_2(j) + \mathbf{n}(j), \end{aligned} \tag{4.16}$$

where $\tilde{S}_2(j) = [\tilde{\mathbf{u}}_2, \ldots, \tilde{\mathbf{u}}_{K(j)}, \tilde{\mathbf{v}}_2, \ldots, \tilde{\mathbf{v}}_{K(j)}]$ and $\tilde{\mathbf{u}}_k = U_k \mathbf{a}_k$ and $\tilde{\mathbf{v}}_k = V_k \mathbf{a}_k$.

As in the synchronous case, the MMSE receiver is $\mathbf{m}(j) = d(j) R_2^{-1}(j) \mathbf{p}(j)$, where $d(j) = 1/(1 + \mathbf{a}_1^H(j) S_1^H R_2^{-1}(j) S_1 \mathbf{a}_1(j))$, $R_2(j) = \tilde{S}_2(j) \tilde{S}_2^H(j) + \sigma^2 \mathbf{I}_N$ and $\mathbf{p}(j) = S_1 \mathbf{a}_1(j)$. The SIR achieved by user 1 using the data from the j^{th} transmission is given by

$$SIR_1(j) = \mathbf{a}_1(j)^H S_1^H (\tilde{S}_2(j) \tilde{S}_2^H(j) + \sigma^2 \mathbf{I}_N)^{-1} S_1 \mathbf{a}_1(j). \tag{4.17}$$

Assume that the delay spread of the multipath channel is very small compared to the processing gain. Then in a large system where $K/N = \alpha$, $N, K \to \infty$, Theorem 3.2 in [91] about the limiting SIR of user 1 for asynchronous Gaussian channel can be extended to the asynchronous multipath channel case. As in [91], the empirical

distribution of the delays of the different users, relative to the desired user is assumed to converge to a fixed distribution, $G(\tau)$,where the delay d relative to user 1 is given by $d = \lfloor \tau N \rfloor$. The empirical distribution of the powers of the users is assumed to converge to a fixed distribution, $F(p)$.

Theorem 2 *$SIR_1(j)$ converges to $SIR_1(j)^* = \beta \sum_{l=1}^{L} |a_{1l}(j)|^2$ in probability as $N \to \infty$, where*

$$\beta = \int_0^1 w(x)dx \tag{4.18}$$

and

$$w(x) = \frac{1}{\sigma^2 + \alpha E_P E_\tau \{I(P, \int_0^\tau w(z)dz) 1_{\tau \geq x} + I(P, \int_\tau^1 w(z)dz) 1_{\tau \leq x}\}} \tag{4.19}$$

where E_P and E_τ denote the expectation with respect to the power distribution $F(P)$ and the delay distribution $G(\tau)$ respectively, $I(P, \beta) = \frac{P}{1+P\beta}$ and $1_{\tau \geq x}$ is an indicator function that is 1 if $\tau \geq x$ and 0 otherwise. The solution to $w(x)$ exits and is unique in a class of function $w(x) \geq 0$.

Proof First, under the assumption that $\mathbf{s}_{1l}, l = 1, \ldots, L$ are independent random sequences, from Theorem A.4 in [22], we have $\mathbf{s}_{1l_1}^H (S_2(j) S_2^H(j) + \sigma^2 \mathbf{I}_N)^{-1} \mathbf{s}_{1l_2} \xrightarrow{P} 0$ as $N \to \infty$ when $l_1 \neq l_2$. Denote $\beta_l = \mathbf{s}_{1l}^H (S_2(j) S_2^H(j) + \sigma^2 \mathbf{I}_N)^{-1} \mathbf{s}_{1l}$. The power of user k is $P_k = \sum_{l=1}^{L} |a_{kl}|^2$. Since the delay spread is very small, we can neglect the effect of the delay spread. Then the variance of an element of matrix $\tilde{S}_2(j)$ is the same as that of the same element of matrix $\mathbf{S}_1 \mathbf{D}_1^{\frac{1}{2}}$ in [91] when the powers of the interference users here are the same as the powers of the users in the signal model in [91]. Following exactly the same steps to prove Theorem 3.2 in [91], we can show that $\beta_l \xrightarrow{P} \beta$. Therefore, $SIR_1 \xrightarrow{P} SIR_1^*$ follows. □

After the receiver combines the outputs of MMSE detector for J transmissions of the same packet using the optimal combiner, the SIR_1 converges to

$$SIR_1^* = \beta \sum_{j=1}^{J} \sum_{l=1}^{L} |a_{1l}(j)|^2 \tag{4.20}$$

in probability. Since the interference and noise at the output of MMSE receiver is Gaussian, we can use (4.9) to calculate bit error rate.

The effective signature matrix of size $N \times (2K(j)-1)L$ for the j^{th} transmission can be denoted as $S(j) = [S_1\ S_2(j)]$. As in the synchronous case, the decorrelator is $S^+(j) = (S(j)^T S(j))^{-1} S(j)^T$ if the inverse exists. The interferences are completely eliminated, the covariance matrix of the Gaussian noise is $\sigma^2(S(j)^H S(i))^{-1}$. For user 1, the noise covariance R_{n1} is the first $L \times L$ sub-block of $\sigma^2(S(j)^H S(j))^{-1}$. With the assumption that the signature sequences of the different multipath components are independent, it is straightforward to extend Theorem 3.3 in [91] about the SIR of decorrelator in asynchronous AWGN channel to asynchronous multipath channel case. In multipath channels, we have $R_{n1} \to \sigma^2/(1-2\alpha L)$ as $N \to \infty$ when $2\alpha L < 1$. Therefore, $SIR_1(j)$ converges to $SIR_1^*(j) = \sum_{l=1}^{L} |a_{1l}(j)|^2(1-2\alpha L)/\sigma^2$ in probability. After combing outputs of the decorrelator for J transmission, we have $SIR_1 \xrightarrow{P} SIR_1^*$ where

$$SIR_1^* = \frac{(1-2\alpha L)}{\sigma^2} \sum_{j=1}^{J} \sum_{l=1}^{L} |a_{1l}(j)|^2. \tag{4.21}$$

It is straightforward to show that the matched filer receiver in the asynchronous multipath channel has the same asymptotic performance as in the synchronous multipath situation [22]. Basically, because the random signatures are used, the effective interference of a particular user at the output of the matched filter is only related to its power and has nothing to do with its relative delay. However, in a finite system that uses the spreading signatures such as Gold sequences which have special crosscorrelation properties, the crosscorrelation in the synchronous cases are typically less than in the asynchronous case. Therefore, the asymptotic result for the matched filter here is not applicable to such a system.

4.3 System Throughput and Delay

In this section, we study the throughput and delay of the slotted and unslotted CDMA random access systems. Since both the offered load and bandwidth is infinite, we normalized the offered load by the processing gain N. The throughput which is defined as the the average number of packets successfully transmitted in a packet duration is also normalized by the processing gain.

In the CDMA random access system with packet combining, the bit error rate is decreasing with the number of transmission increasing. The packet success probability is different for the packet with different number of transmissions. We assume that the length of the packet is L_p. Suppose that the packet fails in $J-1$ transmissions, then the packet success probability in the J^{th} transmission is given by

$$P_{ps}(J) = (1 - P_{be}(J))^{L_p} \tag{4.22}$$

The packet failure probability in the J^{th} transmission the is $P_{pf}(J) = 1 - P_{ps}(J)$. The unconditional packet success probability after J transmissions can be found as

$$P_{ps}^{J} = P_{ps}(J) \prod_{j=1}^{J-1} P_{pf}(j) \tag{4.23}$$

Denote $N_J(t)$ as the number of packets that are transmitted the J^{th} time in the current packet duration. As we see in Section III, the bit error rate converges to a deterministic limit in large systems. Under this condition, it is shown [83] that $N_J(t)$ in a slotted system is a Poisson random variable with the rate

$$G(J) = G(1) \prod_{j=1}^{J-1} P_{pf}(j), \tag{4.24}$$

where $G(1)$ is the new arrival rate, and $N_J(t), J = 1, 2, \ldots$ are mutually independent. In an unslotted system, denote N_f^J as the number of packets that fail in the J^{th} transmission. Since the new arriving packets are Poisson, N_f^1 is a Poisson random variable with rate $G(1)P_{pf}(1)$. We assume that the delays between two consecutive

transmissions are mutually independent random variables with an exponential distribution. By Burke's Theorem [8], a Poisson process after a random delay with exponential distribution is still a Poisson process. Therefore, in an unslotted system, the number of packets that are transmitted the second time in a packet duration is a Poisson random variable with rate $G(2)$. By inducing, we know that $N_J(t), J = 1, 2, \ldots, \infty$ are independent Poisson random variables with the mean given in (4.24).

The offered load can be expressed as

$$G = \sum_{J=1}^{\infty} G(J) = G(1) \sum_{J=1}^{\infty} \prod_{j=1}^{J-1} P_{pf}(j). \tag{4.25}$$

The normalized throughput is given by

$$\begin{aligned} S &= \frac{1}{N} \sum_{J=1}^{\infty} E(N_J) P_{ps}^J \\ &= \frac{G(1)}{N} \sum_{J=1}^{\infty} P_{ps}(J) \prod_{j=1}^{J-1} P_{pf}(j). \end{aligned} \tag{4.26}$$

It is shown [83] that $\sum_{J=1}^{\infty} P_{ps}(J) \prod_{j=1}^{J-1} P_{pf}(j) = 1$. The normalized throughput becomes

$$S = \frac{\alpha}{\sum_{J=1}^{\infty} \prod_{j=1}^{J-1} P_{pf}(j)}. \tag{4.27}$$

The delay is defined as the average number of transmissions of a packet. It is given by

$$D = \sum_{J=1}^{\infty} J P_{ps}^J \tag{4.28}$$

4.4 Numerical Results and Discussions

In this section, we present simulation and analysis results to show the performance of both slotted and unslotted CDMA random access systems. We assume that the receiver has the knowledge of the channel state information and delays of all the users. In a practical system, channel state and the delays can be estimated either blindly or by using training sequences. However, channel estimation is out of the

scope of this work. In simulations, the number of paths of the channel L is 2. All the paths of different users are independent complex Gaussian random variables with the same variance. The channel in each transmission is independent. The packet length is $L_p = 128$.

Fig. 4.1 and Fig. 4.2 show the bit error rate of slotted and unslotted CDMA systems for different SNRs. We plot the BER of 100 independent runs in which spreading signatures are independently generated. In simulation, the spreading signature at the second path is the shifted replica of the original spreading signature; whereas in analysis, we assume that the spreading signatures at different paths are independent. From Fig. 4.1 and Fig. 4.2, one sees that BER in simulations spread around the asymptotic limit. When the processing gain increases, it is expected that the spread around the asymptotic limit becomes more narrow. In AWGN channel, it is shown [61] that MMSE receiver converges to the decorrelator when SNR tends to infinity. However, it is observed in Fig. 4.1 and Fig. 4.2 that MMSE receiver has better performance even when SNR is very high. This can be explained as follows. Consider the signal model for the synchronous CDMA in (4.2). The effective signature of user k in j^{th} transmission is $\mathbf{s}_k(j)\mathbf{a}_k(j)$. As SNR tends to infinity, the MMSE receiver converges to a vector that is orthogonal to the range space of the effective signatures of the interference users. The dimension of this space is $K-1$. If $a_{kl}, l = 1, \ldots, L$ are all equal, the asymptotic SIR of the MMSE receiver is $(1-\alpha)SNR$ when $\alpha < 1$. On the other hand, the asymptotic SIR of the multipath decorrelator is $(1-\alpha L)SNR$ when $\alpha L < 1$. Therefore, the MMSE receiver has approximate $10log(\frac{1-\alpha}{1-\alpha L})$ dB advantage over the decorrelator receiver when SNR is high. The similar conclusion can be drawn for the unslotted CDMA systems. We also see from Fig. 4.1 and Fig. 4.2 that the bit error rate after three transmissions is much less than that after one transmission for all the linear receivers. Fig. 4.3 plots bit error rate attained for different normalized offered load. When $\alpha > \frac{1}{L}$ in the

slotted CDMA system and $\alpha > \frac{1}{2L}$ in the unslotted CDMA system, the decorrelator does not exist. Thus, decorrelator is not suitable for the system with moderate offered load in multipath channels. When offered load is very high, MMSE receiver has almost the same bit error rate as the matched filter receiver. In high offered load regime, there is no sufficient degree of freedom for the MMSE receiver to suppress the interference. Therefore, MMSE receiver tends to have the same performance as the matched filter receiver. Fig. 4.4 shows the bit error rate versus the number of transmissions. It is seen that the bit error rate decreases linearly with the number of transmissions increasing.

The normalized throughput and average delay for a slotted CDMA system is shown in Fig. 4.5 and Fig. 4.6. The throughput and average delay of narrow band ALOHA are also plotted in the figures. In the ALOHA system, we assume that there is no noise. Therefore, the packet can be successfully transmitted if there is no collision. The CDMA system with MMSE receiver and packet combining has the best performance. Its throughput is much higher than ALOHA systems for all the offered traffic load. When the normalized offered load is lower (¡0.8), the CDMA system using MMSE receiver but without packet combining has almost the same throughput as the system with packet combing. However, when the normalized offered load increases, its throughput decreases dramatically. When the normalized offered load is high, the MMSE receiver without packet combining does not have sufficient degree of freedom to effectively suppress the interference. The packet success probability decreases very fast with respect to the increase of the normalized offered load when the normalized offered load is great than one. However, if the receiver combines J packets, it gets J fold interference and noise suppression. Therefore, even when the normalized offered load is very high (> 1), the receiver with the packet combining still can suppress the interference with the number of packet transmissions increasing. This is the reason why the system with packet combining has high throughput when

normalized offered load is high. If the system uses packet combing, the throughput of the systems employing MMSE receiver and matched filter tend to be the same when normalized offered load tends to infinity. This is because, as we observed in Fig. 4.3, the bit error rates of the MMSE receivers and matched filters tends to be the same when the normalized offered load is very large. The throughput of the system with matched filter and without packet combing is much lower than the ALOHA system. This seems to contradict the observation [16] that the CDMA random access system with the matched filter receiver has almost the same throughput as the ALOHA system. This is due to the following reasons. First, effect of additive noise is not considered in [16]. The unsuccessful transmissions are assumed to be caused only by the multiple-access interference. Second, forward error correction code is used in [16]. It is observed [16] that as the block error correction capability increases, the effective throughput increases until it reaches a maximum, after which further coding reduces the effective throughput. In the systems considered here, if we uses the error correction code, the effective throughput can be improved. Finally, we consider the fading channel in which the packet success probability is much lower than in the AWGN channel when SNR is the same. In Fig.4.6 we see that the average delay of the system with packet combing is much smaller than that of the system without packet combing. This is because, with the packet combing, the packet success probability increases with the number of transmissions. If no packet combing, the packet success probability is the same no matter how many times the packet is transmitted. The normalized throughput and average delay for an unslotted CDMA system is shown in Fig. 4.7 and Fig. 4.8. Similarly as in the slotted CDMA system, packet combining improves the performance of an unslotted CDMA system.

4.5 Summary

The system performance of the CDMA random access systems in multipath fading channels are analyzed for large systems in which the offered load and the processing gain tend to infinity but their ratio is fixed. The linear MMSE multiuser receiver has much better performance than the matched filter single user receiver. However, without packet combining, when the normalized offered load is greater than one in slotted systems and is greater than half in unslotted systems, linear MMSE receiver cannot effectively suppress the multiple-access interference; thus the throughput decreases to zero in high offered load region. With packet combining, the receiver not only gets a diversity gain in fading channels but also obtain an interference and noise suppression gain. With the number of transmissions increases, the packet success probability increases even when the offered load is very large. Therefore, packet combing improves the system performance for all the offered load. Unlike in the CDMA system without packet combining, the throughput of CDMA system with packet combing tends to a finite value when the normalized offered load is very large. The CDMA system with MMSE receiver and packet combing has much higher throughput than the ALOHA system for all the offered load.

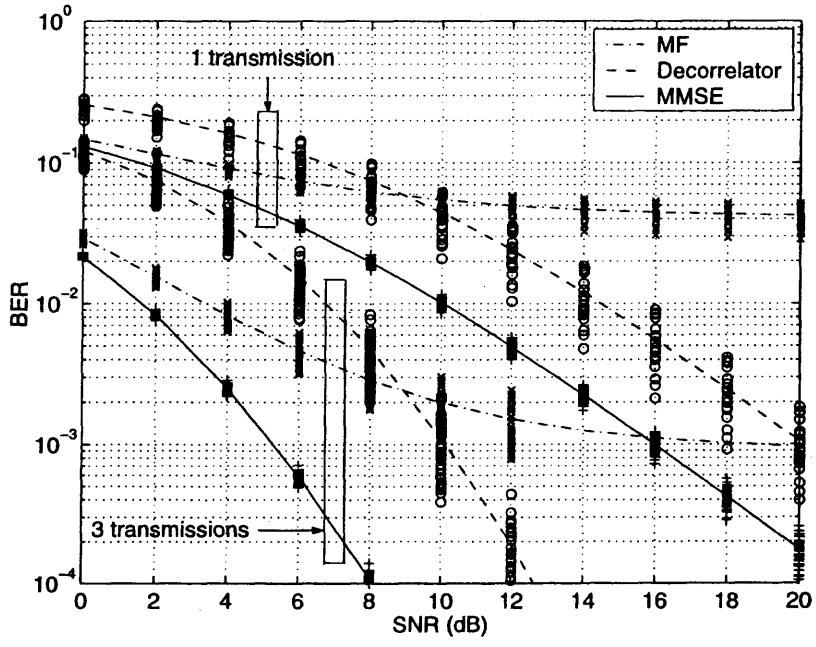

Figure 4.1 BER versus SNR for the slotted CDMA system. $\alpha = 3/8$, $L = 2$, Processing gain $N = 64$ in simulation.

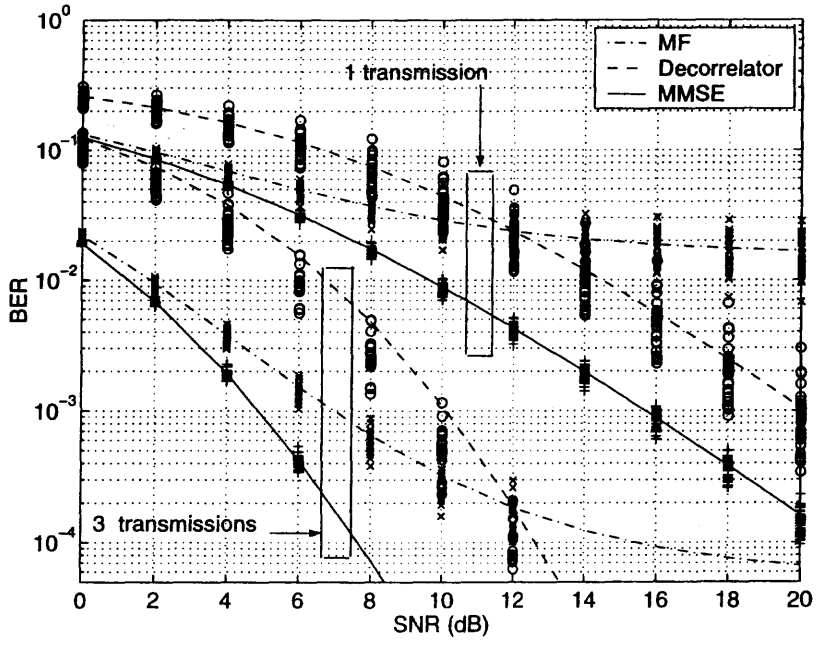

Figure 4.2 BER versus SNR for the unslotted CDMA system. $\alpha = 3/16$,$L = 2$, Processing gain $N = 64$ in simulation.

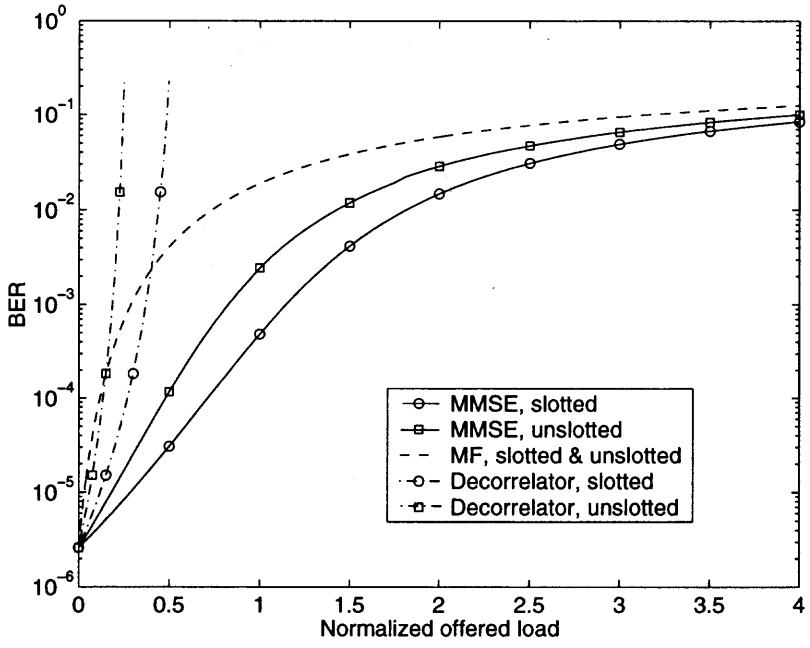

Figure 4.3 BER versus normalized offered load. $SNR = 20dB$, $L = 2$. The number of transmissions $Nrt = 3$.

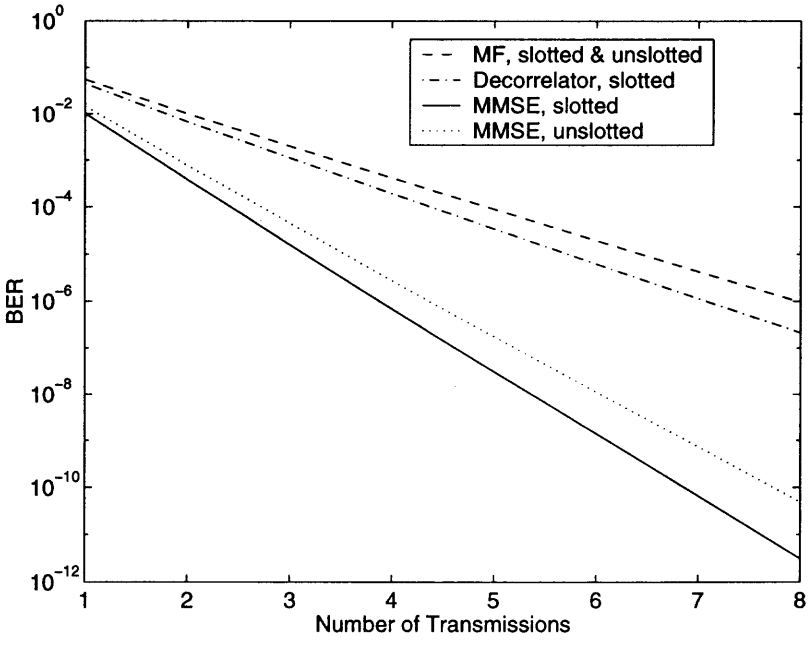

Figure 4.4 BER versus the number of transmissions. $SNR = 10dB$, $\alpha = 3/8$, $L = 2$.

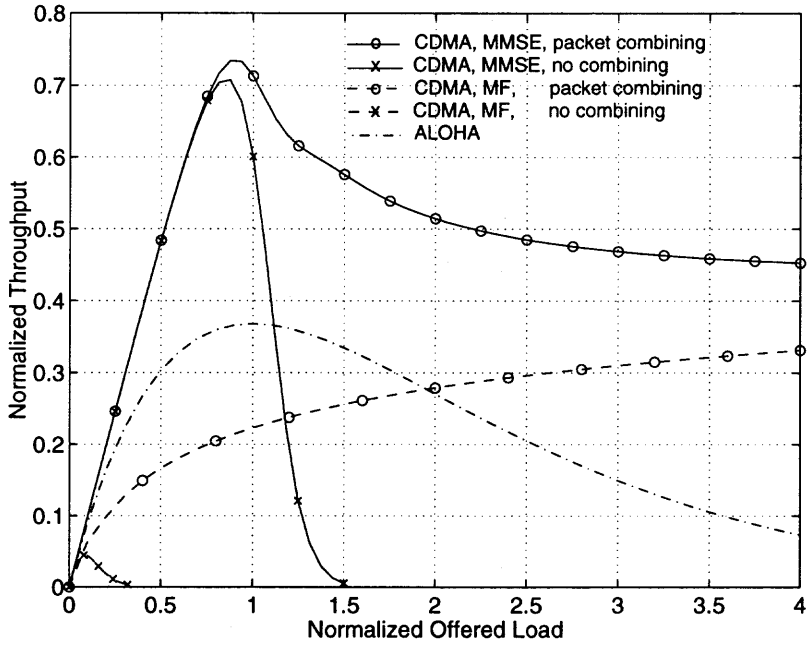

Figure 4.5 Normalized throughput of the slotted CDMA system. $SNR = 20dB$, $L = 2$.

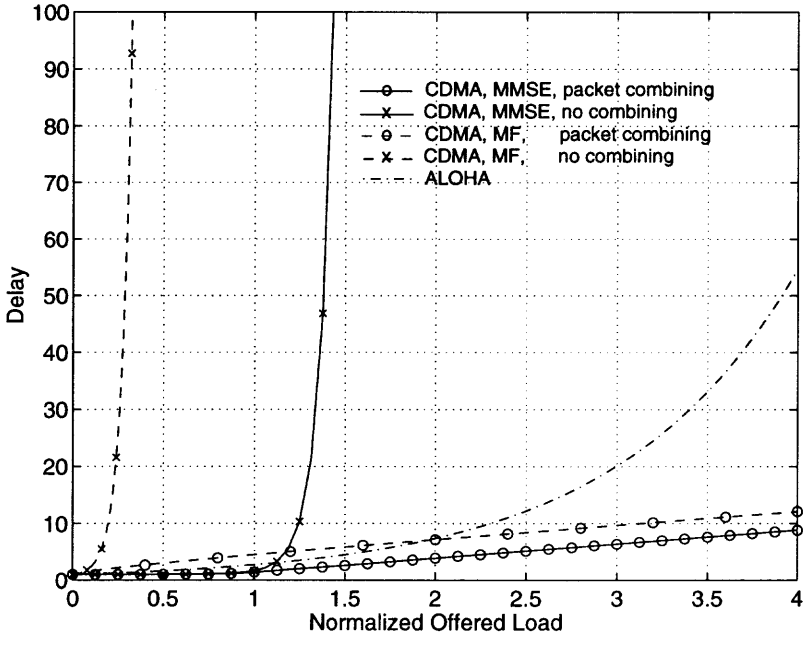

Figure 4.6 Average delay of the slotted CDMA system. $SNR = 20dB$, $L = 2$.

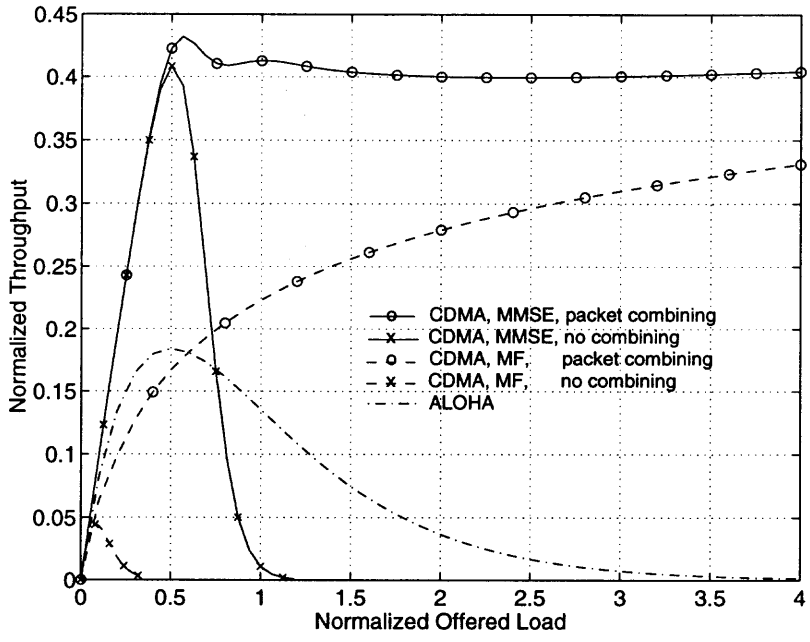

Figure 4.7 Normalized throughput of the unslotted CDMA system. $SNR = 20dB$, $L = 2$.

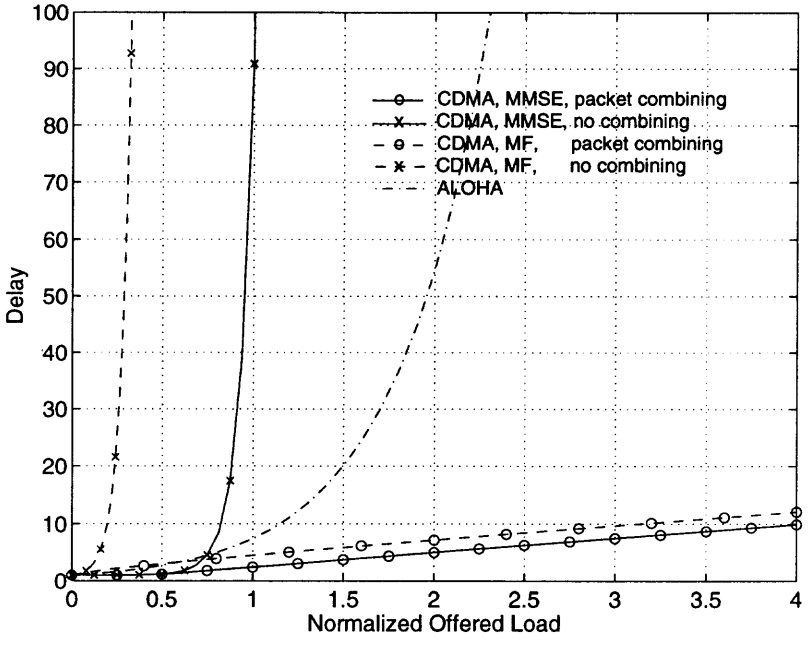

Figure 4.8 Average delay of the unslotted CDMA system. $SNR = 20dB$, $L = 2$.

CHAPTER 5

CONCLUSIONS AND FUTURE DIRECTIONS

5.1 Conclusions

This dissertation investigates two techniques, namely interference suppression technique and diversity technique, to improve the system performance of CDMA systems. Specifically, in interference suppression technique, we study the reduced-rank MMSE receiver and reduced-rank minimum variance receiver for DS-CDMA system. In diversity technique, we study the MC-CDMA systems with transmit diversity and packet CDMA random access systems with packet combining.

In Chapter 2, we first develop reduced-rank MMSE receiver for DS-CDMA system. When the covariance matrix of the received signal is known, it was shown that reduced-rank MMSE receiver has worse performance compared with the full-rank MMSE receiver. However, when the covariance matrix is estimated from an finite number of data samples, our analysis and simulations show that the reduced-rank MMSE receiver that choose proper eigenvalues and eigenvectors outperforms the full-rank receiver, especially when the desired signal is in a low dimensional subspace and the power of different users are different. An adaptive reduced-rank MMSE receiver is then developed based on a subspace tracking algorithm. Compared with the RLS full-rank adaptive receiver, the adaptive reduced-rank MMSE receiver has larger output SIR, but higher complexity. We then investigate the reduced-rank minimum variance receiver that can be blindly implemented. The minimum variance receiver can be implemented in the same structure as a generalized sidelobe canceler. The simulations demonstrate that the reduced-rank minimum variance receiver outperforms the full-rank minimum variance receiver. To further understand the reason why the reduced-rank MMSE receiver has better performance, we study the probability density function of the output SNR of linear MMSE estimators based on a general linear signal model. The pdf of output SNR of full-rank MMSE estimator

that uses direct inverse of the covariance matrix is derived. An asymptotic pdf of the reduced-rank MMSE estimator using principle component inverse of the covariance matrix is also derived. From these pdfs, we see the advantage of the reduced-rank MMSE estimator.

In chapter 3, the multicarrier CDMA system with transmit diversity is studied. The linear block space-time code which is originally proposed for a narrow band system is applied to a wideband MC-CDMA system. We then proposed four schemes to jointly decode the space-time codes and suppress multiple access interference. These four schemes are maximum ratio combiner, orthogonal resorting combiner, MMSE combiner and MMSE multiuser detector. It is shown that the MMSE combiner is the best tradeoff between the performance and the complexity. Channel estimation using pilot channels pilot symbols are then studied for the multicarrier CDMA systems. While the channel estimator using pilot channels has better performance, it reduces the number of spreading codes available for mobile users, thereby reduces the number of users in a cell.

In chapter 3, we investigate the CDMA random access systems with packet combining in fading channels. The performance of both the slotted CDMA system and unslotted CDMA system with random spreading signature is analyzed. The analysis is based on large systems in which the offered load and the processing gain tend to infinity but their ratio is fixed. In such large systems, it is relatively easy to character the effect of multiple-access interference. We first analyze the bit error rate of the MMSE receiver, decorrelator and matched filter receiver in fading channels. The packet that fails in a transmission is not discarded; the receiver combines all the data of the same packet from different transmissions. By doing so, the receiver obtains a interference suppression gain and a diversity gain. The interference suppression gain is due to the fact that in each retransmission of the same packet, the interference is generally uncorrelated. Since the fading is independent in each

retransmission, a diversity gain is obtained by packet combining. It is shown that the bit error rate decreases with the number of transmissions increasing. We then analyze the system throughput and average delay. From the analysis for both the slotted CDMA and unslotted CDMA systems, it is seen that multiuser detection and packet combining substantially improve the performance of CDMA random access systems.

5.2 Future Directions

To implement reduced-rank MMSE receiver or reduced-rank minimum variance receiver, a subspace tracker that can track both the signal space and eigenvalues associated with the basis of the signal space is required. The subspace algorithm should have reasonable complexity and convergence speed. In the simulations, we observed that the PAST algorithm [113] and LORAF3 algorithm [80] has the same order of complexity as RLS adaptive filter but their convergence is very slow. On the other hand, other subspace tracking algorithms [18, 80] have much larger computation complexity. Developing efficient subspace tracking algorithms with practical complexity will be a very interesting and challenging research direction.

In chapter 3, we apply the space-time coding to a wideband system multicarrier CDMA system. Most of the space-time coding schemes assume that the fading channel is not frequency selective. Although such space-time coding also work well in frequency selective fading channel, they are not optimal for such channels. A simple space-time coding [54] has been proposed for multipath channels. Space-time coding that can fully exploit the diversity provided by frequency-selective fading channel will be a fruitful research area.

In the CDMA random access system with packet combining studied in chapter 4, we did not use any coding. We combine the packets at the bit level. When coding is applied to the transmitted data, combing the packets at code level will have better

performance than combing the packets at the bit level. Therefore, the research on packet combing, decoding and multiuser detection for CDMA random access system is worthy to be pursued.

APPENDIX A

DERIVATION OF THE SECOND PARTIAL DERIVATIVE OF $\widehat{MSE}_R$ IN EQ. 2.26

In this appendix, we derive $\mathbf{H}_{ij}$ and F_{ii} in Eq. 2.26 . Let's denote the last two terms in Eq. 2.22 as $M1 = \hat{\mathbf{c}}_r^T \mathbf{C} \hat{\mathbf{c}}_r$ and $M2 = 2\hat{\mathbf{c}}_r^T \mathbf{p}$. We first derive the first and second partial derivatives of $M1$. The gradient of $M1$ along $\hat{\mathbf{u}}_i$ is given by

$$\begin{aligned} \mathbf{g}1_i &= \frac{\partial M1}{\partial \hat{\mathbf{u}}_i} \\ &= 2\frac{\partial \hat{\mathbf{c}}_r^T}{\partial \hat{\mathbf{u}}_i}\mathbf{C}\hat{\mathbf{c}}_r \\ &= \frac{2}{\hat{\lambda}_i}(\mathbf{p}\hat{\mathbf{u}}_i^T + \mathbf{p}^T\hat{\mathbf{u}}_i\mathbf{I}_N)\mathbf{C}\hat{\mathbf{c}}_r. \end{aligned} \tag{A.1}$$

Define $\mathbf{z}_i = \frac{2}{\hat{\lambda}_i}\mathbf{C}\hat{\mathbf{c}}_r$ and $\mathbf{X}_i = \hat{\mathbf{u}}_i\mathbf{p}^T + \mathbf{p}^T\hat{\mathbf{u}}_i\mathbf{I}_N$. Then $\mathbf{g}1_i$ can be expressed as $\mathbf{g}1_i = \mathbf{X}_i^T\mathbf{z}_i$. And we have

$$\frac{\partial \mathbf{z}_i^T}{\partial \hat{\mathbf{u}}_j} = \frac{2}{\hat{\lambda}_i\hat{\lambda}_j}\mathbf{X}_j^T\mathbf{C}. \tag{A.2}$$

Then the Hessian matrix of $M1$, $\mathbf{H}1_{ji}$, is given by

$$\begin{aligned} \mathbf{H}1_{ji} &= \frac{\partial \mathbf{g}1_i^T}{\partial \hat{\mathbf{u}}_j}|_P \\ &= \frac{\partial \mathbf{z}_i^T}{\partial \hat{\mathbf{u}}_j}\mathbf{X}_i|_P \\ &= \frac{2}{\lambda_i\lambda_j}\mathbf{X}_j^T\mathbf{C}\mathbf{X}_i \quad i \neq j \end{aligned} \tag{A.3}$$

and

$$\begin{aligned} \mathbf{H}1_{ii} &= \frac{\partial \mathbf{g}1_i^T}{\partial \hat{\mathbf{u}}_i}|_P \\ &= \frac{\partial(\mathbf{z}_i^T\mathbf{X}_i)}{\partial \hat{\mathbf{u}}_i}|_P \\ &= (\frac{\partial \mathbf{z}_i^T}{\partial \hat{\mathbf{u}}_i}\mathbf{X}_i + [\frac{\partial \mathbf{x}_{i1}^T}{\partial \hat{\mathbf{u}}_i}\mathbf{z}_i, \ldots, \frac{\partial \mathbf{x}_{iN}^T}{\partial \hat{\mathbf{u}}_i}\mathbf{z}_i])|_P \\ &= (\frac{2}{\hat{\lambda}_i^2}\mathbf{X}_i^T\mathbf{C}\mathbf{X}_i + [\mathbf{Y}_1\mathbf{z}_i, \ldots, \mathbf{Y}_N\mathbf{z}_i])|_P \\ &= \frac{2}{\lambda_i^2}\mathbf{X}_i^T\mathbf{C}\mathbf{X}_i + \frac{2}{\lambda_i}[\mathbf{Y}_1\mathbf{C}\mathbf{c}_r, \ldots, \mathbf{Y}_N\mathbf{C}\mathbf{c}_r], \end{aligned} \tag{A.4}$$

where $\{\mathbf{x}_{ij}, j = 1, \ldots, N\}$ are columns of matrix $\mathbf{X}_i$ and matrices $\{\mathbf{Y}_j, j = 1, \ldots, N\}$ are defined as

$$\mathbf{Y}_j = \mathbf{P}_j + \mathbf{p}(j)\mathbf{I}_N. \tag{A.5}$$

Here $\mathbf{P}_j$ is a matrix whose jth column is vector $\mathbf{p}$ and other columns are zero vectors. $M1$ can also be expressed as

$$\begin{aligned} M1 &= \mathbf{p^T} \sum_{j=1}^{r} \frac{\hat{\mathbf{u}}_j \hat{\mathbf{u}}_j^T}{\hat{\lambda}_j} \mathbf{C} \sum_{j=1}^{r} \frac{\hat{\mathbf{u}}_j \hat{\mathbf{u}}_j^T}{\hat{\lambda}_j} \mathbf{p} \\ &= \mathbf{p}^T \left(\frac{\hat{\mathbf{u}}_i \hat{\mathbf{u}}_i^T}{\hat{\lambda}_i} + \sum_{\substack{j=1 \\ j \neq i}}^{r} \frac{\hat{\mathbf{u}}_j \hat{\mathbf{u}}_j^T}{\hat{\lambda}_j}\right) \mathbf{C} \left(\frac{\hat{\mathbf{u}}_i \hat{\mathbf{u}}_i^T}{\hat{\lambda}_i} + \sum_{\substack{j=1 \\ j \neq i}}^{r} \frac{\hat{\mathbf{u}}_j \hat{\mathbf{u}}_j^T}{\hat{\lambda}_j}\right) \mathbf{p} \\ &= \frac{1}{\hat{\lambda}_i^2} \mathbf{p}^T \hat{\mathbf{u}}_i \hat{\mathbf{u}}_i^T \mathbf{C} \hat{\mathbf{u}}_i \hat{\mathbf{u}}_i^T \mathbf{p} + \frac{2}{\hat{\lambda}_i} \mathbf{p}^T \hat{\mathbf{u}}_i \hat{\mathbf{u}}_i^T \mathbf{C} \sum_{\substack{j=1 \\ j \neq i}}^{r} \frac{\hat{\mathbf{u}}_j \hat{\mathbf{u}}_j^T}{\hat{\lambda}_j} \mathbf{p} + \mathbf{p}^T \sum_{\substack{j=1 \\ j \neq i}}^{r} \frac{\hat{\mathbf{u}}_j \hat{\mathbf{u}}_j^T}{\hat{\lambda}_j} \mathbf{C} \sum_{\substack{j=1 \\ j \neq i}}^{r} \frac{\hat{\mathbf{u}}_j \hat{\mathbf{u}}_j^T}{\hat{\lambda}_j} \mathbf{p} \end{aligned} \tag{A.6}$$

The first partial derivative of $M1$ with respect to $\hat{\lambda}_i$ is given by

$$\frac{\partial M1}{\partial \hat{\lambda}_i} = -\frac{2}{\hat{\lambda}_i^3} p^T \hat{\mathbf{u}}_i \hat{\mathbf{u}}_i^T \mathbf{C} \hat{\mathbf{u}}_i \hat{\mathbf{u}}_i^T p - \frac{2}{\hat{\lambda}_i^2} p^T \hat{\mathbf{u}}_i \hat{\mathbf{u}}_i^T \mathbf{C} \sum_{j=1 j \neq i}^{r} \frac{\hat{\mathbf{u}}_j \hat{\mathbf{u}}_j^T}{\hat{\lambda}_j} p \tag{A.7}$$

Then the second partial derivative of $M1$ with respect to $\hat{\lambda}_i$ is found as

$$\frac{\partial^2 M1}{\partial \hat{\lambda}_i^2}|_P = \frac{6}{\lambda_i^4} p^T \mathbf{u}_i \mathbf{u}_i^T \mathbf{C} \mathbf{u}_i \mathbf{u}_i^T p + \frac{4}{\lambda_i^3} p^T \mathbf{u}_i \mathbf{u}_i^T \mathbf{C} \sum_{\substack{j=1 \\ j \neq i}}^{r} \frac{\mathbf{u}_j \mathbf{u}_j^T}{\lambda_j} p \tag{A.8}$$

It is easily shown that the second term in the above equation is equal to zero and $\mathbf{u}_i^T \mathbf{C} \mathbf{u}_i = \lambda_i$. Thus, we have

$$\frac{\partial^2 M1}{\partial \hat{\lambda}_i^2}|_P = \frac{6}{\lambda_i^3} \mathbf{p}^T \mathbf{u}_i \mathbf{u}_i^T \mathbf{p} \tag{A.9}$$

We next determine the derivatives of $M2$. $M2$ can also be expressed as

$$M2 = 2 \sum_{i=1}^{r} \frac{(\mathbf{p}^T \hat{\mathbf{u}}_i)^2}{\hat{\lambda}_i} \tag{A.10}$$

The gradient of $M2$ along $\hat{\mathbf{u}}_i$ is given by

$$\begin{aligned} \mathbf{g}2_i &= \frac{\partial M2}{\partial \hat{\mathbf{u}}_i} \\ &= \frac{4}{\hat{\lambda}_i} \mathbf{p}^T \hat{\mathbf{u}}_i \mathbf{p} \end{aligned} \tag{A.11}$$

It is seen from (37) that we have $\mathbf{H}2_{ij} = \frac{\partial \mathbf{g}2_i^T}{\partial \hat{\mathbf{u}}_j} = \mathbf{0}$ for $i \neq j$. And $\mathbf{H}2_{ii}$ is obtained as

$$\begin{aligned} \mathbf{H}2_{ii} &= \frac{\partial \mathbf{g}2_i^T}{\partial \hat{\mathbf{u}}_i}|_P \\ &= \frac{4}{\lambda_i}\mathbf{W} \end{aligned} \tag{A.12}$$

where the ith column of matrix $\mathbf{W}$ is $\mathbf{p}(i)\mathbf{p}$. The second derivative of $M2$ with respect to $\hat{\lambda}_i$ at point P is given by

$$\frac{\partial^2 M2}{\partial \hat{\lambda}_i^2}|_P = \frac{4(p^T\mathbf{u}_i)^2}{\lambda_i^3} \tag{A.13}$$

Finally, F_{ii} in (2.26) is given by $F_{ii} = \frac{\partial^2 M1}{\partial \hat{\lambda}_i^2}|_P - \frac{\partial^2 M2}{\partial \hat{\lambda}_i^2}|_P$, and $\mathbf{H}_{ij}$ in (2.26) is given by $\mathbf{H}_{ij} = \mathbf{H}1_{ij} - \mathbf{H}2_{ij}$.

REFERENCES

1. S. M. Alamouti, "A simple transmit diversity technique for wireless communications," *IEEE Journal on Select Areas in Communications*, vol. 16, pp. 1451–1458, Oct. 1998.

2. P. D. Alexander, M. C. Reed, J. A. Asenstorfer, and C. B. Schlegel, "Iterative multiuser interference reduction: Turbo CDMA," *IEEE Trans. Commun.*, vol. 47, pp. 1008–1015, July 1999.

3. T. W. Anderson, "Asymptotic theory for principal component analysis," *Annals of Mathematical Statistics*, vol. 34, pp. 122–148, 1963.

4. A. Annamalai and V. K. Bhargava, "Analysis of unslotted direct-sequence spread spectrum multiple access network with packet combing," *Electronics Letters*, vol. 33, pp. 1673–1674, Sept. 1997.

5. A. Annamalai and V. K. Bhargava, "Throughput performance of slotted DS/CDMA ALOHA with packet combing over generalized fading channels," *Electronics Letters*, vol. 33, pp. 1195–1197, July 1997.

6. P. A. Bello, "Characterization of randomly time-variant linear channels," *IEEE Trans. Commun. Syst.*, vol. CS-11, pp. 360–393, Dec. 1963.

7. C. Berrou and A. Glavieux, "Near optimum error correcting coding and decoding: Turbo-Codes," *IEEE Trans. Comm*, vol. COM-44, pp. 1261–1271, Oct. 1996.

8. D. Bertsekas and R. Gallager, *Data Networks*. Englewood Cliffs, NJ: Prentice-Hall, 1992.

9. A. M. Y. Bigloo, T. A. Gulliver, and V. K. Bhargava, "Maximum-likelihood decoding and code combing for DS/SSMA slotted ALOHA," *IEEE Trans. Commun.*, vol. 45, pp. 1602–1612, Dec. 1997.

10. J. Boccuzzi, S.U.Pillai, and J. H. Winters, "Adaptive antenna arrays using sub-space techniques in a mobile radio environment with flat fading and CCI," in *IEEE 49th Vehicular Technology Conference*, pp. 50–54, May 1999.

11. J. K. Cavers, "An analysis of pilot symbol assisted modulation for Rayleigh fading channels," *IEEE Trans. Veh. Technol.*, vol. 40, pp. 686–693, Nov. 1991.

12. J. K. Cavers, "Pilot symbol assisted modulation and differential detection in fading and delay spread," *IEEE Trans. Commun.*, vol. 43, pp. 2206–2212, July 1995.

13. D. Chase, "Code combining – A maximum-likelihood decoding approach for combining an arbitrary number of noisy packets," *IEEE Trans. Commun.*, vol. 33, pp. 385–393, May 1985.

14. D. G. M. Cruickshank, "Suppression of multiple access interference in a DS-CDMA system using Wiener filtering and parallel cancellation," *Proc. IEE Commun.*, vol. 143, pp. 226–230, Aug. 1996.

15. D. N. C.Tse and S. V. Hanly, "Linear multiuser receivers: effective interference, effective bandwidth and user capacity," *IEEE Trans. Inform. Theory*, vol. 45, pp. 641–657, Mar. 1999.

16. P. W. de Graaf and J. S. Lehnert, "Performance comparison of a slotted ALOHA DS/SSMA network and a multichannel narrow-band slotted ALOHA network," *IEEE Trans. Commun.*, vol. 46, pp. 544–552, Apr. 1998.

17. D. Divsalar, M. K. Simon, and D. Raphaeli, "Improved parallel interference cancellation for CDMA," *IEEE Trans. Commun.*, vol. 46, pp. 258–268, Feb. 1998.

18. E. M. Dowling, L. P. Ammann, and R. D. DeGroat, "A TQR-iteration based adaptive SVD for real time angle and frequency tracking," *IEEE Trans. Signal Processing*, vol. 42, pp. 914–926, Apr. 1994.

19. A. Duel-Hallen, "Decorrelation decision-feedback detectors for asynchronous code-division multiple-access channels," *IEEE Trans. Commun.*, vol. 41, pp. 285–290, Feb. 1993.

20. A. Duel-Hallen, "A family of multiuser decision-feedback detectors for asynchronous code-division multiple-access channels," *IEEE Trans. Commun.*, vol. 43, pp. 421–434, Feb/March/April 1995.

21. D. J. Edelbute, J. M. Fisk, and G. L. Kinnison, "Criteria for optimum-signal-detection theory for arrays," *J. Am. Stat. Assoc.*, pp. 199–205, June 1966.

22. J. Evans and D. N. Tse, "Linear multiuser receivers for multipath fading channels," *IEEE Trans. Inform. Theory*, vol. 46, pp. 2059–2078, Sept. 2000.

23. R. Fantacci, "An efficient RAKE receiver architecture with pilot signal cancellation for downlink communications in DS-CDMA indoor wireless networks," *IEEE Trans. Commun.*, vol. 47, pp. 823–827, June 1999.

24. J. S. Goldstein and I. S. Reed, "Reduced-rank adaptive filtering," *IEEE Trans. Signal Processing*, vol. 45, p. 492496, Feb. 1997.

25. J. S. Goldstein and I. S. Reed, "Subspace selection for partially adaptive sensor array processing," *IEEE Trans. Aerosp. Electron. Syst.*, vol. 33, pp. 539–543, Apr. 1997.

26. J. S. Goldstein and I. S. Reed, "Subspace selection for partially adaptive sensor array processing," *IEEE Transactions on Aerospace and Electronic Systems*, vol. 33, pp. 539–544, April 1997.

27. J. S. Goldstein, I. S. Reed, and L. L. Scharf, "A multistage representation of the Wiener filter based on orthogonal projections," *IEEE Trans. Inform. Theory*, vol. 44, pp. 2943–2959, Nov. 1998.

28. G. H. Golub and C. F. V. Loan, *Matrix Computations.* The Johns Hopkins University Press, 1996.

29. X. Gui and T. S. Ng, "Performance of Asynchronous Orthogonal Multicarrier CDMA Systems in Frequency-Selective Fading Channel," *IEEE Trans. Commun.*, vol. 47, pp. 1084–1090, July 1999.

30. A. M. Haimovich, "The eigencanceler: adaptive radar by eigenanalysis methods," *IEEE Trans. Aerosp. Electron. Syst.*, vol. 32, pp. 532–542, Apr. 1996.

31. A. M. Haimovich and Y. Bar-Ness, "An eigenanalysis interference canceler," *IEEE Trans. Signal Processing*, vol. 39, pp. 76–84, Jan. 1991.

32. A. R. Hammons and H. E. Gamal, "On the Theory of Space-Time Codes for PSK Modulation," *IEEE Trans. Inform. Theory*, vol. 46, pp. 524–542, Mar. 2000.

33. R. C. Hanumara, "An alternate derivation of the distribution of the conditioned signal-to-noise ration," *IEEE Trans. Antennas and Propagation*, vol. AP-34, pp. 463–464, Mar. 1986.

34. S. Hara and R. Prasad, "Design and Performance of Multicarrier CDMA System in Frequency-Selective Rayleigh Fading Channels," *IEEE Trans. Vehicular Technology*, vol. 48, pp. 1584–1594, Sept. 1999.

35. A. Hiroike, F. Adachi, and N. Nakajima, "Combined effects of phase sweeping transmitter diversity and channel coding," *IEEE Trans. Vehicular Technology*, vol. 41, p. 170176, May 1992.

36. B. M. Hochwald and T. L. Marzetta, "Unitary space-time modulation for multiple-antenna communications in Rayleigh flat fading," *IEEE Trans. Inform. Theory*, vol. 46, pp. 543–564, Mar. 2000.

37. M. Honig, U. Madhow, and S. Verdu, "Blind multiuser detection," *IEEE Trans. Inform. Theory*, vol. 41, pp. 944–960, July 1995.

38. M. L. Honig and J. S. Goldstein, "Adaptive reduced-rank residual correlation algorithms for DS-CDMA interference suppression," in *32nd Asilomar Conf. Signals, Syst. Comput.*, (Pacific Grove and CA), pp. 1106–1110, November 1998.

39. A. Host-Madsen and K. Cho, "MMSE/PIC multiuser detection for DS/CDMA systems with inter- and intra-cell interference," *IEEE Trans. Commun.*, vol. 47, pp. 291–299, Feb. 1999.

40. A. L. C. Hui and L. B. Letaief, "Successive interference cancellation for multiuser asynchronous DS/CDMA detectors in multipath fading links," *IEEE Trans. Commun.*, vol. 46, pp. 384–391, March 1998.

41. D. L. Jagerman, "Some properties of the Erlang loss function," *The Bell System Technical Journal*, vol. 53, pp. 525–551, Mar. 1974.

42. W. C. Jakes, *Microwave Mobile Communications.* New York: Wiley, 1974.

43. A. Johansson and S. Svensson, "Multistage interference cancellation in multi-rate DS/CDMA on a mobile radio channel," in *IEEE Vehicular Technology Conference*, (Atlanta GA), pp. 666–670, May 1996.

44. D. H. Johnson and D. E. Dudgeon, *Array Signal Processing: Concepts and Techniques.* Englewood Cliffs, NJ: Prentice-Hall, 1993.

45. S. Kallel, "Analysis of a type II hybrid ARQ scheme with code combining," *IEEE Trans. Commun.*, vol. 38, pp. 1133–1137, Aug. 1990.

46. M. Kaveh and A. J. Barabell, "The statistical performance of the MUSIC and the Minimum-Norm algorithms in resolving plane waves in noise," *IEEE Trans. Acoustics Speech and Signal Processing*, vol. ASSP-34, pp. 331–340, Apr. 1986.

47. S. T. Kay, *Fundamentals of Statistical Signal Processing: Estimation Theory.* Englewood Cliffs, NJ: Prentice-Hall, 1993.

48. I. P. Kirsteins and D. W. Tufts, "Rapidly adaptive nulling of interference," in *High Resolution Methods in Underwater Acoustics* (M. Bouvet and G. Bienvenu, eds.), pp. 220–249, Springer-Verlag: New York, 1991.

49. I. P. Kirsteins and D. W. Tufts, "Adaptive detection using low rank approximation to a data matrix," *IEEE Trans. Aerosp. Electron. Syst.*, vol. 30, pp. 55–67, Jan. 1994.

50. R. Kohno, H. Imai, M. Hatori, and S. Pasupathy, "An adaptive canceler of cochannel interference for spread-spectrum multiple-access communication networks in a power line," *IEEE J. Select. Areas Commun.*, vol. 8, pp. 691–699, May 1990.

51. R. Kohno, H. Imai, M. Hatori, and S. Pasupathy, "Combination of an adaptive array antenna and a canceler of interference for direct-sequence spread-spectrum multiple-access systems," *IEEE J. Select. Areas Commun.*, vol. 8, pp. 675–682, May 1990.

52. S. Kumar and S. Nanda, "High data-rate packet communications for cellular networks using CDMA: algorithms and performance," *IEEE J. Select. Areas Commun.*, vol. 17, pp. 472–490, Mar. 1999.

53. W. Y. Kuo and M. P. Fitz, "Design and analysis of transmitter diversity using intentional frequency offset for wireless communications," *IEEE Trans. Vehicular Technology*, vol. 46, pp. 871–881, Nov. 1997.

54. E. Lindskog and A.Paulraj, "Transmit diversity scheme for channels with intersymbol interference," in *Proc. ICC 2000*, (New Orleans and USA), pp. 307–311, June 2000.

55. F. Ling, "Optimal reception, performance bound, and cutoff rate analysis of references-assisted coherent CDMA communications with applications," *IEEE Trans. Commun.*, vol. 47, pp. 1583–1591, Oct. 1999.

56. C.-L. Liu and K. Feher, "Pilot symbol aided coherent M-ary PSK in frequency-selective fast Rayleigh fading channels," *IEEE Trans. Commun.*, vol. 42, pp. 54–62, Jan. 1994.

57. H. Liu and K. Li, "A decorrelating RAKE receiver for CDMA communications over frequency-selective fading channels," *IEEE Trans. Commun.*, vol. 47, pp. 1036–1045, July 1999.

58. R. Lupas and S. Verdu, "Linear multiuser detector for synchronous code-devision multiple-access channels," *IEEE Trans. Inform. Theory*, vol. 35, pp. 123–136, Jan. 1989.

59. R. Lupas and S. Verdu, "Near-far resistance of multiuser detectors in asynchronous channels," *IEEE Trans. Commun.*, vol. 38, pp. 496–508, Apr. IEEE Trans. Commun.

60. U. Madhow, "Blind adaptive interference suppression for the near-far resistant acquisition and demodulation of direct-sequence CDMA signals," *IEEE Trans. Signal Proc.*, vol. 45, pp. 102–112, Jan. 1997.

61. U. Madhow and M. Honig, "MMSE interference suppression for direct-sequence spread spectrum CDMA," *IEEE Trans. Commun.*, vol. 42, pp. 3178–3188, Dec. 1994.

62. D. Mitra and J. A. Morrison, "Erlang capacity and uniform approximations for shared unbuffered resources," *IEEE/ACM Trans. Networking*, vol. 2, pp. 558–570, Dec. 1994.

63. U. Mitra, R. Vijayakumar, and K. M. Wasserman, "Stability of CDMA data networks with fixed and adaptive MMSE receivers," in *Proc. 33rd Asilomar Conference on Signals, Systems and Computers*, (Pacific Grove CA), pp. 197–201, Oct. 1999.

64. M. Moher, "Turbo-based multiuser detection," *Proc. 1997 Int. Symp. on Inf. Th.*, July 1997.

65. P. Monsen, "Digital transmission performance on fading dispersive diversity channels," *IEEE Trans. Commun.*, vol. 21, p. 3339, Jan. 1973.

66. R. K. Morrow and J. S. Lehnert, "Packet throughput in slotted ALOHA DS/SSMA radio systems with random signature sequences," *IEEE Trans. Commun.*, vol. 40, pp. 1223–1230, July 1992.

67. P. Patel and J. Holtzman, ""Analysis of a simple successive interference cancellation techniques for spread-spectrum multiple-access systems"," *IEEE Journal of Selected Areas in Communications*, vol. 12, pp. 796–807, June 1994.

68. C. D. Peckham, A. M. Haimovich, T. F. Ayoub, J. S. Goldstein, and I. S. Reed, "Reduced-rank STAP performance analysis," *IEEE Trans. Aerosp. Electron. Syst.*, vol. 36, pp. 664–676, Apr. 2000.

69. H. V. Poor and S. Verdu, "Probability of error in MMSE multiuser detection," *IEEE Trans. Inform. Theory*, vol. 43, pp. 868–871, May 1997.

70. J. G. Proakis, *Digital Communications.* McGraw-Hill, 1995.

71. P. B. Rapajic, "Performance analysis of slotted ALOHA/CDMA system with adaptive MMSE receivers," *IEICE Trans. Fundamentals*, vol. E80-!, pp. 2485–2492, Dec. 1997.

72. D. Raychaudhuri, "Performance analysis of random access packet-switched code division multiple access systems," *IEEE Trans. Commun.*, vol. 29, pp. 895–900, June 1981.

73. I. Reed, J. Mallett, and L. Brennan, "Rapid convergence rate in adaptive arrays," *IEEE Trans. Aerospace Electron. Syst.*, vol. AES-10, pp. 853–863, Nov. 1974.

74. S. Roy and H.-Y. Wang, "Performance of CDMA slotted ALOHA multiple access with multiuser detection," in *Proc. IEEE Wireless Commun. and Network. Conf. (WCNC'99)*, (New Orleans and LA), pp. 839–843, 1999.

75. T. Sato, H. Okada, T. Yamazato, M. Katayama, and A. Ogawa, "Throughput analysis of DS/SSMA unslotted ALOHA system with fixed packet length," *IEEE J. Select. Areas Commun.*, vol. 14, p. 4, 750-756 1996.

76. J. B. Schodorf and D. B. Williams, "A constrained optimization approach to Multiuser detection," *IEEE Trans. Signal Processing*, vol. 45, pp. 258–262, Jan. 1997.

77. N. Seshadri and J. H. Winters, "Two signaling schemes for improving the error performance of frequency-division -duplex (FDD) transmission systems using transmitter antenna diversity," *Int. J. Wire. Inform. Net.*, vol. 1, p. 1, 49-59 1994.

78. S. Souissi and S. B. Wicker, "A diversity combining DS/CDMA system with convolutional encoding and Viterbi decoding," *IEEE Trans. Vehicular Technology*, vol. 44, pp. 304–312, May 1995.

79. J. Storey and F. A. Tobagi, "Throughput performance of an unslotted direct-sequence SSMA packet radio network," *IEEE Trans. Commun.*, vol. 37, pp. 814–823, Aug. 1989.

80. P. Strobach, "Low-Rank Adaptive Filters," *IEEE Trans. Signal Processing*, vol. 44, pp. 2932–2947, Dec. 1995.

81. Y. Sun, "Network diversity of random access slotted CDMA networks," in *Proc. 33rd Asilomar Conference on Signals, Systems and Computers*, (Pacific Grove and CA), pp. 1606–1610, Oct. 1999.

82. Y. Sun, "Multiuser detection using network diversity for random access packet-switched CDMA networks," in *Proc. 34th Conference on Information Science and Systems*, (Princeton and NJ), pp. TA3–1, Mar. 2000.

83. Y. Sun, "Network diversity of random access packet-switched CDMA networks - part I: multiuser detection," *Submitted to IEEE Trans. Signal Processing*, Jan. 2000.

84. Y. Sun, "Network diversity of random access packet-switched CDMA networks: optimum multiuser detection," *Submitted to IEEE Trans. Signal Processing*, Jan. 2000.

85. V. Tarokh, H. Jafarkhani, and A. R. Calderbank, "Space-Time Block Codes from Orthogonal Designs," *IEEE Trans. Inform. Theory*, vol. 45, pp. 1456–1467, July 1999.

86. V. Tarokh, A. Naguib, N. Seshadri, and A. R. Calderbank, "Space-Time Codes for High Data Rate Wireless Communication: Performance Criterion in the Presence of Channel Estimation Errors, Mobility, and Multiple Paths," *IEEE Trans. Commun.*, vol. 47, pp. 199–206, Feb. 1999.

87. V. Tarokh, N. Seshadri, and A. R. Calderbank, "Space-Time Codes for High Data Rate Wireless Communication: Performance Criterion and Code Construction," *IEEE Trans. Inform. Theory*, vol. 44, pp. 744–765, Mar. 1998.

88. M. K. Tsatsanis, "Inverse filtering criteria for CDMA systems," *IEEE Trans. Signal Processing*, vol. 45, pp. 102–112, Jan. 1997.

89. M. K. Tsatsanis and G. B. Giannakis, "Optimal decorrelating receivers for DS-CDMA systems: a signal processing framework," *IEEE Trans. Sig. Proc.*, vol. 44, pp. 3044–3054, Dec. 1996.

90. M. K. Tsatsanis and Z. Xu, "Performance analysis of minimum variance CDMA receivers," *IEEE Trans. Signal Processing*, vol. 46, pp. 3014–3022, Nov. 1998.

91. K. Tse and D. N. C. Tse, "Effective interference and effective bandwidth of linear multiuser receivers in Asynchronous CDMA systems," *IEEE Trans. Inform. Theory*, vol. 46, pp. 1426–1447, July 2000.

92. D. Tufts, I. Kirsteins, and R. Kumaresan, "Data-adaptive detection of a weak signal," *IEEE Trans. Aerosp. Electron. Syst.*, vol. 19, pp. 313–316, March 1983.

93. D. Tufts, R. Kumaresan, and I. Kirsteins, "Data adaptive signal estimation by singular value decomposition of a data matrix," *Proc. IEEE*, vol. 70, pp. 684–685, June 1982.

94. M. K. Varanasi, "A systematic approach to the design and analysis of optimum DPSK receivers for generalized diversity communications over Rayleigh fading channels," *IEEE Trans. com.*, vol. 47, pp. 1365–1375, Sept. 1999.

95. M. K. Varanasi and B. Aazhang, "Multistage detection for asynchronous code-division multiple-access communications," *IEEE Trans. Commun.*, vol. 38, pp. 505–519, April 1990.

96. M. K. Varanasi and B. Aazhang, "Near-optimum detection in synchronous code-division multiple-access systems," *IEEE Trans. Commun.*, vol. 39, pp. 825–836, May 1991.

97. S. Verdu, "Minimum probability of error for asynchronous Gaussian multiple-access channels," *IEEE Trans. Inform. Theory*, vol. IT-32, pp. 85–96, Jan. 1986.

98. S. Verdu and S. Shamai, "Spectral efficiency of CDMA with random spreading," *IEEE Trans. Inform. Theory*, vol. 45, pp. 622–640, Mar. 1999.

99. R. Vijayakumar and K. M. Wasserman, "On Stability of DS-CDMA data networks employing retransmissions with memory," in *Proceeding of the 38th Conference on Decision and Control*, (Phoenix, Arizona), pp. 3544–3549, Dec. 1999.

100. A. J. Viterbi, "Very low-rate convolution codes for maximum theoretical performance of spread-spectrum multiple-access systems," *IEEE Journal on Selected Areas in Communications*, vol. 8, pp. 614–649, May 1990.

101. X. Wang and H. V. Poor, "Blind multiuser detection: A subspace approach," *IEEE Trans. Inform. Theory*, vol. 44, pp. 677–691, Mar. 1998.

102. X. Wang and H. V. Poor, "Iterative (Turbo) soft interference cancellation and decoding for coded CDMA," *IEEE Trans. Commun.*, vol. 47, pp. 1046–1061, July 1999.

103. M. Wax and T. Kailath, "Detection of signals by information theoretic criteria," *IEEE Trans. Acoust. Speech Signal Processing*, vol. ASSP-33, pp. 387–392, Apr. 1985.

104. V. Weerackody, "Diversity for direct-sequence spread spectrum system using multiple transmit antennas," in *Proc. IEEE ICC'93*, pp. 1775–1779, May 1993.

105. S. B. Wicker, "Adaptive rate error control through the use of diversity combing and majority-logic decoding in a hybrid-ARQ protocol," *IEEE Trans. Commun.*, vol. 39, pp. 380–385, Mar. 1991.

106. S. Wicker, *Error Control Systems for Digital Communication and Storage.* Englewood Cliffs, NJ: Prentice-Hall, 1995.

107. J. H. Winters, "The diversity gain of transmit diversity in wireless systems with Rayleigh fading," *IEEE Trans. Vehicular Technology*, vol. 47, pp. 119–123, Feb. 1998.

108. A. Wittneben, "A new bandwidth efficient transmit antenna modulation diversity scheme for linear digital modulation," in *Proc. IEEE ICC'93*, pp. 1630–1634, May 1993.

109. G. W. Wornell and M. D. Trott, "Efficient signal processing techniques for exploiting transmit antenna diversity on fading channels," *IEEE Trans. Signal Processing*, vol. 45, pp. 191–205, Jan. 1997.

110. Z. Xie, R. T. Short, and C. K. Rushforth, "A family of suboptimum detectors for coherent multiuser communications," *IEEE J. Select. Areas Commun.*, vol. 8, pp. 683–690, May 1990.

111. G. Xue, J. Weng, T. Le-Ngoc, and S. Tahar, "Adaptive multistage parallel interference cancellation for CDMA," *IEEE J. Select. Areas Commun.*, vol. 17, pp. 1815–1827, Oct. 1999.

112. B. Yang, "An extension of the PASTd algorithm to both rank and subspace tracking," *IEEE Signal Processing Letters*, vol. 2, pp. 179–182, Sept. 1995.

113. B. Yang, "Projection approximation subspace tracking," *IEEE Trans. Signal Processing*, vol. 44, pp. 95–107, Jan. 1995.

114. K.-W. Yip and T.-S. Ng, "Efficient simulation of digital transmission over WSSUS channels," *IEEE Trans. Commun.*, vol. 43, pp. 2907–2913, Dec. 1995.

115. J. Zhang, E. K. P. Chong, and D. N. C. Tse, "Output MAI distributions of MMSE multiuser receivers in DS-CDMA systems," *submitted for publication.*

116. Z. Zvonar and D. Brady, "Suboptimal multiuser detector for frequency-selective Rayleigh fading synchronous CDMA channels," *IEEE Trans. Commun.*, vol. 43, pp. 154–157, February/March/April 1995.